PROBABILISTIC FUZZY MULTI-OBJECTIVE OPTIMAL POWER FLOW USING PARTICLE SWARM OPTIMIZATION

PRAKAIPETCH MUANGKHIEW

A Thesis Submitted in Partial Fulfillment of the Requirements for
the Degree of Master of Engineering in Electrical Engineering
Suranaree University of Technology
Academic Year 2021

การหาคำตอบการไหลของกำลังไฟฟ้าที่เหมาะสมที่สุดแบบความน่าจะเป็นหลายวัตถุประสงค์โดยใช้วิธีฟัซซี่ร่วมกับการหาค่าเหมาะสมที่สุดของกลุ่มอนุภาค

นางสาวประกายเพชร ม่วงเขียว

PROBABILISTIC FUZZY MULTI-OBJECTIVE OPTIMAL POWER FLOW USING PARTICLE SWARM OPTIMIZATION

Suranaree University of Technology has approved this thesis submitted in partial fulfillment of the requirements for a Master's Degree.
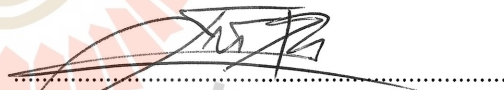
Thesis Examining Committee

....

(Asst. Prof. Dr. Parnjit Damrongkulkamjorn)

Chairperson

....

(Assoc. Prof. Dr. Keerati Chayakulkheeree)

Member (Thesis Advisor)

....
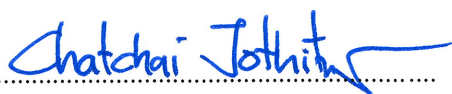
(Assoc. Prof. Dr. Thanatchai Kulworawanichpong)

Member

....

(Asst. Prof. Dr. Uthen Leeton)

Member

....　　　　...

(Assoc. Prof. Dr. Chatchai Jothityangkoon)　　(Assoc. Prof. Dr. Pornsiri Jongkol)

Vice Rector for Academic Affairs and　　　　　Dean of Institute of Engineering

Quality Assurance

ประกายเพชร ม่วงเขียว : การหาคำตอบการไหลของกำลังไฟฟ้าที่เหมาะสมที่สุดแบบความ
น่าจะเป็นหลายวัตถุประสงค์โดยใช้วิธีฟัซซี่ร่วมกับการหาค่าเหมาะสมที่สุดของกลุ่มอนุภาค.
อาจารย์ที่ปรึกษา : รองศาสตราจารย์ ดร. กีรติ ชยะกุลคีรี, 139 หน้า.

คำสำคัญ : ความน่าจะเป็นการไหลของกำลังไฟฟ้าที่ดีที่สุด, การหาค่าเหมาะสมที่สุดที่มีหลาย
วัตถุประสงค์, ฟังก์ชันความพึงพอใจแบบฟัซซี่, ต้นทุนรวม, กำลังงานไฟฟ้าสูญเสีย,
แรงดันไฟฟ้าเบี่ยงเบน

วิทยานิพนธ์นี้นำเสนอการหาคำตอบการไหลของกำลังไฟฟ้าที่เหมาะสมที่สุดแบบความ
น่าจะเป็นหลายวัตถุประสงค์โดยใช้วิธีฟัซซี่ร่วมกับการหาค่าเหมาะสมที่สุดของกลุ่มอนุภาค ในวิธีการ
ที่นำเสนอจะใช้การหาค่าเหมาะสมที่สุดของกลุ่มอนุภาคในการหาคำตอบการไหลของกำลังไฟฟ้าที่
เหมาะที่สุดแบบหลายวัตถุประสงค์ โดยใช้ค่าฟังก์ชันความพึงพอใจแบบฟัซซี่ของแต่ละวัตถุประสงค์
โดยในวิทยานิพนธ์นี้ได้พิจารณาการลดต้นทุนรวมของระบบ การลดกำลังงานสูญเสียของระบบ และ
ลดการเบี่ยงเบนขนาดแรงดันไฟฟ้าของระบบ อีกทั้งยังแก้ปัญหาทั้งสามพร้อมกันด้วยแนวคิดฟังก์ชัน
ความพึงพอใจแบบฟัซซี่ ในขณะเดียวกันการหาคำตอบการไหลของกำลังไฟฟ้าที่เหมาะสมที่สุดแบบ
ความน่าจะเป็นหลายวัตถุประสงค์จะใช้วิธีการหาค่าเหมาะสมที่สุดของกลุ่มอนุภาค โดยทดสอบบน
ระบบมาตรฐาน IEEE 30 บัส และ ระบบมาตรฐาน IEEE 30 บัสที่ถูกปรับแต่งด้วยการเพิ่มเครื่อง
กำเนิดไฟฟ้าของโรงไฟฟ้าพลังงานแสงอาทิตย์ และเครื่องกำเนิดไฟฟ้าของโรงไฟฟ้าพลังงานลม
นอกจากนี้กำลังไฟฟ้าของเครื่องกำเนิดไฟฟ้าพลังงานแสงอาทิตย์และพลังงานลมจะใช้ฟังก์ชันความ
หนาแน่นของความน่าจะเป็นในการอธิบายการแจกแจงความน่าจะเป็นของตัวแปรสุ่มแบบต่อเนื่อง
ของการแผ่รังสีแสงอาทิตย์และความเร็วลม ดังนั้นวิธีที่นำเสนอจึงสามารถพิจารณาความไม่แน่นอน
ของกำลังไฟฟ้าจากพลังงานแสงอาทิตย์ กำลังไฟฟ้าจากพลังงานลม และกำลังไฟฟ้าของโหลดของ
ประเทศไทยในรูปแบบของฟังก์ชันความหนาแน่นของความน่าจะเป็นโดยใช้การจำลองสถานการณ์
แบบมอนติคาร์โลร่วมด้วย ทั้งนี้วิธีการที่นำเสนอในการแก้ไขปัญหาการไหลของกำลังไฟฟ้าได้ทำการ
เปรียบเทียบผลลัพธ์กับวิธีอื่นๆ ภายใต้ข้อมูล ข้อจำกัด และตัวแปรควบคุมของระบบชุดเดียวกัน จาก
ผลการทดสอบพบว่าวิธีที่นำเสนอให้ผลลัพธ์ที่ดีกว่าวิธีอื่นเมื่อพิจารณาต้นทุนรวม กำลังงานไฟฟ้า
สูญเสีย และแรงดันไฟฟ้าเบี่ยงเบน อีกทั้งวิธีการที่นำเสนอเมื่อพิจารณาทั้งสามปัญหาพร้อมกันนั้นมี
ประสิทธิภาพและประสิทธิผลกว่าวิธีอื่นอีกด้วย

สาขาวิชาวิศวกรรมไฟฟ้า   ลายมือชื่อนักศึกษา ปร.กายเพชร ม่วงเขียว
ปีการศึกษา 2564   ลายมือชื่ออาจารย์ที่ปรึกษา

PRAKAIPETCH MUANGKHIEW : PROBABILISTIC FUZZY MULTI-OBJECTIVE
OPTIMAL POWER FLOW USING PARTICLE SWARM OPTIMIZATION. THESIS
ADVISOR : ASSOC. PROF. KEERATI CHAYAKULKHEEREE, D.Eng., 139 PP.

Keyword : Probabilistic optimal power flow/Multi-objective optimization/Fuzzy
satisfaction function/ Total system cost/ Active power loss/ Voltage
magnitude deviation

This research presents the probabilistic fuzzy multi-objective optimal power flow (PFMOOPF) using particle swarm optimization (PSO). In the proposed method, PSO is used to solve the multi-objective optimal power flow (MOOPF) incorporating the fuzzy satisfaction function (FSF) of the individual objective function. The objective function considered in this research is the total system cost minimization, active power loss minimization, and voltage magnitude deviation minimization. The PFMOOPF using PSO is verified on the modified IEEE 30-bus test system with integrated wind power plant (WPP) and photovoltaics power plant (PVPP) generators. In addition, the output power of PVPP and WPP generators is based on the probabilistic density function (PDF) of solar irradiance and wind speed. Therefore, the proposed PFMOOPF can incorporate the uncertainties of PVPP, WPP, and load based on PDF, and the OPF results were assessed using Monte-Carlo simulation (MCS). The efficiency and effectiveness of the proposed method in solving the results compared to the existing methods under identical system data, various constraints, and control variables. The results showed that the proposed method can provide better solutions for total system cost, active power loss, and voltage magnitude deviation minimizations, than other methods. Moreover, the proposed method is more efficient and effective, when solving a multi-objective solution, than other existing methods.

School of Electrical Engineering   Student's Signature ....

Academic Year 2021   Advisor's Signature ....

ACKNOWLEDGEMENT

Prakaipetch Muangkhiew

TABLE OF CONTENTS

TABLE OF CONTENTS (Continued)

TABLE OF CONTENTS (Continued)

TABLE OF CONTENTS (Continued)

LIST OF TABLES

LIST OF FIGURES

LIST OF FIGURES (Continued)

LIST OF ABBREVIATIONS

APL	=	active power loss
APLM	=	active power loss minimization
ED	=	Economic dispatch
FSF	=	fuzzy satisfactory function
MCS	=	Monte-Carlo simulation
MO	=	multi-objective
MOOPF	=	multi-objective optimal power flow
OPF	=	Optimal power flow
PDF	=	probability density function
PFMOOPF	=	probabilistic fuzzy multi-objective optimal power flow
PLF	=	probabilistic load flow
POPF	=	probabilistic optimal power flow
PPSPGSA	=	phasor particle swarm optimization and gravitational search algorithm
PSO	=	Particle swarm optimization
PSO-OPF	=	Particle swarm optimization based optimal power flow
PVPP	=	photovoltaic power plants
SVC	=	Static VAR compensators
TSC	=	Total system cost
TSCM	=	Total system cost minimization
VMD	=	voltage magnitude deviation
VMDM	=	voltage magnitude deviation minimization
WPP	=	wind power plants
EGA	=	Enhanced genetic algorithm
BHBO	=	Black-hole-based optimization
EGA-DQLF	=	Quadratic Load Flow solution with Enhanced genetic algorithm
FMOOPF	=	fuzzy multi-objective optimal power flow

LIST OF NOMENCLATURES

σ^2	=	the variance of PDF.
$|MVA_{Li}|$	=	the MVA flow of line i.
$|V_{Gi}|$	=	the voltage magnitude of generator at bus i.
$|V_i|$	=	the voltage magnitudes at bus i.
$|V_i^{ref}|$	=	the reference value of the voltage magnitude at bus i.
$|V_j|$	=	the voltage magnitudes at bus j.
$|V_{Li}|$	=	the voltage magnitude at load bus i.
μ	=	the mean value of PDF.
a_i, b_i, c_i	=	the cost coefficients parameters of generator i.
APL	=	the active power loss.
APL_{max}	=	the maximum acceptable active power loss obtained by TSCM and VMDM.
APL_{min}	=	the minimum active power loss obtained by APLM.
B_{ij}	=	the imaginary of admittance between buses i and j.
c	=	the scale parameter of the Weibull distribution.
$f_S(S)$	=	the PDF of solar irradiance.
OB_i	=	the objective function to be optimized.
$f_{Pd}(P_d)$	=	the PDF of load demand.
$f_v(v)$	=	the Weibull PDF of wind speed.
$\mathbf{g}$	=	the equality constraints representing nonlinear power flow equations.
G_{ij}	=	the active parts of admittance between buses i and j.
$g_{L,ij}$	=	the conductance of line L between buses i and j.
$gbest_i^t$	=	the best group position of particle i at iteration t
$\mathbf{h}$	=	the system operating constraints.
k	=	the shape parameter of the Weibull distribution.
MVA_{Li}	=	the MVA flow of line i.

LIST OF NOMENCLATURES (Continued)

NB	=	the buses total number.
NC	=	the shunt compensators total number.
p_m	=	the position of particle i
$pbest_m^t$	=	the best particle position of particle i at iteration t
v_m^t	=	the particle i 's velocity at iteration t
c_1, c_2	=	the acceleration constants
$gbest_m^t$	=	the best group position of particle i at iteration t
r_1, r_2	=	the random values within the range of [0,1]
t	=	the total number of iterations
w	=	the inertia weight factor
NG	=	the generators total number.
NL	=	the branches total number.
N_{obj}	=	the objectives total number.
NPQ	=	the PQ buses total number.
NT	=	the transformers total number.
NTL	=	the transmission line total number.
PNF	=	the penalty factor.
P_d	=	the load demands.
P_{Di}	=	the active power load demand at bus i.
P_{Gi}	=	the active power generation at bus i.
P_{pvn}	=	the nominal output power of the PV unit.
P_{PVPPi}	=	the active power PVPP generation at bus i.
P_{WPPi}	=	the active power WPP generation at bus i.
Q_{ci}	=	the shunt VAR compensator.
Q_{Di}	=	the reactive power load demand at bus i.
Q_{Gi}	=	the reactive power generation at bus i.
R_c	=	the certain irradiance points.
S	=	the solar irradiance on the PV module surface.
$S.D.$	=	the standard deviation.

LIST OF NOMENCLATURES (Continued)

S_{stc}	=	the solar irradiance at standard test conditions.
$T_{i\text{-}j}$	=	the transformer taps changing.
TSC	=	the total system cost.
TSC_{max}	=	the maximum acceptable total system cost obtained by APLM and VMDM.
TSC_{min}	=	the minimum total system cost obtained by TSCM.
$\boldsymbol{u}$	=	the column vector of control variables.
v	=	the wind speeds.
v_{ci}	=	the cut-in wind speed.
v_{co}	=	the cut-out wind speed.
VMD	=	the voltage magnitude deviation.
VMD_{max}	=	the maximum acceptable voltage magnitude deviation obtained by TSCM and APLM.
VMD_{min}	=	the minimum voltage magnitude deviation obtained by VMDM.
v_n	=	the nominal wind speeds.
$\boldsymbol{x}$	=	the vector of dependent variables.
δ_{ij}	=	the phase difference of voltages between bud i and bus j.
λ_{APL}	=	the fuzzy satisfaction function of active power loss.
λ_{OB}	=	the fuzzy satisfaction function of individual objective.
λ_T	=	the overall fuzzy satisfaction function.
λ_{TSC}	=	the fuzzy satisfaction function of total system cost.
λ_{VMD}	=	the fuzzy satisfaction function of voltage magnitude deviation.
Superscript		
~	=	probabilistic density function variable.
L	=	lower limit.
U	=	upper limit.

CHAPTER 1

INTRODUCTION

1.1 General Introduction

An important analysis tool for the control and operation of electric power system is optimal power flow (OPF), which gained widespread attention in today's electrical system control and operation, especially for economic operations. The OPF model is a famous problem for power system operation and planning, illustrating the problem of power plants in determining optimal operating levels. To meet the demands imposed during a typical power system network with the aim of reducing operating costs. The main goal of the OPF solution is to obtain the optimal control variable of the system that optimizes the objective function that optimizes the objective function within the constraints of the system. Therefore, with different objective in power system operation, the OPF can be defined as a multi-objective security constraint optimization problem.

In the last decades, many variable optimization methods have been used to solve complex constrained optimization problems for example OPF problems. The OPF problem are created using a multi-objective problem under a set of operative constraint. These constraints include equality and inequality constraints. Therefore, the multi-objective optimization is an important part of optimization activities. The classic approach to solving such problems focuses on aligning multiple objectives to a individual objective. For the multi-objective optimization can be defined conflicting objectives by the Pareto optimal method or a fuzzy decision method to separate the best compromise solution from the tradeoff front.

On the other hand, the OPF assessment is one of the guidelines used to determine the state of the electrical system. But in an unstable energy system such as renewable energy, a conditional OPF assessment cannot accurately solve the state of the system. However, a more general formulation of the probabilistic

optimal power flow (POPF) problem is assumed that random disturbances in the system load can be represented as random disturbances in all the OPF variables.

1.2 Problem Statement

Economic growth and population growth are the key factors to drive economic activities to raise people's living standards. Renewable and alternative energy is part of strengthening energy security through the use of domestic energy feedstocks to reduce the import and dependence of petroleum-based energy. which is a major cause of climate change problems. In the past, Thailand has a policy to continuously support the production of renewable energy and alternative energy in the form of electricity, heat and biofuels. Therefore, the proportion of such energy consumption increases every year. However, providing enough energy to meet growing demand and being greener is a key mission within Thailand's ministry of energy responsibility (Alternative Energy Development Plan: AEDP, 2018). Combining large amounts of renewable energy, such as wind and solar, into the power system presents significant operational challenges due to uncertainty. With highly penetrating renewable energy integrated into the power system, the rapidly increasing uncertainty presents many challenges to the operation of power systems. The POPF has become a powerful and indispensable analytical tool to deal with the uncertainty for power system operation.

Electric utilities are looking at a continuous economic operating scenarios and generation scheduling to reduce the generation cost, power transfer constraints, operating security, and reliable constraints. Over the past two decades, the OPF problem has received a lot of attention. Due to its ability to solve problems to find the optimal solution that takes the security into account system and operational requirements. Meanwhile, a classical OPF is a power flow solution. The control variables must be confidently adjusted to support the objective function of minimizing such total system cost, active power losses, and voltage magnitude deviation while satisfying physical and functional constraints to control, dependent variables, and variable functions. So, the classical OPF apart from similar optimization problems, also makes it more difficult to solve.

The classical mathematical programming approach have modified the previous OPF approach, and its capability has been successfully proven. Recently, combining one or more objectives from both categories has been the focus of the task to find the best compromise solutions that meets economic and technical requirements at the same time. Because optimization problems are continuously developed, various methods have been developed to find OPF solutions. Various optimization techniques are used to troubleshoot OPF to determine the best operating conditions for the power system and control variables in the power system. Previously, deterministic methods such as nonlinear programming, Newton-based method, Gradient method, Quadratic Programming method, and the simplex method have been used to solve OPF problems.

With discrete and continuous control variables, even in the absence of discrete control variables, the OPF problem is non-convex due to the existence of the non-linear (AC) power flow equality limits. That's very difficult to get the best solution with a given method. Therefore, the latest intelligent computational tool with random optimization methods has solved the OPF problem. However, due to the high complication of the OPF problem, some studies, therefore, offers approximation models for simplicity, but the best solutions to global OPF problems remain challenging with different formulas and search techniques. In the OPF problems, the objectives typically conflict with each other, making it impossible to optimize each objective at the same time. Almost all real engineering problems have multiple objectives, such as cost reduction, loss reduction, minimizing voltage deviation, etc. This is a difficult but realistic problem, a common approach to multi-objective optimization is to combine each objective functions into an individual composite function or combine an individual objective to the constraint set. In the previous case, determining an individual objective can be achieved using methods such as utility theory, weighted sum method, etc. But the problem lies in choosing the right weight or utility function to determine the preferences of decision-makers. In practice, precise and accurate selection of these weights can be very difficult, for those who are familiar with the extent of the problem. This drawback is that scaling is required between objectives, and sometimes a small perturbation in the weights can lead to very

different solutions. In another case, the problem is that moving an objective to a set of constraints requires defining the constraints for each of these original objectives. This can be quite presuming.

This thesis focuses on POPF methods applied to power systems with uncertain load, photovoltaic power plant (PVPP), and wind power plant (WPP) generations. Therefore, the Monte-Carlo simulation (MCS) is applied to solve the POPF problem. Meanwhile, this thesis introduces the method for solving OPF, with multiple objectives using a fuzzy trade-off concept. The proposed probabilistic fuzzy multi-objective optimal power flow (PFMOOPF) was resolved by particle swarm optimization (PSO) and tested with the modified IEEE 30-bus test system compared to the existing OPF methods.

1.3   Research Objectives

The main objectives of this thesis are as follow,

1) To solve the OPF problem with multi-objective including the total system cost minimization, active power loss minimization, and voltage magnitude deviations minimization.

2) To apply the fuzzy satisfactory function method for multi-objective decision problems.

3) To study the behavior of variables in power systems with integrated WPP and PVPP generators.

4) To solve multi-objective OPF with fuzzy satisfactory function using PSO considering PVPP, WPP, and load uncertainty using probabilistic model and Monte-Carlo simulation.

1.4   Scope and limitations

The PFMOOPF using PSO method is developed for determining the OPF solution with several load flow control variables. The multi-objective OPF can be formulated by stochastic optimization problem. The proposed method will be investigated and compared by IEEE 30-bus test system with four cases, as follow;

1) Develop OPF and test with the modified IEEE 30-bus test system, considering the total system cost minimization

2) Develop OPF and test with the modified IEEE 30-bus test system, considering the active power losses minimization.

3) Develop OPF and test with the modified IEEE 30-bus test system, considering the voltage magnitude deviations minimization.

4) Develop OPF and test with the modified IEEE 30-bus test system, considering the multi-objective minimization in 1), 2), and 3) under fuzzy satisfactory function.

5) The investigation of PVPP, WPP, and load uncertainty using probabilistic density function (PDF) and Monte-Carlo simulation (MCS) for the above MOOPF will be carried out.

6) The simulations result with the modified IEEE 30-bus test system has been as case study including single-objective and multi-objective by MATLAB programming.

1.5   Conception

This thesis's significant contribution is applying the fuzzy concept by PSO for determining OPF solutions in multi-objective problems. The probabilistic fuzzy multi-objective OPF (PFMOOPF) problem is formulated with the optimization problem to minimize the total system cost, the active power losses, and voltage magnitude deviations for optimal several control variables with integrated PVPP, WPP, and load uncertainty. The OPF formulation includes the voltage magnitude at PVPP and WPP buses are considered to control variables. Meanwhile, the output power of PVPP, WPP, and load is based on the probability density function (PDF) of solar irradiance, wind speed, and load demand. However, the simulations result with IEEE 30-bus test system has been a case study including individual objectives and multi-objectives by MATLAB programming. The computational concept can be illustrated in Figure1.1.
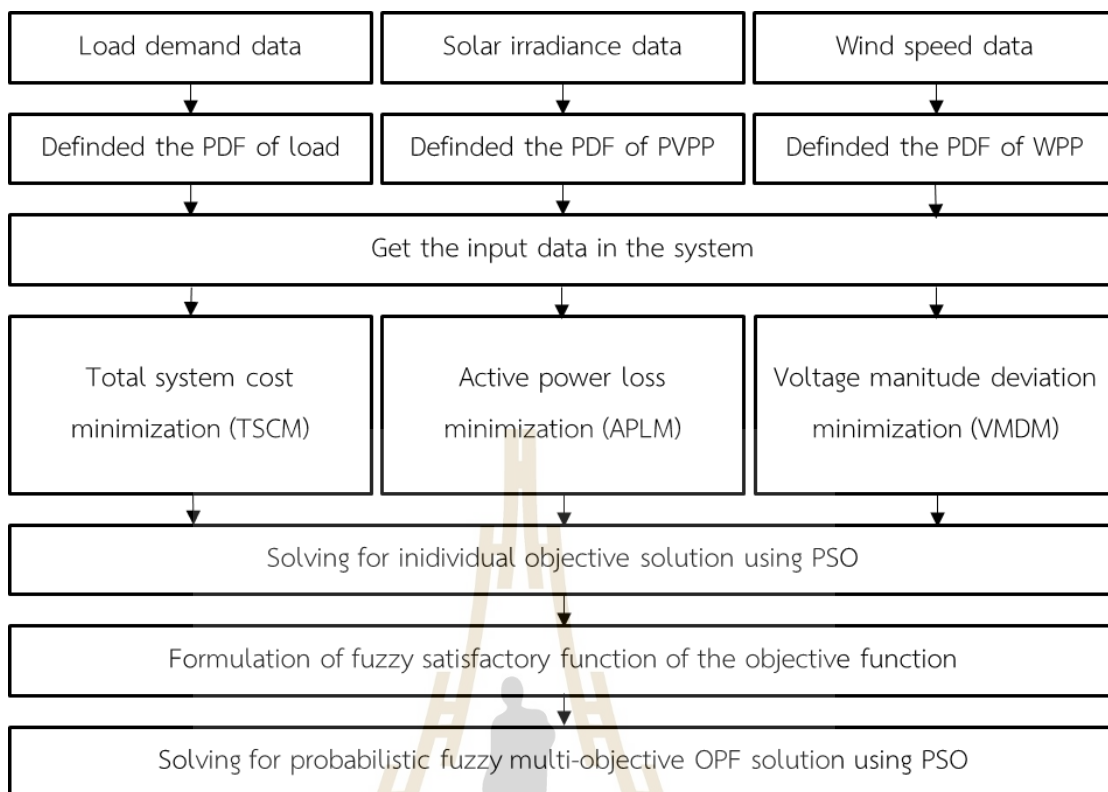
Figure 1.1 The computational concept of the proposed

The organization of this thesis are as follow,

Chapter 1 is the introduction of the thesis. Chapter 2 addresses the literature survey on related works. The OPF solution using PSO is illustrated in Chapter 3. Then, further improved on the proposed OPF solving multi-objective OPF is addressed in Chapter 4. In addition, the uncertainties of load, solar, and wind power generations are incorporated to the proposed method using Monte-Carlo simulation in Chapter 5. Lastly, Chapter 6 conclude this thesis.

1.6   Research Benefits

The PFMOOPF will be able to solve for optimal operation of control variables in the power system. The probabilistic model can handle the uncertainty of power system with integrated WPP, PVPP generation, and load uncertainty. The proposed method is expected in providing positive effects, such as reducing the total system cost, as well as reducing the active power losses and voltage magnitude deviation, under fuzzy satisfactory function concept and PSO.

CHAPTER 2

LITERATURE REVIEW

2.1   Introduction

In the operation and planning of power systems, there are various concerns and studies that need to be developed in optimal power flow (OPF) analysis. Today, the OPF problem is vast and continues to be a growing subject for the global power system research community. Many kinds of research have been proposed by considering the objective of total system cost minimization, active power loss minimization, voltage magnitude deviations minimization, etc. However, the reviews of existing works on OPF are addressed in this chapter, which provides some of the relevant research to compare the result of different methods. The OPF kinds of literature were categorized into different objectives, problem formulations, and optimization tools.

2.2   Literature Overview

Related research in the thesis can be classified into three groups: the individual objective OPF, the multi-objective OPF, and the probabilistic OPF. Each research group classified offers a different approach to problem-solving. However, most of the optimization research involved in the review focuses on the objective of minimizing total system cost, active power loss, and voltage magnitude deviation. This section overview presents an overview of the relevant research in tabular form. Firstly, Table 2.1 shows the kinds of literature on OPF under the individual objective. Table 2.2 presents the literature OPF under the multi-objective. Meanwhile, Table 2.3 shows the literature on Probabilistic OPF. However, a detailed description of the mentioned references contained in the tables in each group can be found in Sections 2.4, 2.5, and 2.6

Table 2.1 The OPF under the individual objective

Year	Author	Objective	Description
1974	O.Alsac and B.Stott	- Minimize total system cost.	- Use Optimal load-flow program. - Tested with the IEEE 30-bus standard load-flow test system. - This proposal expands the scope of problem determination and solution model by incorporating absolute emergency stop constraints.
2002	M.A. Abido	- Minimize total system cost. - Voltage profile improvement. - Voltage stability enhancement.	- Used Particle swarm optimization (PSO). - Tested with IEEE 30-bus test system. - Represented the cost curves of generators by piecewise quadratic function.
2002	A. G. Bakirtzis et al.	- Minimize total operation cost.	- Used Enhanced Genetic Algorithm (EGA). - Tested with IEEE 30-bus test system and the 3-area IEEE RTS96. - Simulating the best and worst operation costs of proposed method by 20 test runs.

Table 2.1 The OPF under the individual objective (Continued)

Year	Author	Objective	Description
2010	A. Bhattacharya et al.	- Minimize the active power losses.	- Used Biogeography Based Optimization (BBO). - Tested with IEEE 30-bus and IEEE 57-bus power system. - Found that optimal solutions BBO method is better than GCA, SOA, L-SaDE, SPSO, CLPSO and PSO.
2013	B. Emre, et al.	- Minimize total system cost. - Minimize system loss.	- Used PSO. - Obtain cost curves considering Valve Point Loading Effect. - Tested on IEEE 14 and 30 buses system with generation PV. - The total system loss values and total generation cost found the proposed hybrid PSO method are lower than literature.

Table 2.1 The OPF under the individual objective (Continued)

Year	Author	Objective	Description
2014	H.R.E.H. Bouchekara	- Minimize total system cost. - Minimize total active transmission losses. - Minimize total reactive transmission losses. - Minimize the deviation of load voltage. - Minimize the index of stability.	- Used Black-hole-based optimization (BHBO). - Tested on IEEE 30-bus test system and Algerian 59-bus network systems. - The proposed solution gives better results than GA, PSO, etc.
2015	R. P. Singh et al.	- Minimize total system cost. - Minimize transmission active power loss. - Minimize total voltage deviation.	- Used PSO with an aging leader and challengers (ALC-PSO). - Tested with the modified IEEE 30-bus test system. - The proposed ALC-PSO provides better quality results compared to other result literature.
2016	H. J.Touma	- Minimize total system cost.	- Used Whale optimization algorithm (WOA). - Tested with IEEE 30-bus test system. - Using B-coefficients data for test system.

Table 2.1 The OPF under the individual objective (Continued)

Year	Author	Objective	Description
2017	D.P. Ladumor et al.	- Minimize total system cost. - Voltage profile improvement. - Minimize active power loss.	- Used Grey Wolf Optimizer algorithms (GWO). - Tested with IEEE 30-bus test system. - Found that the results of proposed method were clear that using SVC gave the best results for all three cases.
2017	U. Khaled et al.	- Minimize total system cost.	- Used PSO. - Tested with IEEE 30-bus test system. - Add renewable energy sources such as wind and PV. - PSO has been suggested to select the optimal hourly load flow with the integration of Renewable Power Distribution (DG) generation.
2018	M. Abdo et al.	- Minimize quadratic fuel cost. - Minimize piecewise quadratic cost. - Minimize quadratic fuel cost considering the valve point effect.	- Used Developed Grey Wolf Optimizer (DGWO). - Tested with IEEE 30-bus test system. - The DGWO is proven compared to conventional GWO and other well-known optimization techniques.

Table 2.1 The OPF under the individual objective (Continued)

Year	Author	Objective	Description
2019	T. T. Nguyen	- Minimize total electricity generation fuel cost. - Minimize total power losses. - Minimize total emission of all generators. - Minimize voltage deviation. - Minimize L index.	- Used Novel Improved Social Spider Optimization Algorithm (NISSO). - Tested with IEEE 30-, 57- and 118- bus system. - The results have advantages over SSO such as simpler application, fewer control parameters, faster convergence with optimized solutions, and more stable search capabilities.
2021	P. Muangkhiew and K. Chayakulkheeree	- Minimize total system cost.	- Used PSO. - Tested on IEEE 30-bus test system. - Found that the result of proposed method is better than deterministic method, EGA method, and GWO method.

Table 2.2 The OPF under the multi-objective

Year	Author	Objective	Description
2010	M. S. Kumari et al.	- Minimize total system cost. - Minimize loss. - Minimize voltage stability index.	- Used Decoupled Quadratic Load Flow (DQLF) solution with EGA. - Tested on IEEE 30-bus test system. - Found that EGA–DQLF with SPEA method showed superiority over PSO–Fuzzy method.
2011	S. Sivasubramani et al.	- Minimize total system cost. - Minimize real power loss. - Minimize voltage stability index (L-index).	- Used Multi-objective harmony search (MOHS). - Tested with IEEE 30-bus test system. - The MOHS method can provide best Pareto solution with better distribution than NSGA-II method with different objectives.
2012	C. Kumar et al.	- Minimize total system cost. - Minimize active power loss. - Minimize multi-objective.	- Used PSO. - Tested with IEEE 14-bus system. - The multi-objective considered fuel cost and active power loss. - Found that optimal solutions PSO method is better than Evolutionary programming (EP).

Table 2.2 The OPF under the multi-objective (Continued)

Year	Author	Objective	Description
2013	M. R. Adaryani et al.	- Minimize total system cost. - Voltage profile improvement. - Voltage stability enhancement. - Minimize total power losses. - Minimize total emission cost.	- Used Artificial bee colony (ABC) algorithm. - Tested with IEEE 9-bus system, IEEE 30-bus test system and IEEE 57-bus system. - That ABC algorithm results in lower fuel cost than those previously reported in the literature.
2015	M. Ghasemi et al.	- Minimize total system cost. - Improvement of voltage profile. - Piecewise quadratic fuel cost functions. - Quadratic cost curve with valve point loadings.	- Used Teaching-learning-based optimization using Lévy mutation operator (LTLBO). - Tested with IEEE 30-bus and IEEE 57-bus system. - Implemented the goal to near global optimal settings of the control variables and their superiority compared to other methods.

Table 2.2 The OPF under the multi-objective (Continued)

Year	Author	Objective	Description
2015	A. A. El-Fergany et al.	- Minimize total fuel cost of generating units. - Minimize total network real power losses. - Minimize total network reactive power losses (series reactance). - Minimize voltage security index.	- Used GWO and differential evolution (DE). - Tested with IEEE 30-bus and 118-bus systems. - Tested to find the best compromise of multi-objective functions by fuzzy Pareto front method.
2017	X. Yuan et al.	- Minimize total system cost. - Minimize emissions.	- Used improved strength Pareto evolutionary algorithm (ISPEA2). - Tested with the IEEE 30-bus and 23 IEEE 57-bus systems. - Found that the ISPEA2 method can produce the best Pareto optimal solutions for the multi-objective OPF problem better than other methods.

Table 2.2 The OPF under the multi-objective (Continued)

Year	Author	Objective	Description
2018	M. A. Taher et al.	- Minimize total system cost. - Minimize gas emission reduction. - Minimize active power loss. - Improve voltage profile. - Voltage stability enhancement.	- Used Moth flame optimization (MFO). - Tested with IEEE 30-, 57-, and 118-bus systems. - The proposed algorithm is based on 15 case studies in terms of different individual and multi-objective functions. - Found that IMFO was able to find a more accurate and better OPF solution compared to other techniques.
2019	Z. Ullah et al.	- Minimize total system cost. - Minimize active power loss. - Minimize load bus voltage deviations.	- Used Phasor PSO and a gravitational search algorithm (hybrid PPSOGSA). - Tested with IEEE 30-bus test system. - Forecast the output power of WT and PV generators based on the real-time measurements. - The multi-objective OPF problem can be solved using a weighted sum method.

Table 2.2 The OPF under the multi-objective (Continued)

Year	Author	Objective	Description
2020	M.A. Ilyas et al.,	- Minimize total system cost. - Minimize real power loss. - Minimize carbon emission.	- Used Paper review using Fuzzy Membership Function (FMF). - Tested with modified IEEE-30 bus system with integration of renewable energy resources. - The constraint satisfaction was achieved using penalty function approach (PFA) and to develop true Pareto front (PF).
2021	M. K. Ahmed et al.	- Minimize active power loss. - Minimize total system cost. - Minimize voltage deviation.	- Used PSO and Genetic algorithms (GA). - Tested on IEEE 30-bus test system. - Used fuzzy set theory to consider multi-objective functions. - The results showed that PSO was much better than GA.

Table 2.2 The OPF under the multi-objective (Continued)

Year	Author	Objective	Description
2021	E. Naderi et al.	- Minimize total generation cost. - Minimize active power transmission losses. - Minimize emission.	- Used Fuzzy adaptive hybrid configuration oriented to a joint self-adaptive PSO and differential evolution algorithms (FAHSPSO-DE). - Tested with IEEE 30-bus, 57-bus, and 118-bus test systems. - Found that the FAHSPSO-DE can handle different scales, multi-objective, and non-convex optimization problem.
2021	A. K. Khamees et al.	- Minimize fuel cost. - Minimize wind generation cost. - Minimize active power losses. - Minimize voltage security index.	- Used Mayfly Algorithm. - Used the fuzzy-based Pareto front technique in multi-objective (MO) optimization. - Study the impact of changes in Weibull parameters, fine cost coefficients and return cost coefficients on wind power generation costs.

Table 2.2 The OPF under the multi-objective (Continued)

Year	Author	Objective	Description
2022	S. Li et al.	- Minimize total system cost. - Minimize active power loss. - Minimize voltage deviation. - Minimize emission.	- Used non-dominated sorting genetic algorithm (NSGA-II). - Used adaptive crossover non-dominated sorting differential evolution (ACNSDE) and Superiority of feasible (SF) - Tested with modified IEEE-30 bus system incorporating renewable energy sources. - Tested with IEEE 57-bus systems to verify the effectiveness of the proposed approach in handling large-scale problems.
2022	P. Muangkhiew and K. Chayakulkheeree	- Minimize total system generation cost. - Minimize active power losses. - Minimize load bus voltage deviations.	- Used F-PSO. - Tested with IEEE 30-bus test system. - A fuzzy satisfactory function is used to solve for the best solution of multi-objective coordinately with PSO.

Table 2.3 Probabilistic OPF

Year	Author	Objective	Description
2007	S. Conti et al.	- Solved load flow problem in distribution networks with solar photovoltaic (PV) distributed generation.	- Used Deterministic load-flow (DLF). - The models are included in a radial distribution probabilistic load flow (PLF) program developed using Monte Carlo techniques. - Comparison between Deterministic Load Flow (DLF) and PLF analyses is also performed.
2008	J. Hetzer et al.	- Minimize total system cost.	- Used Economic dispatch (ED). - Develop a model to integrate the wind power conversion system into the ED problem.
2014	Y. Li et al.	- Considered the relationship of wind speed and load after different distributions.	- Used Probabilistic Optimal Power Flow (POPF). - Tested on IEEE 14-, 118-bus system and an actual utility system in the southwest of China. - Found that the correlations between wind speeds and loads have significant impacts on the outputs of POPF.

Table 2.3 Probabilistic OPF (Continued)

Year	Author	Objective	Description
2014	K. Chayakulkheeree	- The review of different POPF methods.	- Load uncertainty is a normal probability distribution function (PDF) with the concept of using historical total daily or annual load profile. - Proposes the frameworks for more realistic probabilistic modeling of system loads and renewable energy.
2015	H. Zhang et al.	- Minimize the total power loss with carbon emission consideration of the whole power network.	- Used Interior-point algorithm and Monte-Carlo sampling (MCS) method. - Tested with modified IEEE 14-bus system. - Maintain the lowest carbon emissions and the lowest energy loss. - Wind power variation and load variation are considered probabilistic variations.

Table 2.3 Probabilistic OPF (Continued)

Year	Author	Objective	Description
2018	D. Fang et al.	- Minimize root-mean-square (RMSE).	- Used MCS method. - Tested with modified IEEE 14-bus test network. - Uncertainties of wind energy resources (wind speeds, wind directions and power outputs of wind-based generation system). - Uncertainties during the assessment of line dynamic thermal rating (DTR).
2018	U. Chhor et al.	- Minimize total system cost.	- Used Probabilistic optimal power dispatch (POPD) using linear programming (LP). - Solve the power generation dispatch with price-based real-time demand response (PRDR). - The expected short-term load forecast is shown with the probability distribution function.

Table 2.3 Probabilistic OPF (Continued)

Year	Author	Objective	Description
2019	G. Li et al.	- Minimize fuel cost of power generation.	- Tested on IEEE 30-bus test system. - POPF calculation method that considers the relationship between PV output and load.
2019	K. Rojanaworahiran et al.	- Minimize the total cost. - Minimize the total real power loss.	- Used PSO. - Tested with IEEE 30-bus test system and PDF of power system variables. - Consider the probabilistic of load and solar power uncertainties. - This method can be applied to infiltration of high PVPP with unstable load or other variables in emerging power systems.
2020	M.U. Keerio et al.	- Minimize g active power loss. - Minimize voltage deviation.	- Use NSGA-II algorithm. - Tested on IEEE 30-bus test system. - Appropriate probability distribution functions are considered to model them with Monte-Carlo simulation technique for wind and solar power generation.

Table 2.3 Probabilistic OPF (Continued)

Year	Author	Objective	Description
2022	P. Muangkhiew and K. Chayakulkheeree	- Minimize total system cost. - Minimize active power loss. - Minimize voltage magnitude deviation.	- Calculated FMOPF using PSO. - Tested on IEEE 30-bus test system. - Using PDF for load, PVPP, and WPP with MCS.

2.3   OPF under the individual objective

The optimal power flow (OPF) problem is a complex optimization problem, especially considering the limitations of the system. The OPF problem is a non-linear and smooth optimization problem. O.Alsac and B.Stott (1974) previously extended problem definitions and solution schemes by incorporating potential downtime constraints in this approach. To achieve the optimal operating point of the system with stable state security. The controllable system volume in the base case problem is optimized within scope for some defined purposes so as not to violate other volume limits in baseline or emergency system operating conditions

After years of OPF development, M.A. Abido (2002) studied the optimal setting of the OPF problem control variable by a particle swarm optimization (PSO) technique. The PSO method is a derivative-free optimization method for solving the OPF problem. The assumptions set in the objective function are highly optimized. The proposed method has a different objective reflecting the reduction of fuel cost, voltage profile improvement, and voltage stability enhancement. The results of the proposed guidelines have been compared with those reported in the literature recently, tested on IEEE 30-bus standard test systems.

At the same time, A. G. Bakirtzis et al. (2002) presented an optimal current solution (OPF) with both continuous and discrete control variables using an advanced genetic algorithm (EGA). There are the unit active power output and the voltage magnitude of the generator bus as a modeled continuous control variable, while the

transformer tap settings and switchable dividers are the discrete variables. Lastly, there are several operational limitations, such as branch flow, Load bus voltage, and the response capability of the generator. This is included in the penalty in the GA fitness function.

The optimal reactive power flow is an optimization problem with at least one objective of reducing active power loss for a fixed production schedule. The generator bus voltages, transformer tap settings, and reactive power output of the compensating devices placed on various busbars are the control variables in the system. At the same time, Aniruddha B. et al. (2010) presented a solution for optimal reactive energy flow of various types under operational constraints by using the Biogeography-Based Optimization (BBO) technique. BBO searches for the global optimum mainly through two stages: Migration and Mutation. However, BBO are used to solve the problem of optimal reactive power flow for power systems to reduce active power loss tested on IEEE 30-bus and IEEE 57-bus standards.

Belgin Emre et al. (2013) describe OPF with the total system cost function as considered the objective function by using the PSO method to fix the problem. The proposed OPF formula contains detailed generator limits, including power generation limits of active and reactive and test valve point load effects, tested on the standard IEEE 14 and 30 bus test systems. Therefore, the results of this proposed showed that the PSO technique developed within the domain of this study produces results at a lower cost than studies available in the literature.

H.R.E.H. Bouchekara (2014) presented an algorithm. meta-heuristic Inspired by nature to solve the problem of optimal power flow in the electrical system. This algorithm was inspired by the phenomenon of black holes. A black hole is a region of spacetime where gravity is so strong that nothing (no particles or even electromagnetic radiation such as light) can escape from black hole. The developed method namely the black hole-based optimization method shows the effectiveness of the proposed method. It has been tested on the standard IEEE 30-bus test system for various objectives. In addition, to establish the scalability and suitability of the proposed method for large and active power systems. The system was tested on an actual Algeria

59 bus power system. Lastly, the results are compared with other methods reported in the literature.

Rudra Pratap Singh et al. (2015) presented the solution to the power system OPF problem using a combination of PSO with an aging leader and challengers (ALC-PSO). The study was performed on a modified IEEE 30-bus test power system with different objectives reflecting the reduction in fuel cost or active power loss or the total voltage deviation. Later, Haider J.Touma (2016) presented a new strategy to solve the Economic Dispatch problem, the latest meta-heuristic optimization approach called the Whale Optimization Algorithm. The proposed method was validated on an IEEE 30-Bus test system to reduce production costs. Dilip P Ladumor et al. (2017) presented a paper that introduced defined OPF problems equipped with shunt-connected Flexible AC transmission (FACT) device known as Static VAR Compensator (SVC) by a meta-heuristic Grey Wolf Optimizer (GWO) algorithm. There are three objective functions consisting of total system fuel Cost, voltage magnitude deviation, and active power loss considered OPF problems. The proposed methodology applies to standard IEEE 30-bus test systems with and without SVC devices to determine the quality and performance of the proposed approach (GWO).

Extensive loads often cause voltage drop problems in the power system, which can be solved by adding renewable energy sources such as wind power plants and photovoltaic (PV) plants to the busbars. This option can increase the efficiency and reliability of the system while also reducing the generated power cost. So, Usama Khaled et al. (2017) presented an hourly load flow suitable for distributed generation with the consolidation of renewable energy resources using PSO, a modified intelligent technique in the 30-bus IEEE system under different operating conditions. In addition, PV and wind power plants have been used on selected buses to assess their benefits as renewable distributed generation (DG). Meanwhile, the different solar radiation and wind speeds for the Dammam site in Saudi Arabia were used locally to study the potential of the integration of renewable energy resource and their impact on the operation of the electrical system. However, the results of this proposed system prove that the use of renewable energy sources such as DG reduces the overall production and operating costs of the power system.

Next, Mostafa Abdo et al. (2018) presented an effective solution to OPF by an improved version of a gray wolf optimization technique called the Developed Gray Wolf Optimizer (DGWO). While the GWO is an efficient technique but it may tend to stagnate at local optimization in some cases due to insufficient wolf diversity. Therefore, the DGWO algorithm was proposed to improve the searchability of this optimizer. The DGWO is based on improving the survey process using a random mutation to increase the population diversity while an exploitation process is enhanced by improving the position of populations in a spiral path around the best solution. The adaptive operators are used in DGWO to find a balance between the exploration and exploitation step during the iterative process. The objective function of this work is to reduce quadratic fuel cost, reduce piecewise quadratic cost, and reduce quadratic fuel cost considering the effect of valve point.

However, T. T. Nguyen (2019) proposed the NISSO algorithm for solving the OPF solutions to optimize fuel cost in electricity generation, power loss, polluted emission, voltage deviation, and L index tested on three IEEE systems with 30, 57, and 118 buses. At the same time, the NISSO method was developed to improve the quality of the optimal solution and accelerate the convergence of traditional Social Spider (SSO) optimization. As a result, the proposed method has advantages over SSO such as simplification of operation with few control parameters and less time to adjust control parameters.

2.4 OPF under the multiple objective

In recent years, there is an optimization problem associated with more than one objective function where the task of finding one or more optimal solutions is called multi-objective optimization. The different objectives and constraints of the OPF problem are defined as non-linear constrained multi-objective optimization problems considered in a different formula than the original formula. M. S. Kumari et al. (2010) began to define the problem of multi-objective optimization by setting optimal controls for reducing and wasting fuel costs, loss Index and voltage stability fuel cost index and voltage stability, and finally Fuel cost, loss and voltage stability index, tested on an IEEE 30-bus test system. This work combines the new DQLF solution with EGA

to solve OPF problems. Then, the multi-objective evolutionary algorithm proposed with the EGA–DQLF model for OPF solutions sets the Pareto front. Results using EGA–DQLF versus SPEA methods were compared with results obtained using PSO and Fuzzy maximization methods.

S. Sivasubramani et al. (2011) presented a multi-objective harmony search (MOHS) algorithm for the OPF problem. Elite sorting and rejection distances are used quickly to find and manage the most suitable Pareto front end. Lastly, use a fuzzy-based function to select a compromise solution from the Pareto set. This proposed MOHS method was tested on the IEEE 30-bus test system for different objectives, and the simulation results were also compared with the fast non-dominated sorting genetic algorithm (NSGA-II) method. By comparison, it is clear that the proposed method can produce a truly optimal Pareto solution and well distributed for OPF problems. Subsequently, C.Kumar et al. (2012) presented the solution of the OPF using PSO. The main goal of this article is to examine the feasibility of implementing PSO problems, which consist of various objective functions. The proposed PSO technique has been verified and compared with the Evolutionary Programming (EP) method to standard IEEE 14-bus systems. The results showed that the proposed PSO method was able to find a higher quality solution to the OPF problem effectively.

Meanwhile, M. Rezaei Adaryani et al. (2013) presented the artificial bee colony (ABC) algorithm as the primary optimization tool for optimizing the electrical control variables of the OPF problems. The proposed method is a new efficient method for solving the OPF problem in electric power systems. In this work, different objective functions were chosen for this highly restrictive non-convex nonlinear optimization problem, in which different objective functions consist of convex and non-convex fuel costs, total active power loss, voltage profile improvement, voltage stability enhancement, and total emission cost. The absoluteness and effectiveness of the proposed method have been tested with the IEEE 9-bus system, IEEE 30-bus test system, and IEEE 57-bus system and the simulation results show that the proposed ABC algorithm provides the right solutions for all kinds of objective functions.

Mojtaba Ghasemi et al. (2015) examined the feasibility of implementing an evolutionary approach to solving OPF problems using a novel Teaching-Based

Optimization (TLBO) algorithm using a mutation strategy. Lévy variants for optimal setting of OPF problem control variables. The objective functions in these problems are to reduce fuel costs such as quadratic cost function, piecewise quadratic cost function, cost function with valve point effect, and improvement of the voltage profile, tested on IEEE 30-bus and IEEE 57-bus test systems with different objective functions and compared to methods reported in the literature. At the same time, A. A. El-Fergany et al. (2015) used the grey wolf optimizer and DE algorithms to solve individual and multi-objective OPF problems. Both algorithms are used to optimize individual objective functions including fuel cost, real power loss, reactive power loss, and voltage security index. The best compromise of multi-objective functions uses the fuzzy-based Pareto front approach.

X. Yuan et al. (2017) used the Pareto evolutionary algorithm to solve the multi-objective OPF problems. The original SPEA2, ISPEA2, NSGA2, and r-NSGA2 were used to evaluate IEEE 30-bus and IEEE 57-bus systems with respect to reductions in fuel cost and associated emissions. Compared to other algorithms, the simulation results showed that the ISPEA2 was able to find a well-distributed Pareto set and a better solution. In addition, M. A. Taher et al. (2018) proposed an improved moth flame optimization (IMFO) algorithm to effectively solve the problem of OPF. The MFO concept was inspired by the movement of a moth in the direction of the moon. The IMFO was based on the MFO concept, re-spiralizing the moth's path around the flame. Standard IEEE 30-bus, IEEE 57-bus, and IEEE 118-bus test systems are used to verify and prove the performance and durability of IMFO algorithms. The validation of the proposed method is based on 15 case studies in terms of different individual and multi-objective functions, including minimizing fuel cost, minimizing gas emission, active minimizing power loss, voltage profile improvement, and voltage stability enhancement. The results demonstrated the capability and robustness of the IMFO algorithm in solving OPF problems.

Z. Ullah et al. (2019) presented a mixture of phasor particle swarm optimization (PPSO) and a gravitational search algorithm, namely a hybrid PPSOGSA algorithm, for OPF in power systems with an integrated solar photovoltaic (PV) and wind turbine (WT) generators. The WT and PV generator output power forecasts are based on real-time

measurements and the probabilistic models of solar irradiance and wind speed. The proposed OPF guidelines and solutions have been validated in IEEE 30-bus test systems. The statistical characteristics of the OPF results were assessed using the Monte Carlo method.

Meanwhile, M. A. Ilyas et al. (2020) presented that the inclusion of renewable energy resources (RESs) in an electrical network is a center of attention. This proposed OPF problem is considered a multi-constraint, multi-objective optimal power flow (MOOPF) problem along with optimal RESs integration. While, the objectives of MOOPF are three: the total generation cost, active power loss of the system, and reducing carbon emission of thermal sources. In this work, efficient computational techniques are presented to find the most probable values of control variables in power systems with distributed RES. The IEEE-30 bus system was addressed with RES inclusion, and the final optimization issue was resolved using the Particle Group Optimization (PSO) algorithm.

M. K. Ahmed et al. (2021) presented a single-objective and multi-objective (MO) function, where a reduction in real power loss, fuel cost, and voltage deviation is considered the objectives. In this paper, a multi-objective PSO (MOPSO) method is proposed using fuzzy set theory which was tested on the IEEE 30-bus test system. However, the results showed that MOPSO and revised PSO results were much better than GA and MOGA.

E. Naderi et al. (2021) proposed a new fuzzy adaptive hybrid configuration focused on a joint self-adaptive particle swarm optimization (SPSO) and differential evolution algorithms (FAHSPSO-DE), to deal with multi-objective OPF (MOOPF). The objectives with normal differences such as total system cost, active power losses, and emission are selected. To demonstrate the effectiveness and appropriateness of the proposed approach to solving the OPF problem. They will test on IEEE 30-, 57- and 118-bus test systems also used.

Renewable energy sources are gaining increasing attention due to a number of attractive features such as recycling, integrity, and cleanliness. As a result, more and more renewable energy sources are being penetrated into the power grid. A. K. Khamees et al. (2021) studied a new artificial intelligence (AI) method called the Mayfly

Algorithm (MA) and Aquila Optimizer (AO) to calculate the Weibull distribution parameters. Two AI methods have proven superior and robust for evaluating the two-parameter Weibull distribution as they provide lower error and higher correlation coefficients. Then, individual and multi-objective stochastic optimal power flow (SCOPF) is applied to modified IEEE-30 with two wind farms to reduce total system cost, active power loss, thermal unit emission, and voltage security index (VSI). They use the fuzzy Pareto front technique of multi-objective optimization (MOO) to achieve the best compromise solution.

In addition, S. Li et al. (2022) proposed a modified IEEE 30-bus test system that integrates renewable energy sources as the case study. Meanwhile, the available solar power is used the lognormal probability density function (PDF) to calculate and the available wind power is used the Weibull probability density function to calculate. The optimal power flow with random wind and solar energy is formulated as a multi-objective optimization problem, in which four optimization objectives including total system cost, active power loss, voltage magnitude deviation, and emission, are considered. In addition, to verify the effectiveness of the proposed approach to addressing large-scale problems, another larger test system, such as the IEEE 57 bus system, was selected.

2.5 Probabilistic OPF

With greater uncertainty and variability in smart grids' configurable load flow, It is used to analyze daily working conditions and plan electrical systems for future investments. The problem cannot be solved by considering intermittent power generation and load variation. S. Conti et al. (2007) addressed the LF problem in photovoltaic (PV) DG distribution networks. This model was included in a radial distributed probabilistic load flow (PLF) program developed using Monte Carlo techniques. Meanwhile, a comparison is made between Deterministic Load Flow (DLF) and PLF analyses are also performed. A year later, J. Hetzer et al. (2008) proposed a solution to the electrical power system economic dispatch (ED) by continually searching for alternatives to conventional energy sources, the need to include a wind

power generator (WECS). The uncertain nature of the wind speed is illustrated by the Weibull PDF.

Y. Li et al. (2014) presented a probabilistic optimal power flow (POPF) technique based on the relationship of wind speed correlations after arbitrary probability distributions based on the point estimation method (PEM). The results showed that the relationship between wind speed and wind speed and load had a significant impact on POPF results. At the same time, Keerati Chayakulkheeree (2014) discussed the advantages of probabilistic optimal power flow (POPF) in the analysis of modern power systems, including the frameworks for probabilistic models for system loading and renewable power, which is the behavior of solar and wind energy. An examination of the practical load profiles and behavior of photovoltaic plants is discussed as an illustration. The POPF is one of the interesting tools that provide effective uncertainty management in power system analysis.

Haotian Zhang (2015) presented a probabilistic optimal power flow (POPF) considering probabilistic load and solar power instability. In defining the proposed POPF problem formulations, minimization of the total cost (TCMS) and the minimization of total real power loss (TLMS) are solved by PSO, respectively. In the POPF model, the probabilistic of photovoltaic power plant (PVPP) and load data are combined with the POPF calculation.

Then, Duo Fang (2018) looked at the assessment of uncertainties due to significantly increased penetration levels of unpredictable renewable energy sources, which is illustrated by the example of an actual UK wind farm (WF) and the use of dynamic thermal rating (DTR), instead of static heat rating. The analysis presented shows that there is a complex relationship between the line DTRs and WF power outputs, as both are greatly affected by variations in wind speeds and wind directions. This associated volatility and related uncertainties were modeled using the appropriate PDF and CDF analysis formulas, and then combined with the probabilistic optimal power flow (POPF) analysis, allowing for a more accurate assessment of the risk of cable overload.

At the same moment, Udoum Chhor (2018) presented a probabilistic optimal power dispatch (POPD) using linear programming (LP) for solving the power generation dispatch with price-based real-time demand response (PRDR). The expected short-term

load forecast is represented by a probabilistic distribution function, clearly showing that the proposed method can handle a POPD solution for the actual power distribution based on PRDR using the probable truncated normal distribution (PTNF) function.

Years later, Guoqing Li (2019) proposed presented the influence of uncertainty and the relationship between solar photovoltaic (PV) power output and load on the operating state of the power system. This article is a probabilistic optimal power flow (POPF) calculation method based on the propagation kernel density estimate. Firstly, according to the distribution characteristics of the solar PV output, an adaptive diffusion kernel density estimation of the PV output is modeled, which can transform the kernel function into a linear diffusion process to achieve a modulation of the approximation bandwidth of the nuclear density estimation. Second, the Kendall rank correlation coefficient and the minimum Euclidean distance were used as correlation measures and suitability index of fitting to select the optimal Copula function, and the joint probability distribution model of PV output and load is constructed. Finally, simulation studies will be conducted with the measured data of a Chinese solar PV and the IEEE 30-bus power system. The results showed that considering the relationship between solar PV output and load, it was possible to improve the accuracy of POPF calculation and effectively reduce the total system cost of the power system by using a genetic algorithm (GA). That same year, Kanatip Rojanaworahiran (2019) presented a probabilistic optimal power flow (POPF) based on probabilistic load and solar power uncertainties. In the proposed POPF problem determination, total cost reduction (TCMS) and total real power loss reduction (TLMS) will be solved by PSO respectively. The POPF model, probabilistic solar photovoltaic (PVPP), and load data were combined with POPF calculations tested on an IEEE 30-bus test system and the electrical system variable's probability density function (PDF) was a machine. real generator total loss and have reviewed all expenses.

The POPF model, probabilistic photovoltaic (PVPP), and load data were combined with POPF calculations tested on an IEEE 30-bus test system and the electrical system variable probability density function (PDF) as a machine. active generator total loss and have reviewed all expenses.

CHAPTER 3

OPF CONSIDERING FULL CONTROL VARIABLES[1]

3.1 Introduction

The OPF problem determines the power output of each online generator. The main objective of the OPF problem is to reduce the total system cost (TSC) of the considered power system, which can be achieved by adjusting the output power of all generators connected to the considered electric system. From section 2.3, numerous research has been aimed at minimizing the total system cost for the power system. Total system cost minimization (TSCM) is a key factor for economic performance that benefits both electricity buyers and consumers. Thus, the TSCM for the power system is achieved based on several parameters, one of which is generator allocation.

This chapter presents a particle swarm optimization (PSO) for the determining of OPF solution based on full control variables. The proposed PSO-based OPF (PSO-OPF) problem is defined with the intent of TSCM. The active power generation, generator voltage magnitudes, transformer tap changing, and capacitive reactance optimization are obtained simultaneously. This is a result of the proposed method, tested on the IEEE 30-bus test system. Finally, comparative results of the IEEE 30-bus test system of the proposed method and other available methods are shown and discussed.

3.2 Problem formulation

The OPF problem is known as economic dispatch (ED) considering operating control variables and security constraints. It optimizes the control variable settings in terms of the objective function while satisfying various equality and inequality limit constraints. Thus, the objective function of this chapter is to reduce the overall cost

---

[1] Part of this work was presented at the " 9th International Electrical Engineering Congress (iEECON2021)", Thailand, 2021. (Best Paper Award in Power System Session)

of generating electricity under constraints. Mathematically, the OPF problem can be defined as:

$$\text{Minimize} \quad OB_i(\mathbf{x}, \mathbf{u}) + PNF \tag{3.1}$$

$$\text{Subject to:} \quad \mathbf{g}(\mathbf{x}, \mathbf{u}) = 0 \tag{3.2}$$

$$\mathbf{h}(\mathbf{x}, \mathbf{u}) \le 0 \tag{3.3}$$

In the above equations, OB_i represents the set of objective functions to be minimized. Meanwhile, $\mathbf{g}$ and $\mathbf{h}$, in Equations 3.2 and 3.3, are the sets of necessary equality and inequality constraints, where $\mathbf{x}$ is the vector of dependent variables including:

1. Active power generation of slack bus (P_{G1}).
2. Voltages at load bus (V_L)
3. Reactive power output generation (Q_G)
4. Transmission line flow (S_l).

So, $\mathbf{x}$ can be expressed as:

$$\mathbf{x}^T = [P_{G1}, V_{L1}...V_{LNL}, Q_{G1}...Q_{GNG}, S_{l1}...S_{lNTL}]. \tag{3.4}$$

So, $\mathbf{u}$ can be expressed as:

$$\mathbf{u}^T = [\mathbf{P_G}, |\mathbf{V_G}|, \mathbf{T}, \mathbf{X_C}]. \tag{3.5}$$

Where $\mathbf{u}$ is the control variable vectors, consisting of,

1. Active power output generation (P_G) excluding at the slack bus (P_{G1}).
2. Voltage magnitude at generator bus (V_G).
3. Transformer tap setting (T).
4. Capacitive Reactance (X_C).

$$\mathbf{P_G} = [P_{G2}, P_{G3}, ..., P_{GNG}]_{1 \times (NG-1)} \quad , \tag{3.6}$$

$$|\mathbf{V_G}| = [|V_{G1}|, |V_{G2}|, ..., |V_{GNG}|]_{1 \times NG} \quad , \tag{3.7}$$

$$\mathbf{T} = [T_1, ..., T_{NT}]_{1 \times NT} \quad , \tag{3.8}$$

$$\mathbf{X_C} = [X_{C1}, ..., X_{CNC}]_{1 \times NC} \quad . \tag{3.9}$$

3.3 Objective function: Total system generation cost minimization (TSCM)

In this simulation process of the OPF problem, the objective function is to reduce the total cost of electric power to meet demand and stay within the limitations listed below:

$$\min_u OB_1(\mathbf{x}, \mathbf{u}) = \min_u TSC(\mathbf{x}, \mathbf{u}) + PNF \tag{3.10}$$

where,

$$TSC(\mathbf{x}, \mathbf{u}) = \sum_{i=1}^{NG} (a_i + b_i P_{Gi} + c_i P_{Gi}^2) \tag{3.11}$$

3.4 Constraints

Optimization constraints are as follows:

3.4.1 Equality constraints

In Equation 3.2, **g** is the equality limit constraints, which represent typical load flow equations:

$$P_{Gi} - P_{Di} - V_i \sum_{j=1}^{NB} V_j \left[G_{ij} \cos \delta_{ij} + B_{ij} \sin \delta_{ij} \right] = 0 \tag{3.12}$$

$$Q_{Gi} - Q_{Di} - V_i \sum_{j=1}^{NB} V_j \left[G_{ij} \sin \delta_{ij} - B_{ij} \cos \delta_{ij} \right] = 0 \tag{3.13}$$

Where, i = 1,2,...,NB.

3.4.2 Inequality constraints

The matrix **h** is the inequality limit constrains that included:

- Generator's voltage magnitude limit constraints,

$$|V_i|^L \leq |V_i| \leq |V_i|^U \qquad , i=1,\ldots,NG, \qquad (3.14)$$

- Generator's active power output limit constraints,

$$P_{Gi}^L \leq P_{Gi} \leq P_{Gi}^U \qquad , i=1,\ldots,NG, \qquad (3.15)$$

- Generator's reactive power output limit constraints,

$$Q_{Gi}^L \leq Q_{Gi} \leq Q_{Gi}^U \qquad , i=1,\ldots,NG, \qquad (3.16)$$

- Transformer tap changing limit constraints,

$$T_i^L \leq T_i \leq T_i^U \qquad , i=1,\ldots,NT, \qquad (3.17)$$

- Shunt capacitor limit constraints,

$$Q_{ci}^L \leq Q_{ci} \leq Q_{ci}^U \qquad , i=1,\ldots,NC, \qquad (3.18)$$

- Bus voltage magnitude limit constraints,

$$|V_{Li}|^L \leq |V_{Li}| \leq |V_{Li}|^U \qquad , i=1,\ldots,NPQ, \qquad (3.19)$$

- Line flow limit constraints,

$$|MVA_{Li}| \leq MVA_{Li}^U \qquad , i=1,\ldots,NL. \qquad (3.20)$$

3.5 The OPF Using PSO

Particle Swarm Optimization (PSO) was presented by Kennedy and Eberhart in 1995. The PSO solution is a random search optimization method with the concept that "the populations are defined as swarms, and the possible solutions are the particles". The system is initialized with a stochastic population of solutions and particles are updated in the subsequent releases (iterations). Every time (iteration), each particle will be updated with the best values. Meanwhile, the best value in each iteration is called 'pbest'. And if the value is better than the 'pbest' of the current iteration, the

'pbest' value is replaced and each particle that knows the best value in the group called 'gbest' among 'pbest'. PSO is more computationally efficient in terms of velocities and records the best position ever.

In this section, the population set is defined as Equation (3.21). The particles modify their velocity and current position according to equations (3.22) and (3.23), respectively.

$$\mathbf{p_i} = [\mathbf{P_{Gi}}, \; |\mathbf{V_{Gi}}|, \; \mathbf{T_i}, \; \mathbf{X_{Ci}}]. \tag{3.21}$$

$$v_m^{t+1} = wv_m^t + c_1 r_1 (pbest_m^t - \mathbf{p}_i^t) + c_2 r_2 (gbest^t - \mathbf{p}_m^t) . \tag{3.22}$$

$$\mathbf{p}_m^{t+1} = \mathbf{p}_m^t + v_m^{t+1} . \tag{3.23}$$

The standard parameters of PSO are used for the investigation of this work. A w decreases from 0.9 at the first iteration to 0.4 at the maximum iteration, and c_1 and c_2 are 2.00. The computational procedure of the TSCM can be described in the following step:

Step 1: Obtain power flow input data set.

Step 2: Specify the control variables, dependent variables, and security limits.

Step 3: Formulate the PSO population by Equation (3.21).

Step 4: Run power flow for all populations and compute the objective value by Equations (3.12) and (3.13).

Step 5: Check constraint violations for the population. If the constraint is not violated, go to step 7, otherwise, proceed to step 6.

Step 6: Add the penalty factor to the objective function for population m.

Step 7: Compute TSC by Equation (3.11).

Step 8: Get $pbest_m^t$ and $gbest^t$ of PSO.

Step 9: Determine the velocity of particle m and update the particle's position.

Step 10: Check maximum iteration. If the iteration reaches maximum iteration, go to step 11, otherwise, go to step 4.

Step 11: Obtain the output.

3.6   Simulation Results

The proposed OPF using PSO was validated by IEEE 30-bus test system as shown in Figure 3.1 and the modified IEEE 30-bus test system with additional capacitors connected to bus numbers 12, 15, 17,20, 21, 23, and 29, as shown in Figure 3.2.

The IEEE 30-bus test system data, including network information, generation and load information are given in (O. Alsac, B. Stott., 1974) and control variables including their limits from (A. G. Bakirtzis et al., 2002). The study cases are presented using MATLAB software. The goal of this section is the total system cost.
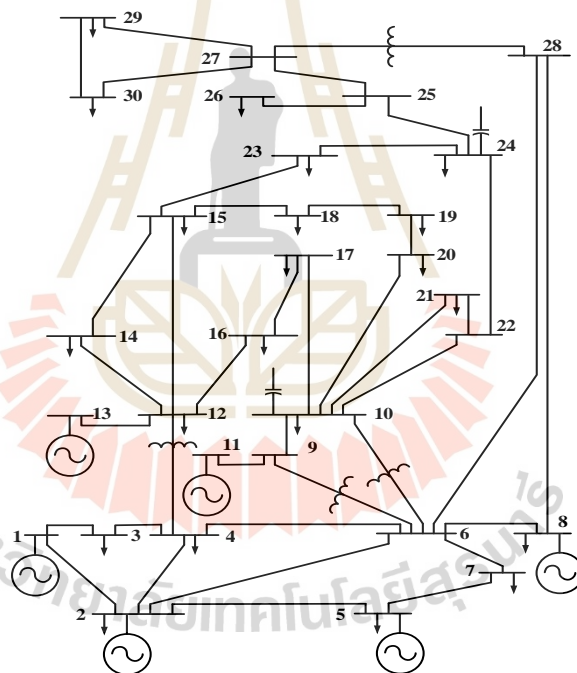
Figure 3.1 The IEEE 30-bus test system
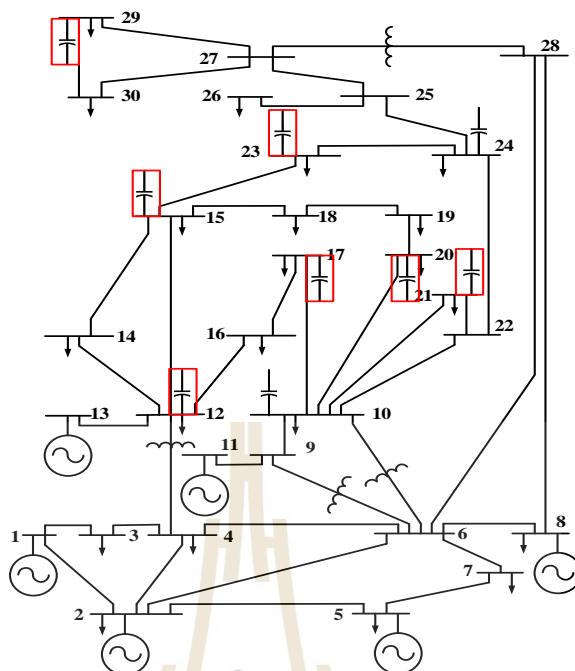
Figure 3.2 The modified IEEE 30-bus test system

This section contains two case studies, consisting of Case I: The base case with IEEE 30-bus test system and Case II: Further capacitors connected with modified IEEE 30-bus test system. For the base case and further capacitors of the base case, the control variables are as shown in Table 3.1.

Table 3.1   The control variables of standard case

Control Variables	Base Case		Further capacitors of the base case	
	Number	At bus number	Number	At bus number
Active power generations	5	2, 5, 8, 11, 13	5	2, 5, 8, 11, 13
Generators' voltage magnitudes	6	1 (slack), 2, 5, 8, 11, 13	6	1 (slack), 2, 5, 8, 11, 13
Transformer tap-changes	4	6-9, 6-10, 4-12, 27-28	4	6-9, 6-10, 4-12, 27-28
Capacitive reactance	2	10, 24	9	10, 12, 15, 17, 20, 21, 23, 24, 29.

3.6.1 Case I: Simulation Results with the Base Case of IEEE 30-Bus Test System

This case study investigates the performance of the proposed PSO-based OPF by comparing it to the widely-used standard case (O. Alsac, B. Stott., 1974), which is the model shown in Figure 3.1. The TSC is compared deterministic method (O. Alsac, B. Stott., 1974) provided in Table 3.2.

In Table 3.2, the Capacitors are connected only to buses 10 and 24. The results show that the total system cost proposed PSO is 799.551 ($/h), which is lower than that of the conventional deterministic method.

Table 3.3 illustrates the base case simulation results from 30 trials of the proposed method. Meanwhile, the minimum and maximum values of TSC received from PSO are 799.551 $/h. and 800.479 $/h., respectively. The average and standard deviation of TSC from 30 trials are 799.643 $/h and 0.195, respectively. Then, the behavior convergence plot of the proposed base case is shown in Figure 3.3., and the plot of 30 trial solutions is also shown in Figure 3.4.

Table 3.2 Comparison results of the IEEE 30-bus test system for TSCM

Control Variables	Deterministic method	Proposed method
Power Generation (P_{Gi}) at Bus (MW)		
2	48.84	48.66
5	21.51	21.30
8	22.15	21.05
11	12.14	11.84
13	12.00	12.00
Generator Voltage ($|V_i|$) Magnitude at Bus (p.u.)		
1	1.05	1.10
2	1.04	1.09
5	1.01	1.06
8	1.02	1.07
11	1.09	1.09
13	1.09	1.08
Transformer Tap-Changing (T_{i-j}) between Buses		
6-9	1.00	1.10
6-10	0.96	0.93
4-12	1.00	1.05
28-27	0.94	1.03
Capacitive Reactance (X_{Ci}) at Bus (p.u.)		
10	-5.26	-44.46
24	-25.00	-9.64
TSC ($/h.)	802.400	**799.551**

Table 3.3 The best, worst, average, and standard deviation of TSC from the Base case 30 trial solutions

	The proposed PSO			
	Best	Worst	Average	S.D.
TSC ($/h)	799.551	800.479	799.643	0.195
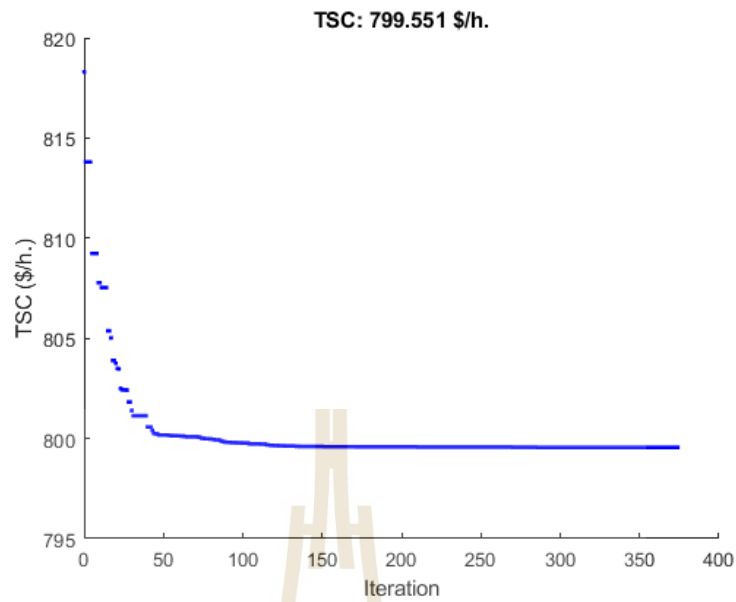
Figure 3.3 The convergence plot of the proposed method for base case
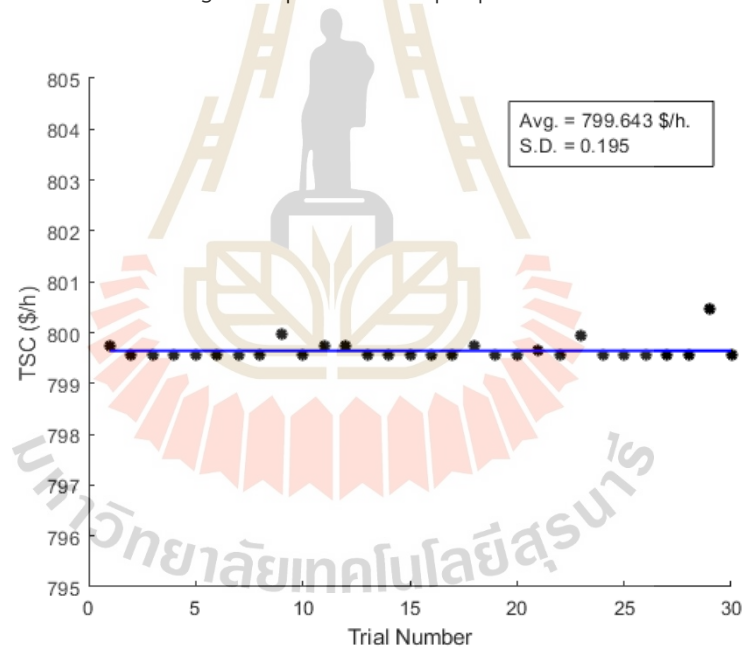
Figure 3.4 The solution with 30 trials of the proposed method run for base case

3.6.2 Case II: Simulation Results of the modified IEEE 30-Bus Test System

In this case, the modified IEEE 30-bus test system with further capacitors is tested by the proposed method and compared with the EGA method (A. G. Bakirtzis et al., 2002), BHBO method (H.R.E.H. Bouchekara, 2014), and EGA-DQLF method (M. S. Kumari et al., 2010), which the model showed in Figure 3.2. Meanwhile, the control variables are shown in Table 3.1. The comparison results with the modified IEEE 30-

bus test system of EGA, BHBO, EGA-DQLF, and the proposed method are given in Table 3.4. The TSC should be lower than Case I because it has more capacitors control variables. Similarly, the proposed PSO of Case II yielded the lowest TSC result of 799.385 $/h, compared to the EGA method, BHBO method, and EGA-DQLF method. Meanwhile, the behavior convergence plot of the proposed PSO for Case II is shown in Figure 3.5. From the results, it can be seen that the proposed method can successfully reduce the TSC considering all load flow variables in the power system.

Table 3.5 illustrates the base case simulation results from 30 trials of the proposed method. The best and worst values of TSC received from PSO are 799.385 $/h. and 800.025 $/h., respectively. The average and standard deviation of TSC from 30 trials are 799.445 $/h and 0.121, respectively. Meanwhile, the convergence plot of the proposed base case is shown in Figure 3.5., and the plot of 30 trial solutions is also shown in Figure 3.6.
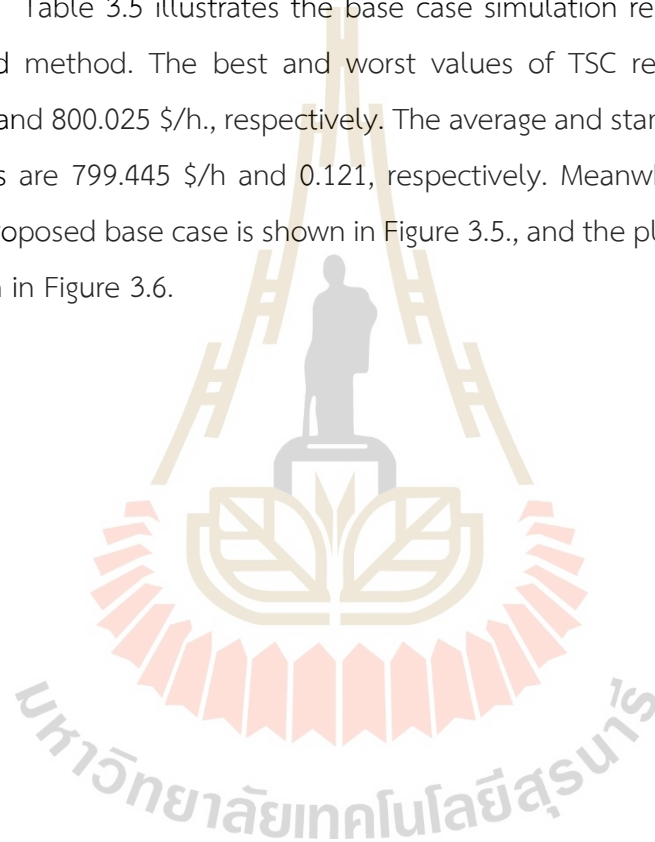
Table 3.4   Comparison results of the modified IEEE 30-bus test system for TSCM

Control Variables	EGA	BHBO	EGA-DQLF	Proposed method
Power Generation (P_{Gi}) at Bus (MW)				
2	48.75	48.35	48.11	48.69
5	21.44	21.53	21.28	21.30
8	21.95	20.02	20.93	21.13
11	12.42	13.42	12.50	11.95
13	12.02	13.41	12.00	12.00
Generator Voltage ($|V_i|$) Magnitude at Bus (p.u.)				
1	1.05	1.10	1.10	1.10
2	1.04	1.08	1.08	1.09
5	1.01	1.05	1.05	1.06
8	1.01	1.06	1.06	1.07
11	1.08	1.08	1.10	1.05
13	1.07	1.07	1.09	1.01
Transformer Tap-Changing ($T_{i\text{-}j}$) between Buses				
6-9	1.01	1.02	0.95	1.03
6-10	0.95	1.00	1.04	1.07
4-12	1.00	1.03	1.00	1.05
28-27	0.96	1.00	0.98	1.04
Capacitive Reactance (X_{Ci}) at Bus (p.u.)				
10	-20.00	-33.23	-25.00	-15.16
12	-20.00	-33.69	-50.00	-2.39
15	-33.33	-28.94	-20.00	-33.08
17	-20.00	-28.16	-20.00	-15.25
20	-20.00	-40.84	-50.00	-45.00
21	-20.00	-36.03	-25.00	-9.08
23	-25.00	-35.74	-25.00	-44.92
24	-20.00	-29.52	-33.33	-14.47
29	-33.33	-37.21	-100.00	-44.97
TSC($/h.)	802.060	799.922	799.560	**799.385**

Table 3.5 The best, worst, average, and standard deviation of TSC from 30 trial solutions

	The proposed PSO			
	Best	Worst	Average	S.D.
TSC ($/h)	799.385	800.025	799.445	0.121
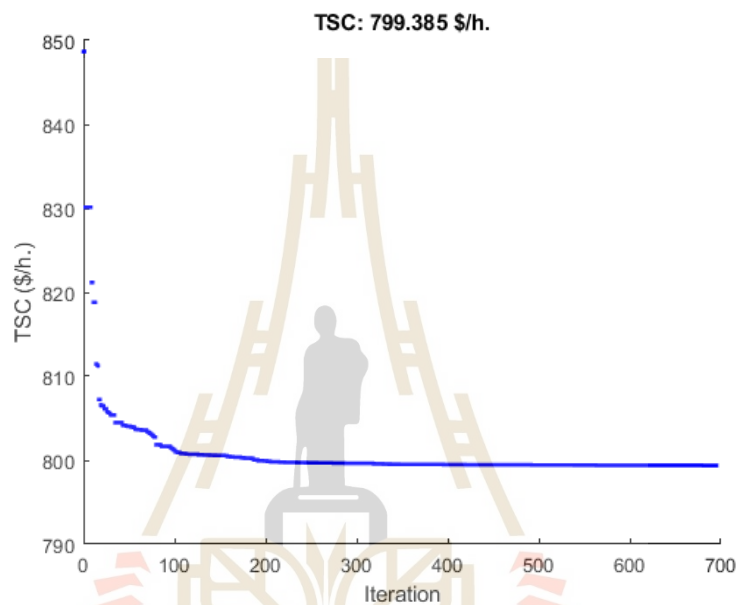
Figure 3.5 The convergence plot of the proposed method of TSCM
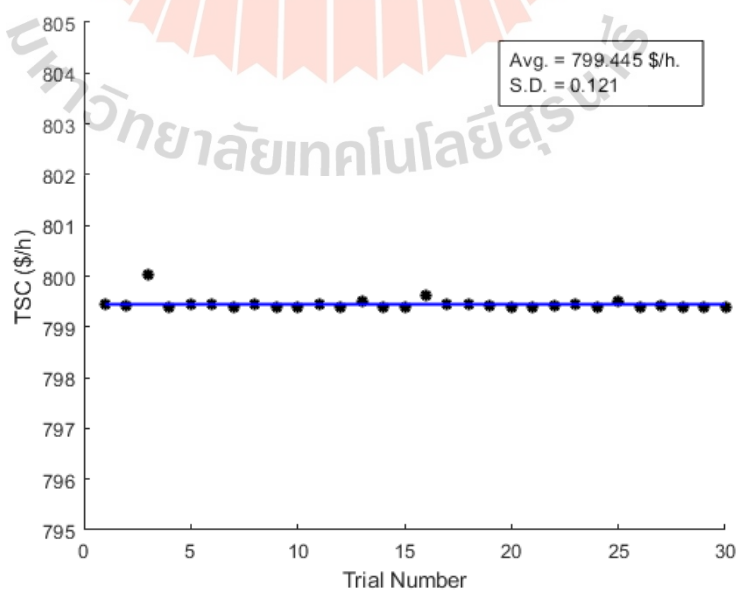
Figure 3.6 The solution with 30 trials of the proposed method run of TSCM

CHAPTER 4

FUZZY MULTI-OBJECTIVE OPF[2]

4.1   Introduction

With the different objectives of operating an electrical system, the OPF can be defined as a multi-objective security constraint optimization problem. The multi-objective (MO) optimization is an important part of optimization activities. Whereas the multi-objective OPF (MOOPF) has been proposed in several kinds of research literature in section 2.4, most of the research is on minimizing total system cost (TSC), active power loss (APL), and voltage deviation (VMD) considering each objective simultaneously.

This section presents the problem of determining the optimal control variable for the purpose, which consists of reducing TSC, APL, and VMD. Meanwhile, the proposed provides three objective functions that are optimized individually and MO at the same time, subjected to several equality limits constraints. Therefore, the proposed fuzzy-MOOPF (FMOOPF) uses the PSO method tested on the modified IEEE 30-bus test system. Lastly, the comparison results with the IEEE 30-bus test system of the proposed method and the kinds of literature are addressed.

4.2   Problem formulation

Mathematically, the OPF problem can be formulated as Equations (4.1), (4.2), and (4.3). Whereas, the dependent variables vector (**x**) can be expressed as Equation (4.4) and the control variables vector (**u**) can be expressed as Equation (4.5). Mathematically, the OPF problem can be defined as:

$$\text{Minimize} \qquad OB_i(\mathbf{x}, \mathbf{u}) + PNF \qquad\qquad (4.1)$$

Subject to: $\boldsymbol{g}(\mathrm{x},\mathrm{u})=0$ (4.2)

$\boldsymbol{h}(\mathrm{x},\mathrm{u})\leq 0$ (4.3)

In the above equations, OB_i represents the set of objective functions to be minimized. Where **x** is the vector of dependent variables including:

1. Active power generation of slack bus (P_{G1}).

2. Voltages at load bus (V_L)

3. Reactive power output generation (Q_G)

4. Transmission line flow (S_l).

So, **x** can be expressed as:

$$\mathbf{x}^T = [P_{G1}, V_{L1}...V_{LNL}, Q_{G1}...Q_{GNG}, S_{l1}...S_{lNTL}].$$ (4.4)

So, **u** can be expressed as:

$$\mathbf{u}^T = [\mathbf{P_G}, |\mathbf{V_G}|, \mathbf{T}, \mathbf{X_C}].$$ (4.5)

Where **u** is the control variable vectors, consisting of,

1. Active power output generation (P_G) excluding at the slack bus (P_{G1}).

2. Voltage magnitude at generator bus (V_G).

3. Transformer tap setting (T).

4. SVCs Reactance values (X_C).

$$\mathbf{P_G} = [P_{G2}, P_{G3}, ..., P_{GNG}]_{1\times(NG-1)} \ ,$$ (4.6)

$$|\mathbf{V_G}| = [|V_{G1}|, |V_{G2}|, ..., |V_{GNG}|]_{1\times NG} \ ,$$ (4.7)

$$\mathbf{T} = [T_1, ..., T_{NT}]_{1\times NT} \ ,$$ (4.8)

$$\mathbf{X_C} = [X_{C1}, ..., X_{CNC}]_{1\times NC} \ .$$ (4.9)

4.3   Objective function

4.3.1   Total system generation cost minimization (TSCM)

This cost depends on the actual amount of power produced by the generator. The generator cost is regarded as a quadratic function, therefore the TSCM of all generators in the system can be considered as Equations (4.10) and (4.11).

$$\min_u OB_1(\mathbf{x},\mathbf{u}) = \min_u TSC(\mathbf{x},\mathbf{u}) + PNF \tag{4.10}$$

where,

$$TSC(\mathbf{x},\mathbf{u}) = \sum_{i=1}^{NG}(a_i + b_i P_{Gi} + c_i P_{Gi}^2) \tag{4.11}$$

4.3.2   Active power loss minimization (APLM)

The transmission power network consists of a large number of wires with high transmission power, which leads to high active power losses and high-power losses. Losses are an important parameter in determining the effect of active energy losses. This will reduce power transfer efficiency and deteriorate the voltage profile. The actual reduction of power loss in the distribution network is therefore very important compared to the transmission system. Therefore, the active power loss (APL) in the transmission line must be reduced by the expression below.

$$\min_u OB_2(\mathbf{x},\mathbf{u}) = \min_u APL(\mathbf{x},\mathbf{u}) + PNF \tag{4.12}$$

where,

$$APL(\mathbf{x},\mathbf{u}) = \sum_{L=1}^{NTL} g_{L,ij}\left[V_i^2 + V_j^2 - 2V_i V_j \cos\theta_{ij} \right]. \tag{4.13}$$

4.3.3   Voltage magnitude deviation minimization (VMDM)

The voltage at the load of the bus is the most important value that contribute greatly to the stable and economical operation of the transmission power network. Therefore, the voltage magnitude deviation (VMD) between the operating and the reference voltage should be taken into account in the OPF problem, and the goal of reducing the VMD can be formulated as:

$$\min_{u} OB_3(\mathbf{x},\mathbf{u}) = \min_{u} VMD(\mathbf{x},\mathbf{u}) + PNF \tag{4.14}$$

where,

$$VMD(\mathbf{x},\mathbf{u}) = \sum_{i=1}^{NL} \left| V_i - V_i^{ref} \right|. \tag{4.15}$$

V_i^{ref} is generally considered as 1 p.u.

4.3.4 Fuzzy Multi-Objective OPF Formulation

In this section, the fuzzy satisfactory function (FSF) is used to solve multi-objective OPF (MOOPF), namely FMOOPF. On account of the FMOOPF method defines fuzzy satisfaction for individual objectives (H. J. Zimmermann, 1987). The proposed method with three objectives is solved by a fuzzy satisfaction method, where the fuzzy satisfaction method is the choice of all feasible solutions. Rather than incorporating the objectives into one objective by a simple sum or weight factor. The FMOOPF problem is concurrently resolved for the optimal solution of TSCM, APLM, and VMDM, based on an FSF. In this way, the FMOOPF can be solved by compromising all objectives. The FSF values λ for individual objective functions consisting of TSCM, APLM, and VMDM are computed and defined as (4.16), (4.17), and (4.18), respectively. Meanwhile, the objective functions in Equations (4.16) to (4.18) are used for FSF as shown in Figures 4.1 to 4.3.

This process determines the FSF associated with each objective, and the best value for each objective is obtained by optimizing each objective. From Figures 4.1 to 4.3, the FSF can take any value in [0,1]. An FSF value of 1 is assigned to the minimum value for each objective. When another objective states that the objective value is greater than the minimum, the FSF is reduced to zero. Lastly, a MOOPF can be defined as a fuzzy maximization problem as in Equation 4.19.

$$\lambda_{TSC} = \begin{cases} 1 & ,\text{for } TSC \le TSC_{\min} \\ \dfrac{-1}{TSC_{\max} - TSC_{\min}} \cdot TSC + \dfrac{TSC_{\max}}{TSC_{\max} - TSC_{\min}} & ,\text{for } TSC_{\min} \le TSC < TSC_{\max} \\ 0 & ,\text{for } TSC \ge TSC_{\max} \end{cases} \tag{4.16}$$

$$\lambda_{APL} = \begin{cases} 1 & ,\text{for } RPL \le RPL_{\min} \\ \dfrac{-1}{APL_{\max} - APL_{\min}} \cdot APL + \dfrac{APL_{\max}}{APL_{\max} - APL_{\min}} & ,\text{for } APL_{\min} \le APL < APL_{\max} \\ 0 & ,\text{for } APL \ge APL_{\max} \end{cases} \qquad (4.17)$$

$$\lambda_{VMD} = \begin{cases} 1 & ,\text{for } VMD \le VMD_{\min} \\ \dfrac{-1}{VMD_{\max} - VMD_{\min}} \cdot VMD + \dfrac{VMD_{\max}}{VMD_{\max} - VMD_{\min}} & ,\text{for } VMD_{\min} \le VMD < VMD_{\max} \\ 0 & ,\text{for } VMD \ge VMD_{\max} \end{cases} \qquad (4.18)$$

$$\text{Maximize} \quad \lambda_T = \min\{\lambda_{TSC}, \lambda_{APL}, \lambda_{VMD}\} + PNF \qquad (4.19)$$
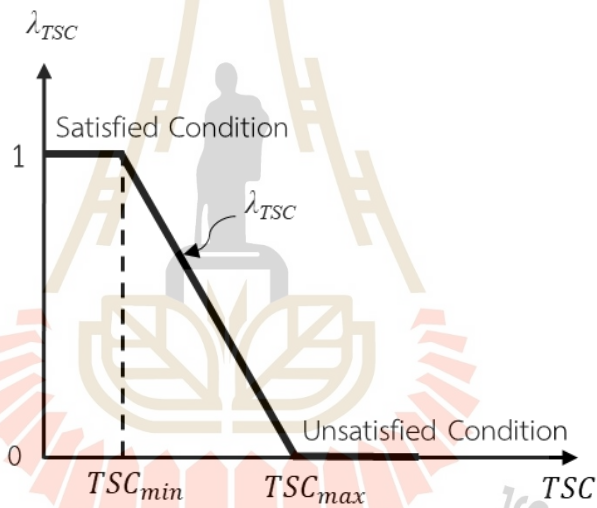
Figure 4.1 FSF of TSC
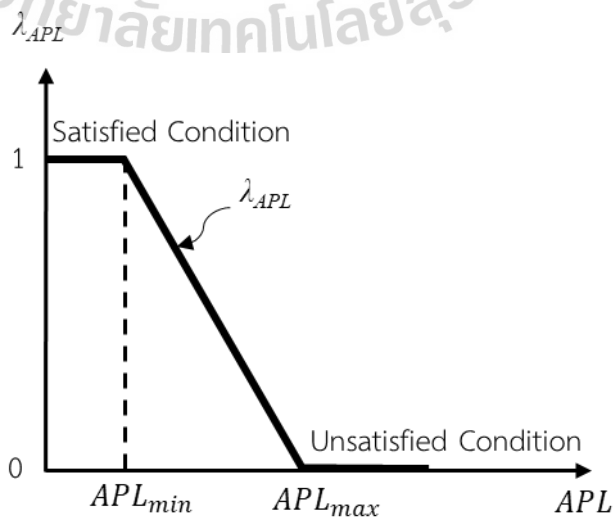
Figure 4.2 FSF of APL
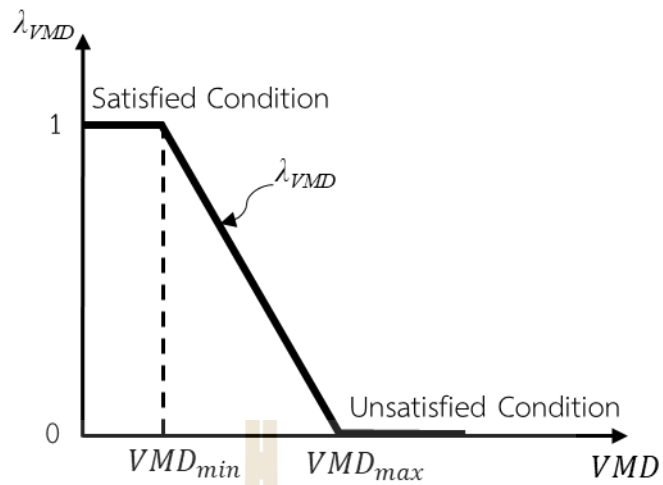
Figure 4.3 FSF of VMD

4.4 Constraints

Optimization constraints are as follows:

4.4.1 Equality constraints

In Equation 4.2, **g** is the equality limit constraints, which represent typical load flow Equations (4.20) and (4.21):

$$P_{Gi} - P_{Di} - V_i \sum_{j=1}^{NB} V_j \left[G_{ij} \cos \delta_{ij} + B_{ij} \sin \delta_{ij} \right] = 0 \qquad (4.20)$$

$$Q_{Gi} - Q_{Di} - V_i \sum_{j=1}^{NB} V_j \left[G_{ij} \sin \delta_{ij} - B_{ij} \cos \delta_{ij} \right] = 0 \qquad (4.21)$$

Where, $i = 1,2,...,NB$.

4.4.2 Inequality constraints

The matrix **h** is the inequality limit constrains that included generator's voltage magnitude, generator's active power output, generator's reactive power output, transformer tap changing, shunt capacitor, bus voltage magnitude, and line flow, can be formulated as Equations (4.22) to (4.28).

$$|V_i|^L \leq |V_i| \leq |V_i|^U \qquad , i=1,...,NG, \qquad (4.22)$$

$$P_{Gi}^L \leq P_{Gi} \leq P_{Gi}^U \qquad , i=1,\ldots,NG, \tag{4.23}$$

$$Q_{Gi}^L \leq Q_{Gi} \leq Q_{Gi}^U \qquad , i=1,\ldots,NG, \tag{4.24}$$

$$T_i^L \leq T_i \leq T_i^U \qquad , i=1,\ldots,NT, \tag{4.25}$$

$$Q_{ci}^L \leq Q_{ci} \leq Q_{ci}^U \qquad , i=1,\ldots,NC, \tag{4.26}$$

$$|V_{Li}|^L \leq |V_{Li}| \leq |V_{Li}|^U \qquad , i = 1,\ldots,NPQ, \tag{4.27}$$

$$|MVA_{Li}| \leq MVA_{Li}^U \qquad , i = 1,\ldots,NL. \tag{4.28}$$

4.5 The FMOOPF Using PSO

In this Section, the set of populations is formulated as Equation (4.29), velocity and current position according to the Equations (4.30) and (4.31), respectively.

$$\mathbf{p_i} = [\mathbf{P_{Gi}}, \ |\mathbf{V_{Gi}}|, \ \mathbf{T_i}, \ \mathbf{X_{Ci}}]. \tag{4.29}$$

$$v_m^{t+1} = wv_m^t + c_1 r_1 (pbest_m^t - \mathbf{p}_i^t) + c_2 r_2 (gbest^t - \mathbf{p}_m^t) . \tag{4.30}$$

$$\mathbf{p}_m^{t+1} = \mathbf{p}_m^t + v_m^{t+1}. \tag{4.31}$$

The procedure for calculating the objective function can be described in the following steps:

Step 1: Get the power flow input data set.

Step 2: Identify the control variables, dependent variables, and security limits.

Step 3: Determine the PSO population.

Step 4: Run power flow for all populations and calculate the objective value.

Step 5: Check constraint violations for the population. If the constraints are not violated, go to step 7, otherwise, proceed to step 6.

Step 6: Add the penalty factor to the objective function for population m.

Step 7: Calculate individual objective function.

Step 8: Get PSO's $pbest_m^t$ and $gbest^t$.

Step 9: Determine the velocity of particle m and update the particle's position.

Step 10: Check for maximum iteration. If the iteration reaches maximum iteration, go to step 11, otherwise, go to step 4.

Step 11: Get the results from minimizing individual objectives.

Step 12: Define an FSF for individual objections.

Step 13: Calculate the power flow of all populations.

Step 14: Compute an FSF for MO.

Step 15: Repeat steps 5-9.

Step 16: Check maximum iteration. If the iteration reaches maximum iteration, repeat steps 14-15 until the maximum iteration is reached.

Step 17: Print the results of objective functions.

4.6   Simulation Results

In this section, the proposed FMOOPF using PSO was validated by the modified IEEE 30-bus test system with additional capacitors, as shown in Figure 3.2 and the capacitors in addition to the control variable base case shown in Table 3.1. In particular, the modified IEEE 30-bus test system furthers capacitors, considering MO including three objective functions: TSC, APL, and VMD.

In Table 4.1, the simulation results of this section consider two cases consisting of individual objectives and MO, compared with the PPSOGSA method (Z. Ullah et al., 2019), tested under the same system data and control variables. To further validate the reliability of the FMOOPF proposed method, 30 trials were performed to determine the best values for individual objectives (TSCM, APLM, and VMDM) and the MO (-λ_T of FMOOPF), where λ_T is the maximum FSF value between the lowest values of λ_{TSC}, λ_{APL}, and λ_{VMD}. Note the minimization of - λ_T is corrected for λ_T maximization.

As simulation results in Table 4.1, when minimizing an individual objective, each objective could result in a higher result for other objectives. As the results obtained from several trials guarantee the reliability of the proposed method. For the first, considering each objective function, when minimizing TSC from TSCM, the lowest value

of TSC is 799.385 $/h. Under this condition, the APL and VMD are 8.709 p.u. and 0.823 p.u., respectively. Meanwhile, the APLM derived from the proposed method is 2.966 p.u, but the best APL condition leads to a maximum resolution of TSC and VMD at 967.342 $/h and 0.888 p.u., respectively. Likewise, VMDM is 0.076, which the lowest VMDM condition is leading to the higher value of TSC and APL at 861.944 $/h and 10.946 p.u., respectively. Hence, a comparison of the proposed and PPSOGSA methods showed that the proposed yielded better results for each objective, including TSCM, ALPM, and VMDM, than those of the PPSOGSA method, as shown in Table 4.1.

However, the MO problems considering simultaneously minimizing TSC, APL, and VMD may be also beneficial to the system depending on operator needs. Thus, the proposed FMOOPF can smoothly resolve conflicting MO problems. As a result, the proposed FMOPF can compromise between TSCM, APLM, and VMDM, under the FSF concept. On the other hand, the PPSOGSA method uses the weighted sum method to solve the MOOP.

Table 4.2 shows individual objectives (TSCM, APLM, and VMDM) and MO (considering all three objective functions simultaneously), with simulation results from 30 trials of the proposed method. For individual objectives, the best and worst values of TSC received from PSO are 799.385 $/h. and 800.025 $/h., respectively. The TSC's average and standard deviations are 799.445 $/h and 0.121, respectively. Meanwhile, the best and worst values of APL from APLM are 2.966 p.u. and 3.486 p.u., respectively. Besides, the average and standard deviation of APL are 3.001 p.u. and 0.114, respectively. The best and worst values of VMD from VMDM are 0.076 p.u. and 0.121 p.u., respectively. In the same way, the VMD's average and standard deviation are 0.087 p.u. and 0.010, respectively. In addition, the MO problem considerations looked at the $-\lambda_T$ values of FMOOPF, where the best and worst values of $-\lambda_T$ are 0.723 and 0.542, respectively. While, the average and standard deviation of $-\lambda_T$ are 0.650 and 0.038, respectively. Lastly, the convergence behaviors of TSCM, APLM, VMDM, and $-\lambda_T$ of FMOOPF are shown in Figures 4.4, 4.5, 4.6, and 4.7, respectively.

Table 4.1 Comparison results of the modified IEEE 30-bus test system for MO

Control Variables	TSCM		APLM		VMDM		MO	
	PPSO GSA	Proposed method	PPSO GSA	Proposed method	PPSO GSA	Proposed method	PPSO GSA	FMOOPF
Power Generation (P_{Gi}) at Bus (MW)								
2	48.58	48.69	80.00	80.00	49.04	80.00	52.66	54.58
5	21.37	21.30	50.00	50.00	44.74	15.00	31.73	34.12
8	21.44	21.13	35.00	35.00	18.41	10.00	34.94	34.99
11	11.94	11.95	30.00	30.00	24.13	17.29	25.28	26.58
13	12.00	12.00	40.00	40.00	14.50	39.35	20.38	27.56
Generator Voltage ($|V_i|$) Magnitude at Bus (p.u.)								
1	1.08	1.10	1.06	1.10	1.01	1.00	1.03	1.02
2	1.07	1.09	1.06	1.10	1.00	1.04	1.02	1.01
5	1.03	1.06	1.04	1.08	1.02	1.02	1.00	0.99
8	1.04	1.07	1.04	1.09	1.01	1.00	1.01	1.00
11	1.09	1.05	1.06	1.03	1.00	0.95	1.01	1.02
13	1.04	1.01	1.05	1.06	1.02	0.95	1.01	1.04
Transformer Tap-Changing ($T_{i\text{-}j}$) between Buses								
6-9	1.02	1.03	1.02	1.10	1.02	0.95	1.03	1.07
6-10	0.95	1.07	0.94	0.97	0.90	1.10	0.91	0.90
4-12	0.96	1.05	0.99	1.05	1.01	0.94	0.98	0.98
28-27	0.98	1.04	0.98	1.05	0.96	1.00	0.97	0.97
Capacitive Reactance (X_{Ci}) at Bus (p.u.)								
10	-1.39	-15.16	-0.26	-44.95	-0.22	-40.83	-0.20	-26.07
12	-0.72	-2.39	-0.47	-30.08	-0.28	-21.22	-0.95	-44.77
15	-0.22	-33.08	-0.21	-28.75	-0.20	-22.91	-0.21	-33.08
17	-0.20	-15.25	-0.20	-15.58	-3.08	-9.84	-1.40	-19.02
20	-0.25	-45.00	-0.22	-45.00	-0.20	-45.00	-0.20	-42.16
21	-0.20	-9.08	-0.20	-9.49	-0.20	-7.36	-0.20	-8.35
23	-0.26	-44.92	-0.29	-44.99	-0.20	-44.94	-0.20	-31.76
24	-0.20	-14.47	-0.20	-14.23	-0.20	-6.29	-0.20	-25.78
29	-0.30	-44.97	-0.37	-45.00	-0.77	-32.15	-0.34	-45.00
TSC ($/h.)	800.528	**799.385**	967.669	967.342	849.613	861.944	829.598	**845.866**
APL (p.u.)	9.027	8.709	3.103	**2.966**	7.420	10.946	6.110	**5.478**
VMD (p.u.)	0.911	0.823	0.891	0.888	0.090	**0.076**	0.110	**0.308**

Table 4.2   The best, worst, average, and standard deviation of individual
objective and MO from 30 trial solutions

	The proposed FMOOPF			
	Best	Worst	Average	S.D.
TSC ($/h)	799.385	800.025	799.445	0.121
APL (p.u.)	2.966	3.486	3.001	0.114
VMD (p.u.)	0.076	0.121	0.087	0.010
-λ_T of FMOOPF	-0.723	-0.542	-0.650	0.038
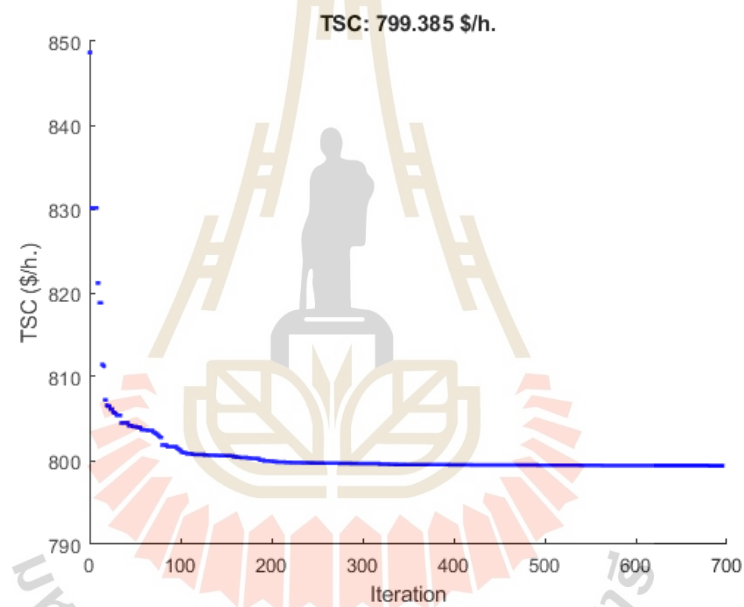
Figure 4.4 The convergence plot of the proposed method of TSCM
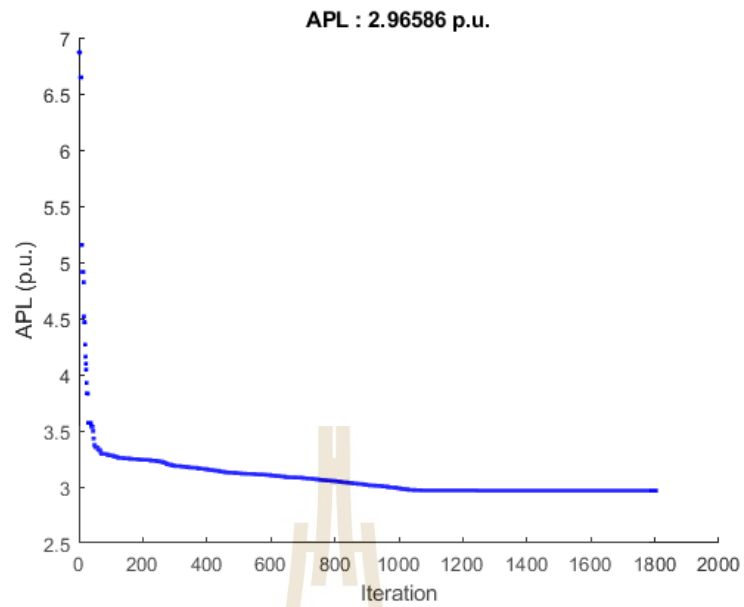
Figure 4.5 The convergence plot of the proposed method of APLM
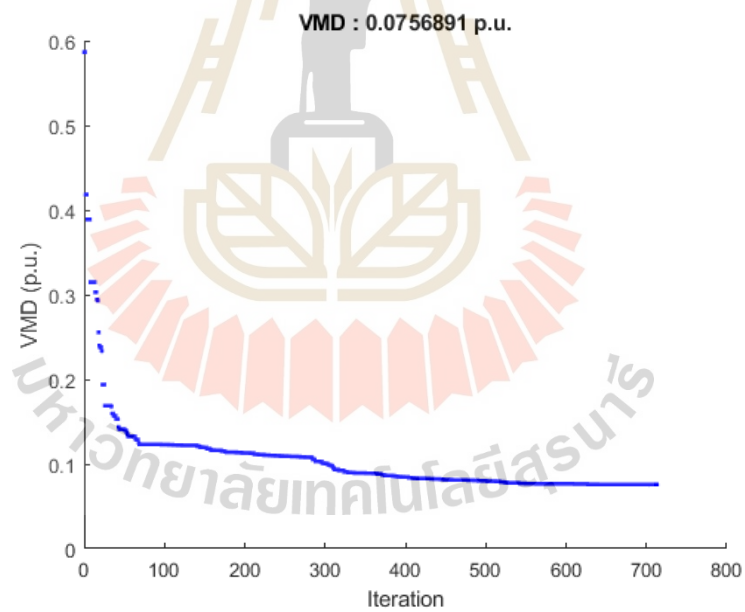
Figure 4.6 The convergence plot of the proposed method of VMDM
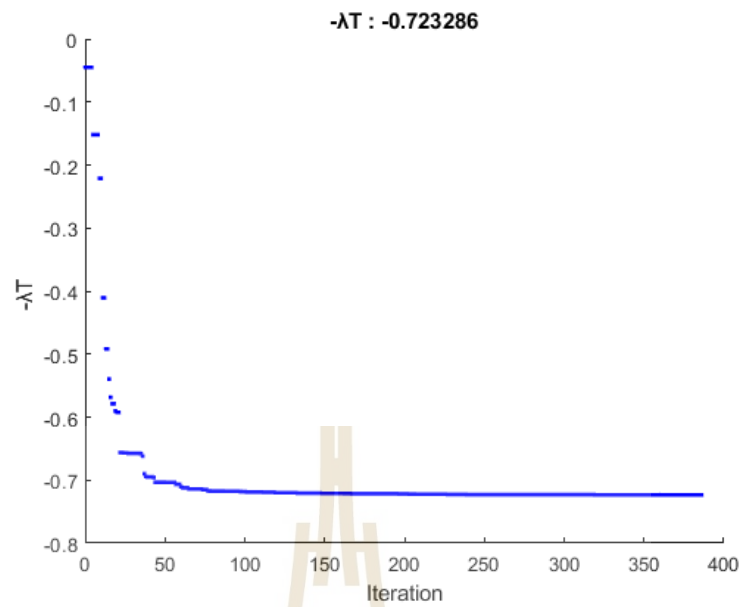
Figure 4.7 The convergence plot of the proposed method of $-\lambda_T$ of FMOOPF

CHAPTER 5

PROBABILISTIC FUZZY MULTI-OBJECTIVE OPF[3]

5.1   Introduction

In the last decade, renewable energy has been heavily pursued and largely infiltrated the power system, and of course, this type of energy is a good alternative to conventional thermal units as renewable energy, especially photovoltaic power plants (PVPP) and wind power plants (WPP), will soon cost less than fossil fuels. Whereas, the problem of PVPP and WPP generation in the power system is the uncertainties of local wind speed and solar radiation. There is also load uncertainty in the power system. Therefore, to properly assess PVPP and WPP generators in the power system, probabilistic load flow (PLF) is one of the effective tools. Recently, accurate stochastic models that accurately describe the behavior of power generation and load demand are critical to the planning and operation of the power system. Therefore, these models need further enhancements to accurately capture the behavior of solar radiation and wind speed. Meanwhile, there are two methods for solving PLF problems: the numerical method and the analytical method. The most commonly used method is the Monte-Carlo simulation (MCS).

This chapter presents the probability density function (PDF) of load, wind speed, and solar radiation uncertainties. It is necessary to calculate system state variables with uncertain properties. Then, load uncertainty is expressed by Normal PDF in the proposed method. Similarly, the solar radiation uncertainty is expressed by the Normal PDF as well as the load uncertainty. Meanwhile, the Weibull PDF is used for modeling wind speed, as proposed by M. R. Patal in 2006, and became a widely used method.

This research proposes the probabilistic fuzzy multi-objective optimal power flow (PFMOOPF) considering photovoltaic power plant (PVPP) generation, wind power

---

[3] Part of this work is accepted for publication in " GMSARN International Journal", 2022.

plant (WPP) generation, and load uncertainty. Then, the objectives considered are individual objectives and MO tested on the modified IEEE 30-bus test system with renewable energy. While objective functions consider TSCM, APLM, and VMDM. Meanwhile, the proposed method can successfully provide the optimal operation of controllable parameters, including the optimal active power generation, the magnitudes of generators' voltages, the tap changing of transformers, and reactance values of capacitors considering load, wind speed, and solar radiation uncertainty in the test system.

5.2 Problem formulation

In this paper, the PFMOOPF problem can be mathematically described by

$$\text{Minimize} \quad OB_i(\tilde{\mathbf{x}}, \tilde{\mathbf{u}}) + PNF \quad , \qquad i = 1, 2, \ldots, N_{\text{obj}} \tag{5.1}$$

$$\text{Subject to:} \quad \boldsymbol{g}(\tilde{\mathbf{x}}, \tilde{\mathbf{u}}) = 0, \tag{5.2}$$

$$\boldsymbol{h}(\tilde{\mathbf{x}}, \tilde{\mathbf{u}}) \leq 0. \tag{5.3}$$

The matrix OB_i represents the set of objective functions that are to be minimized consisting of total system cost (TSC), active power loss (APL), and voltage magnitude deviation (VMD), as shown in Equation (5.1). Meanwhile, $\boldsymbol{g}$ and $\boldsymbol{h}$, in Equations (5.2) and (5.3), are the sets of necessary equality and inequality constraints. However, the vector of probabilistic dependent variables is denoted by $\tilde{\mathbf{x}}$, consisting of,

1. Probabilistic slack bus generated active power ($\tilde{P}_{G1}$),

2. Probabilistic voltage magnitudes at load bus ($\tilde{V}_{Li}$),

3. Probabilistic generators' reactive power output ($\tilde{Q}_{Gi}$), and

4. Probabilistic transmission lines and transformers loading (branches flow) ($\tilde{S}_l$).

Hence, $\tilde{\mathbf{x}}$ can be expressed as:

$$\tilde{\mathbf{x}}^T = [\tilde{P}_{G1}, \tilde{V}_{L1}...\tilde{V}_{LNL}, \tilde{Q}_{G1}...\tilde{Q}_{GNG}, \tilde{Q}_{WPP}, \tilde{Q}_{PVPP}, \tilde{S}_{l1}...\tilde{S}_{lNTL}] \tag{5.4}$$

Whereas, **ũ** is the vector of probabilistic control variables as follow:

$$\tilde{\mathbf{u}}^T = [\tilde{\mathbf{P}}_\mathbf{G}, \left|\tilde{\mathbf{V}}_\mathbf{G}\right|, \tilde{\mathbf{T}}, \tilde{\mathbf{X}}_\mathbf{C}] \tag{5.5}$$

Where $\tilde{\mathbf{P}}_\mathbf{G}$ is the matrix of probabilistic active power generation excluding slack bus generation. $|\tilde{\mathbf{V}}_\mathbf{G}|$ is the matrix of probabilistic voltage magnitude of generator bus including WPP and PVPP. Then, $\tilde{\mathbf{T}}$ is the matrix of probabilistic transformer tap-changing. And $\tilde{\mathbf{X}}_\mathbf{C}$ is the matrix of probabilistic capacitive reactance.

$$\tilde{\mathbf{P}}_\mathbf{G} = [\tilde{P}_{G2}, \tilde{P}_{G3}, ..., \tilde{P}_{GNG}]_{1\times(NG-1)} \quad , \tag{5.6}$$

$$\left|\tilde{\mathbf{V}}_\mathbf{G}\right| = [\left|\tilde{V}_{G1}\right|, \left|\tilde{V}_{G2}\right|, ..., \left|\tilde{V}_{GNG}\right|, \left|\tilde{V}_{WPP}\right|, \left|\tilde{V}_{PVPP}\right|]_{1\times NG} \quad , \tag{5.7}$$

$$\tilde{\mathbf{T}} = [\tilde{T}_1, ..., \tilde{T}_{NT}]_{1\times NT} \quad , \tag{5.8}$$

$$\tilde{\mathbf{X}}_\mathbf{C} = [\tilde{X}_{C1}, ..., \tilde{X}_{CNC}]_{1\times NC} \quad . \tag{5.9}$$

5.3 Objective function

5.3.1 Total system generation cost minimization (TSCM)

In this process of the OPF problem simulation, the objective function is to minimize the overall cost of electricity needed to supply the demands and subject to the constraints considering the uncertainty of load, PVPP and WPP in the system, expressed below:

$$\min_u OB_1(\tilde{\mathbf{x}}, \tilde{\mathbf{u}}) = \min_u TSC(\tilde{\mathbf{x}}, \tilde{\mathbf{u}}) + PNF \tag{5.10}$$

where,

$$TSC(\tilde{\mathbf{x}}, \tilde{\mathbf{u}}) = \sum_{i=1}^{NG}(a_i + b_i P_{Gi} + c_i P_{Gi}^2) \tag{5.11}$$

5.3.2 Active power loss minimization (APLM)

The active power loss (APL) in the transmission lines needs to be minimized taking into account the uncertainty of PVPP and WPP loads in the system as the following expression below.

$$\min_u OB_2(\tilde{\mathbf{x}},\tilde{\mathbf{u}}) = \min_u APL(\tilde{\mathbf{x}},\tilde{\mathbf{u}}) + PNF \tag{5.12}$$

where,

$$APL(\tilde{\mathbf{x}},\tilde{\mathbf{u}}) = \sum_{L=1}^{NTL} g_{L,ij}\left[V_i^2 + V_j^2 - 2V_iV_j\cos\theta_{ij} \right]. \tag{5.13}$$

5.3.3 Voltage magnitude deviation minimization (VMDM)

The voltage magnitude deviation (VMD) between the operating and the reference voltage should be taken into account in the OPF problem and taken into account with the uncertainty of load, PVPP, and WPP. So, the goal of minimizing the VMD can be formulated as:

$$\min_u OB_3(\tilde{\mathbf{x}},\tilde{\mathbf{u}}) = \min_u VMD(\tilde{\mathbf{x}},\tilde{\mathbf{u}}) + PNF \tag{5.14}$$

where,

$$VMD(\tilde{\mathbf{x}},\tilde{\mathbf{u}}) = \sum_{i=1}^{NL}\left| V_i - V_i^{ref} \right|. \tag{5.15}$$

V_i^{ref} is generally considered as 1 p.u.

5.3.4 Probabilistic Fuzzy Multi-Objective OPF Formulation (PFMOOPF)

The PFMOOPF problem was addressed concurrently for an optimal solution of TSCM, APLM, and VMDM based on fuzzy satisfactory function (FSF) concepts. As a result of minimizing the objective function in Equations (5.10) to (5.15), FSF can be determined as shown in Figures 5.1 to 5.3 and Equations (5.16) to (5.8), where OB_i represents individual objectives (TSCM, APLM, and VMDM). Finally, the multi-objective (MO) problem can be formulated as a fuzzy maximization problem as Equation (5.9).

$$\lambda_{TSC} = \begin{cases} 1 & ,\text{for } TSC \leq TSC_{\min} \\ \dfrac{-1}{TSC_{\max} - TSC_{\min}} \cdot TSC + \dfrac{TSC_{\max}}{TSC_{\max} - TSC_{\min}} & ,\text{for } TSC_{\min} \leq TSC < TSC_{\max} \\ 0 & ,\text{for } TSC \geq TSC_{\max} \end{cases} \tag{5.16}$$

$$\lambda_{APL} = \begin{cases} 1 & ,\text{for } RPL \leq RPL_{\min} \\ \dfrac{-1}{APL_{\max} - APL_{\min}} \cdot APL + \dfrac{APL_{\max}}{APL_{\max} - APL_{\min}} & ,\text{for } APL_{\min} \leq APL < APL_{\max} \\ 0 & ,\text{for } APL \geq APL_{\max} \end{cases} \tag{5.17}$$

$$\lambda_{VMD} = \begin{cases} 1 & ,\text{for } VMD \leq VMD_{\min} \\ \dfrac{-1}{VMD_{\max} - VMD_{\min}} \cdot VMD + \dfrac{VMD_{\max}}{VMD_{\max} - VMD_{\min}} & ,\text{for } VMD_{\min} \leq VMD < VMD_{\max} \\ 0 & ,\text{for } VMD \geq VMD_{\max} \end{cases} \tag{5.18}$$

Maximize $\lambda_T = \min\{\lambda_{TSC}, \lambda_{APL}, \lambda_{VMD}\} + PNF$ \hfill (5.19)
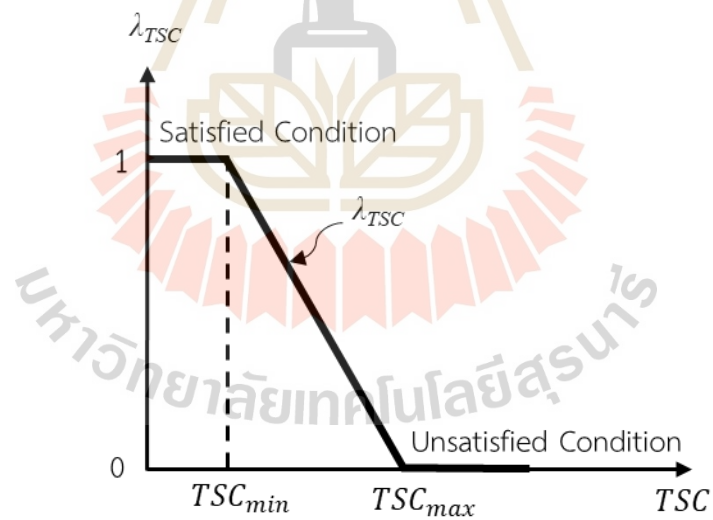
Figure 5.1 FSF of TSC
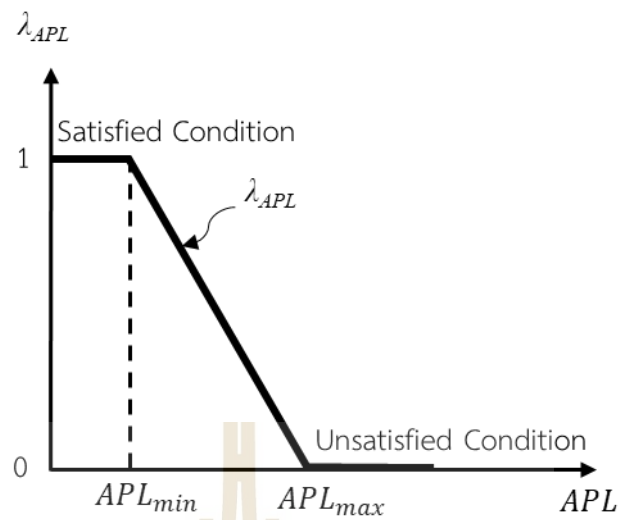
Figure 5.2 FSF of APL
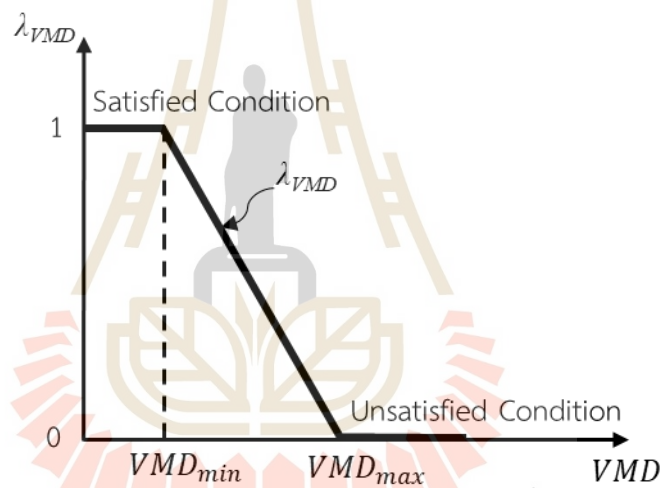
Figure 5.3 FSF of VMD

5.4 Constraints

The limitations of the probabilistic OPF (POPF), including power and function balance, are taken into account in the proposed method.

5.4.1 Equality constraints

In Equation 5.2, **g** is the equality limit constraints considering the uncertainty of load, PVPP, and WPP shown in PDF, representing the general load-flow equation:

$$\tilde{P}_{Gi} + \tilde{P}_{PVi} + \tilde{P}_{WTi} - \tilde{P}_{Di} - \tilde{V}_i \sum_{j=1}^{NB} \tilde{V}_j \left[G_{ij} \cos \tilde{\delta}_{ij} + B_{ij} \sin \tilde{\delta}_{ij} \right] = 0 \tag{5.20}$$

$$\tilde{Q}_{Gi} + \tilde{Q}_{PVi} + \tilde{Q}_{WTi} - \tilde{Q}_{Di} - \tilde{V}_i \sum_{j=1}^{NB} \tilde{V}_j \left[G_{ij} \sin \tilde{\delta}_{ij} - B_{ij} \cos \tilde{\delta}_{ij} \right] = 0 \tag{5.21}$$

where, $i = 1, \ldots, NB$.

5.4.2. System operating limit constraints

The generator constraints are the limit on generators' voltage magnitude, the generators' active, and reactive power operating limit at the ith bus as formulated in Equations (5.22) to (5.24), respectively. Equations (5.25) and (5.26) present transformer tap-changing limits, and the Capacitors setting limits, respectively. Whereas, network operating limit constraints include the limit on bus voltage magnitude and the transmission lines and transformers loading limit as formulated in Equations (5.27) and (5.28), respectively.

$$|V_{Gi}|^L \le |\tilde{V}_{Gi}| \le |V_{Gi}|^U \quad , \quad i = 1, 2, \ldots, NG, \tag{5.22}$$

$$P_{Gi}^L \le \tilde{P}_{Gi} \le P_{Gi}^U \quad , \qquad i = 1, 2, \ldots, NG, \tag{5.23}$$

$$Q_{Gi}^L \le \tilde{Q}_{Gi} \le Q_{Gi}^U \quad , \qquad i = 1, 2, \ldots, NG, \tag{5.24}$$

$$T_i^L \le \tilde{T}_i \le T_i^U \quad , \qquad i = 1, 2, \ldots, NT, \tag{5.25}$$

$$Q_{ci}^L \le \tilde{Q}_{ci} \le Q_{ci}^U \quad , \qquad i = 1, 2, \ldots, NC, \tag{5.26}$$

$$|V_{Li}|^L \le |\tilde{V}_{Li}| \le |V_{Li}|^U , \qquad i = 1, 2, \ldots, NPQ, \tag{5.27}$$

$$|MVA_{Li}| \le M\tilde{V}A_{Li}^U \quad , \qquad i = 1, 2, \ldots, NL. \tag{5.28}$$

5.5   Uncertainty models

A probability model is a model that combines the probability distribution of a random variable, where the random variable represents the possible outcome of an uncertain event. Probability distributions assign probabilities to various possible outcomes. Meanwhile, Monte-Carlo simulation (MCS) is a traditional numerical method for dealing with probability problems. Because MCS can generate random numbers and random sampling with the cumulative density function and replicate the energy flow individually. Therefore, practical probability models are used to make realistic decisions with the MCS concept, often necessary to recognize the uncertainty in the inputs and outcomes of the process. However, this research considers the uncertainty of PVPP, WPP, and load in Thailand. In the proposed, the procedure for calculating the MCS concept can be described in the following steps:

Step 1: Get the power flow input data set.

Step 2: Identify the control variables, dependent variables, and security limits.

Step 3: Set the average total power generation at k = 0 to zeros ($PGT_{AV}^0 = 0$). Set iteration k = 1.

Step 4: Get system load, PVPP, and WPP power generation, from PDFs.

Step 5: Solve OPF for individual objective function (TSC, APL, and VMD in Equations (5.10), (5.12), and (5.14), respectively) using PSO.

Step 6: Define a satisfying fuzzy function for individual objective function.

Step 7: Calculate a satisfying fuzzy function for MO.

Step 8: Solve FMOOPF for λ_T maximization in Equation (5.19), using PSO.

Step 9: Calculate the average total power generation (PGT_{AV}^k) obtained from iterations k

Step 10: If $\left| PGT_{AV}^k - PGT_{AV}^{k-1} \right| > \varepsilon$, k = k+1 and go to Step 4, conversely, if $\left| PGT_{AV}^k - PGT_{AV}^{k-1} \right| \leq \varepsilon$, go to Step 11.

Step 11: Compute the PDF of control and output variables.

Step 12: Stop.

The proposed PFMOOPF is tested with the modified IEEE 30-bus test system consisting of PVPP, WPP, and load for individual objectives and MO. The system data is taken from Z. Ullah et al. in 2019, as shown in Figure 5.4. Therefore, PVPP generation, WPP generation, and load are modeled as uncertain variables as follows.
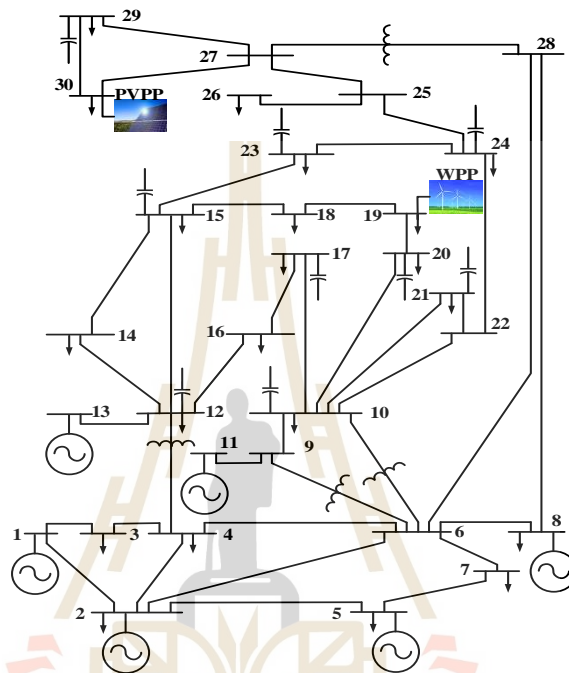
Figure 5.4 The modified IEEE 30-bus test system with renewable energy

5.5.1 PVPP Model

Solar radiation follows a normal distribution probability theory. A normal distribution is a continuous probability distribution of a continuous random variable in which a normal logarithm distribution is given. In the proposed, the PVPP is intermittent and uncertain output, and it is modeled as a continuous random variable of Thailand. In the proposed, Figure 5.5 shows the normal fitting of normalized solar irradiance data after running an MCS. Meanwhile, the mean value 'μ' of solar irradiance is taken as 0.7805 and the variance 'σ^2' is taken as 0.0242. The rated power of PVPP connected at bus 30 is 25 MW.
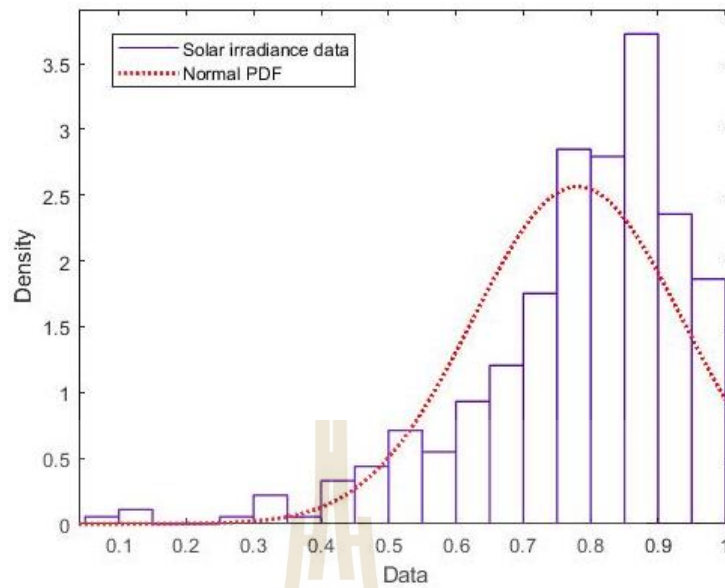
Figure 5.5 The PDF of solar irradiance data

Therefore, the output power generated by the PVPP unit is dependent on solar irradiance, as follows.

$$\tilde{P}_{PVPP_i}(S) = \begin{cases} \tilde{P}_{pvn} \dfrac{S^2}{S_{stc}R_c} & \text{for } S < R_c \quad \text{,for bus } i \\[3mm] \tilde{P}_{pvn} \dfrac{S}{S_{stc}} & \text{for } S \geq R_c \quad \text{,for bus } i \end{cases}.$$

(5.29)

The PDF for the normal random variable, S which is a normal probability distribution of solar irradiance as defined by:

$$f_S(S) = \frac{1}{\sigma\sqrt{2\pi}} \exp\left\{ \frac{-(x-\mu)^2}{2\sigma^2} \right\}.$$

(5.30)

for $-\infty < S < \infty$, $-\infty < \mu < \infty$, $0 < \sigma^2 < \infty$

The mean and variance of the PDF of solar irradiance for normal distribution 'S' are;

$$E(S) = \mu,$$ (5.31)

$$Var(S) = \sigma^2.$$ (5.32)

The random variable is modeled by the normal distribution with mean 'μ' and variance 'σ^2' as shown in Equations (5.31) and (5.32), respectively, then it is simply denoted as;

$$S \sim N(\mu, \sigma^2).$$ (5.33)

5.5.2 WPP model

The power generated by a wind power plant (WPP) depends on the fluctuation of wind speed over time. Due to the high variability of the geographic location of wind resources. Therefore, the probability distribution of wind speed is often characterized by a Weibull distribution. A typical Weibull distribution can take various shapes depending on the parameters. In this research, the wind speed is modeled using a Weibull distribution. In addition, the WPP connected at bus 19 has a rated power (P_{wtn}) of 50 MW with a normal wind speed (v_n) of 10 m/s, cut-in wind speed (v_{ci}) of 2.7 m/s, and cut-out wind speed (v_{co}) of 25 m/s. Moreover, the normalized wind speed is approximated with a two-parameter Weibull distribution. The scale factor 'c' is taken as 0.493 and the shape factor 'k' is taken as 2.459, as in Figure 5.6.
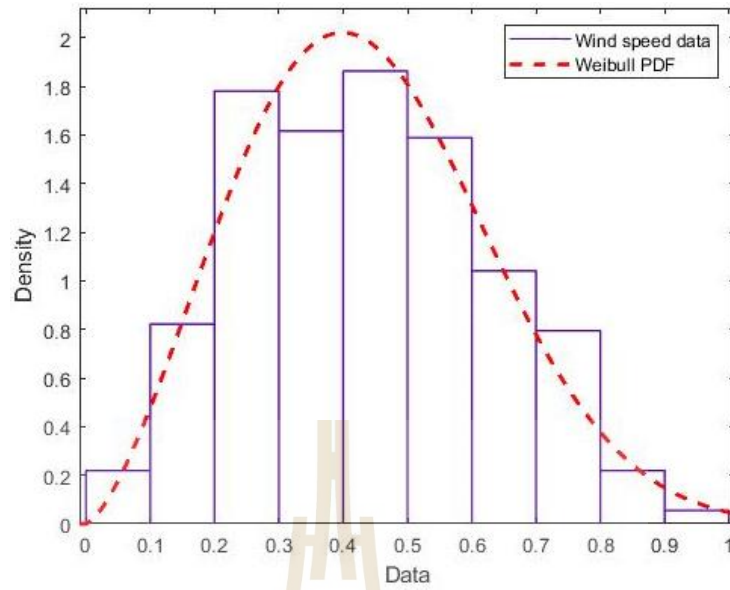
Figure 5.6 The PDF of wind speed data of Thailand

The output power of wind speed (v) of WPP can be analyzed as follows:

$$
\tilde{P}_{WPP}(v) = \begin{cases} 0 & v \leq v_{ci} \\ \dfrac{v - v_{ci}}{v_n - v_{ci}} \cdot P_{wtn} & v_{ci} < v \leq v_n \\ P_{wtn} & v_n < v \leq v_{co} \\ 0 & v \geq v_{co} \end{cases}
\tag{5.34}
$$

Weibull distribution with shape factor (k) and scale factor (c) can be formulated as follows:

$$
f_v(v) = \frac{k}{c} \cdot \left(\frac{v}{c}\right)^{k-1} \cdot e^{-\left(\frac{v}{c}\right)^k} \qquad \text{for } 0 < v < \infty
\tag{5.35}
$$

Mean of Weibull distribution can be formulated as follows:

$$
M_{wbl} = c \cdot \Gamma(1 + k^{-1})
\tag{5.36}
$$

5.5.3 Load Model

Probabilistic load models can be found in several probabilistic load flows. In the same way, in PVPP and WPP, the load is modeled as a continuous random variable of energy consumption in Thailand. Nevertheless, the nature of the load in the normal distribution model is shown in Figure 5.4. Therefore, the load PDF is usually represented by a normal PDF, where the probabilistic load models can be rendered more realistically by daily hourly loading. In Figure 5.7, the active power of the load is assumed to have a normal PDF. Furthermore, the μ is taken as 0.7748 and the σ^2 is taken as 0.0077.
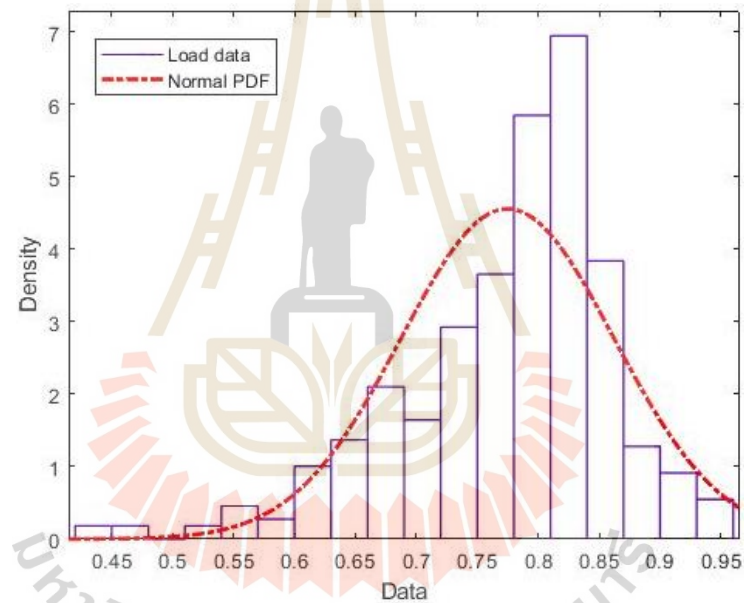
Figure 5.7 The PDF of active power load

The total load connected to the bus can be probabilistically described by a normal distribution. The relevant PDF is as follows:

$$f_{P_d}(P_d) = \frac{1}{\sqrt{(2\pi)}\sigma} \exp\left(-\frac{(P_d-\mu)^2}{2\sigma^2}\right) \tag{5.37}$$

for $-\infty < P_d < \infty$, $-\infty < \mu < \infty$, $0 < \sigma^2 < \infty$

The mean and variance of the PDF of load for normal distribution 'P_d' are;

$$E(P_d) = \mu, \tag{5.38}$$

$$Var(P_d) = \sigma^2. \tag{5.39}$$

The random variable is modeled by the normal distribution with mean 'μ' and variance 'σ^2' as shown in Equations (5.38) and (5.39), respectively.

5.6   Simulation Results

The PFMOOPF simulations were performed on the modified IEEE 30-bus test system consisting of PVPP, WPP, and load, which were studied as individual objectives and MO, as shown in Figure 5.1. The PVPP power generation characteristic is obtained from the solar irradiance data of Thailand, which selected dispatch hour is noon every day because it is the time with the highest solar irradiation. The PVPP is connected to bus 30. The wind speed data is derived from NASA's location in Bangkok, Thailand at noon, just like solar irradiance data. The WPP is connected to bus 19. Like solar irradiance and wind speed, the load characteristic is derived from the load demand of Thailand, which is distributed proportionally across the modified IEEE 30-bus test system.

Tables 5.1 and 5.2 shows the control variables of the proposed PFMOOPF. The PDF in terms of mean and standard deviation (S.D.) for TSCM and APLM is shown in Table 5.1, respectively. Therefore, the PDF in terms of mean and standard deviation (S.D.) for VMDM and MO are shown in Table 5.2, respectively.

Table 5.1   The TSCM and APLM results obtained by proposed PFMOOPF

Control Variables	TSCM		APLM	
	Mean	S.D.	Mean	S.D.
Power Generation (P_{Gi}) at Bus (MW)				
2	32.811	5.849	44.507	14.914

5	16.412	1.399	49.895	1.598
8	10.066	0.766	30.991	6.361
11	10.004	0.066	28.985	4.004
13	12.000	0.009	31.558	7.105

Generator Voltage ($|V_i|$) Magnitude at Bus (p.u.)

1	1.082	0.033	1.054	0.043
2	1.072	0.035	1.055	0.043
5	1.052	0.036	1.046	0.042
8	1.060	0.036	1.054	0.042
11	1.043	0.053	1.042	0.045
13	1.052	0.044	1.061	0.032
19(WPP)	1.063	0.035	1.077	0.023
30(PVPP)	1.081	0.032	1.094	0.019

Transformer Tap-Changing ($T_{i\text{-}j}$) between Buses

6-9	1.013	0.067	1.016	0.066
6-10	0.998	0.081	0.939	0.067
4-12	0.998	0.047	0.969	0.040
28-27	0.998	0.043	0.976	0.039

Capacitive Reactance (X_{Ci}) at Bus (p.u.)

10	-28.347	17.644	-24.748	17.978
12	-22.346	18.682	-18.339	17.556
15	-41.574	6.542	-43.312	5.119
17	-28.599	10.848	-24.160	7.082
20	-43.384	5.293	-44.187	4.292
21	-19.070	12.391	-15.222	7.702
23	-43.759	3.393	-44.628	2.045
24	-25.735	10.402	-23.480	6.717
29	-44.407	2.805	-44.856	1.411

TSC ($/h.)	**486.705**	**90.524**	666.916	112.017
APL (p.u.)	4.401	1.950	**1.194**	**1.805**
VMD (p.u.)	1.433	0.413	1.564	0.336

Table 5.2 The VMDM and MO results obtained by proposed PFMOOPF

Control Variables	VMDM		MO	
	Mean	S.D.	Mean	S.D.
Power Generation (P_{Gi}) at Bus (MW)				
2	48.405	23.666	38.868	7.449

5	31.569	13.573	31.338	5.238
8	20.876	9.724	23.779	7.414
11	19.361	7.518	19.010	5.348
13	27.111	10.364	17.874	5.190
Generator Voltage ($|V_i|$) Magnitude at Bus (p.u.)				
1	0.996	0.025	1.036	0.032
2	1.008	0.043	1.029	0.032
5	1.014	0.013	1.013	0.031
8	0.997	0.016	1.022	0.031
11	1.017	0.046	1.011	0.036
13	0.998	0.033	1.011	0.026
19(WPP)	0.998	0.006	1.014	0.019
30(PVPP)	0.992	0.023	1.040	0.020
Transformer Tap-Changing ($T_{i\text{-}j}$) between Buses				
6-9	1.023	0.050	1.014	0.055
6-10	0.991	0.058	1.006	0.067
4-12	0.999	0.059	1.004	0.042
28-27	0.968	0.033	1.003	0.038
Capacitive Reactance (X_{Ci}) at Bus (p.u.)				
10	-26.914	14.446	-27.570	14.487
12	-26.823	14.268	-24.442	15.428
15	-25.603	12.149	-36.064	9.614
17	-28.881	12.022	-28.078	10.760
20	-34.963	13.213	-37.298	9.629
21	-18.861	12.587	-21.742	12.649
23	-35.257	10.208	-37.993	8.437
24	-15.124	10.644	-25.489	10.274
29	-33.298	11.985	-40.195	7.344
TSC ($/h.)	596.140	93.435	**535.123**	98.046
APL (p.u.)	6.941	4.917	**2.523**	**1.896**
VMD (p.u.)	**0.055**	**0.0205**	0.430	0.148
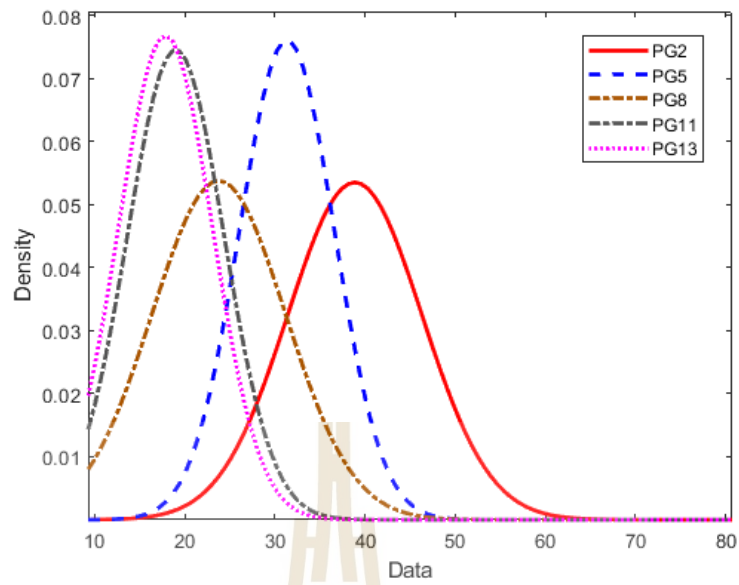
Figure 5.8 The PDF of PFMOOPF for output power of generators
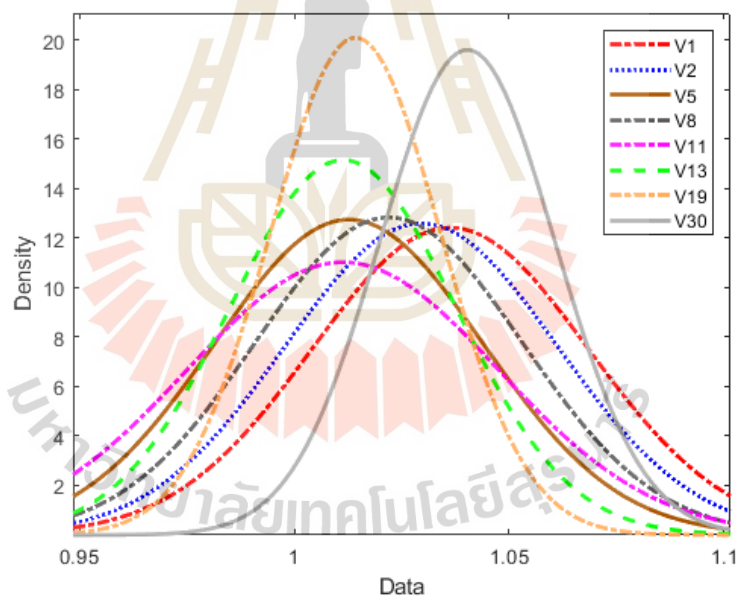
Figure 5.9 The PDF of PFMOOPF for voltage magnitudes of generators
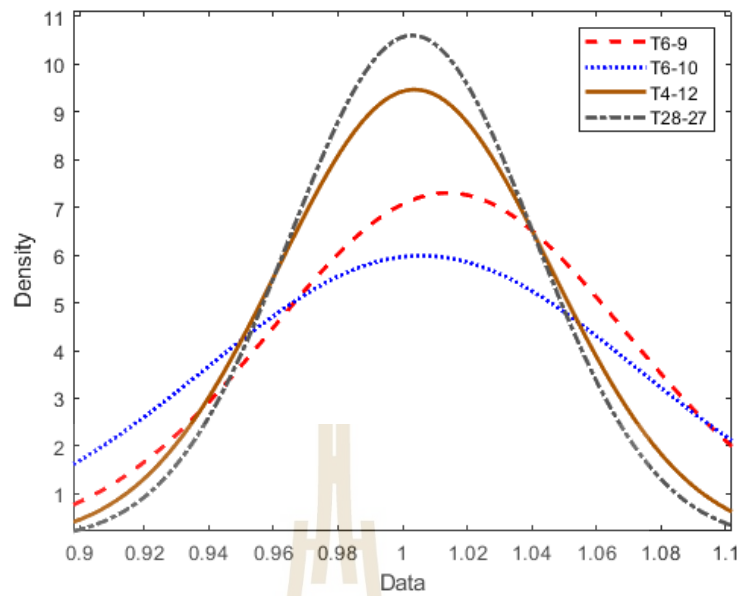
Figure 5.10 The PDF of PFMOOPF for transformer Tap-Changing
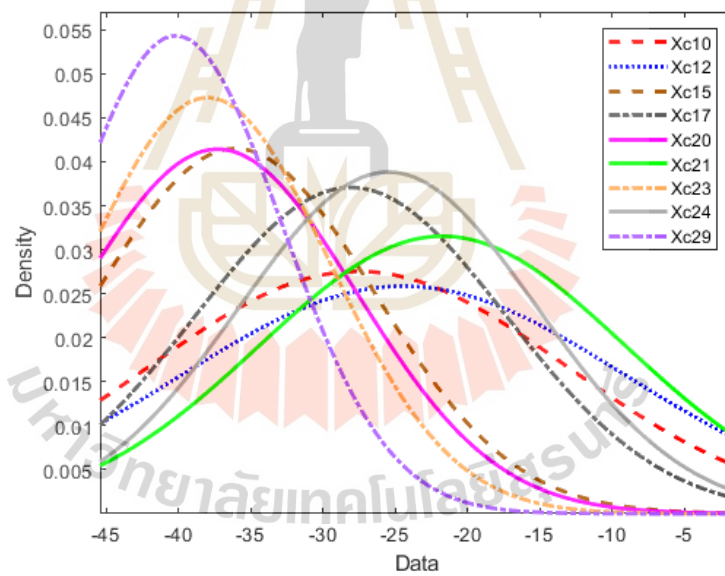
Figure 5.11 The PDF of PFMOOPF for capacitive reactance
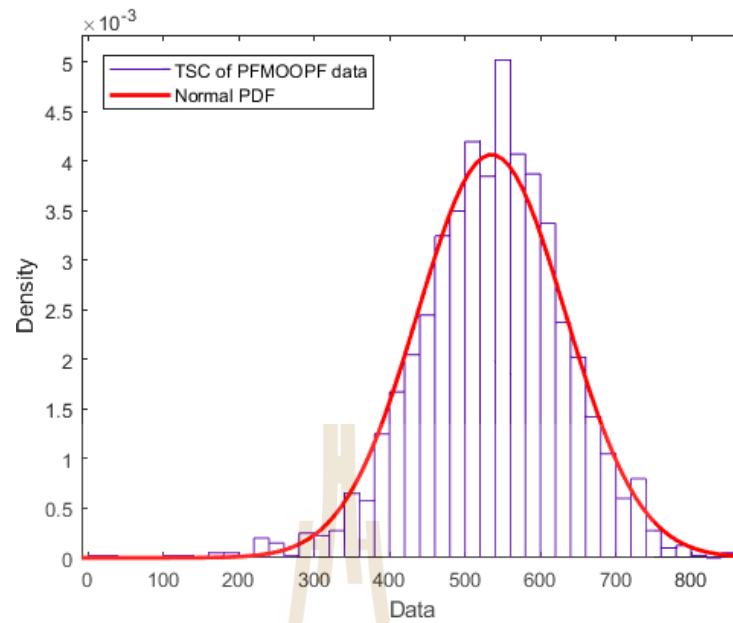
Figure 5.12 The PDF of PFMOOPF for TSC
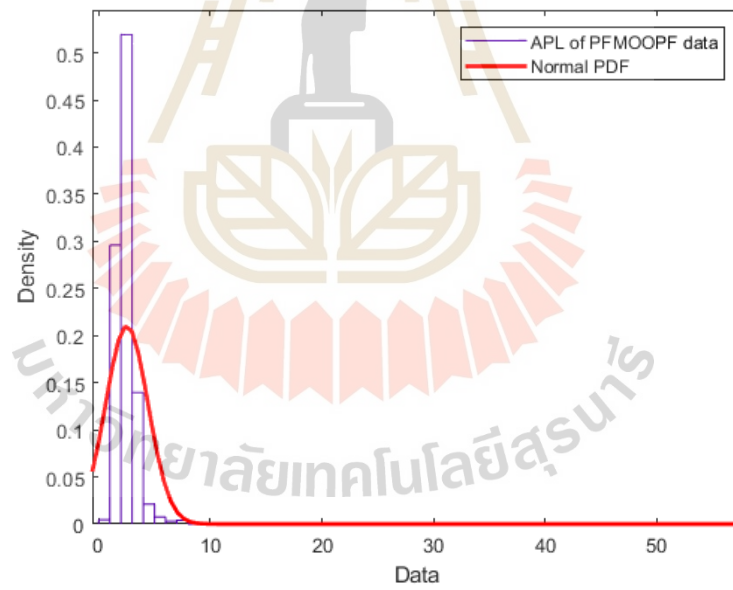
Figure 5.13 The PDF of PFMOOPF for APL
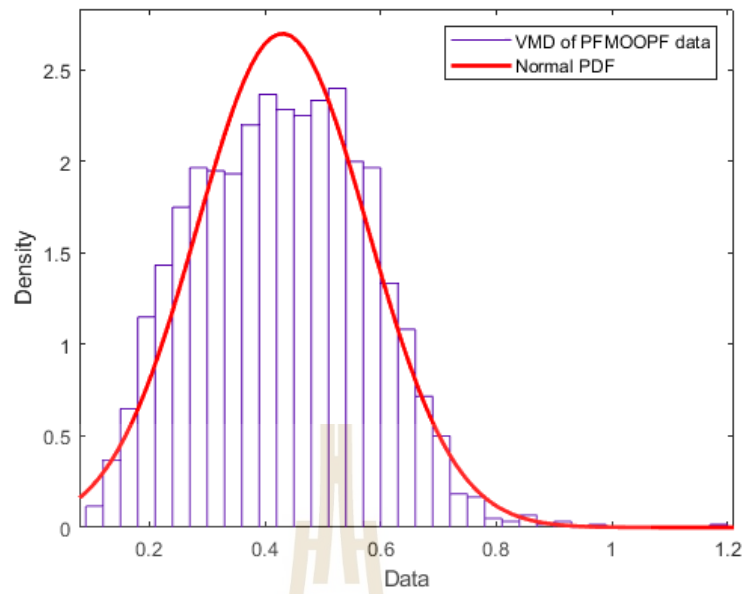
Figure 5.14 The PDF of PFMOOPF for VMD
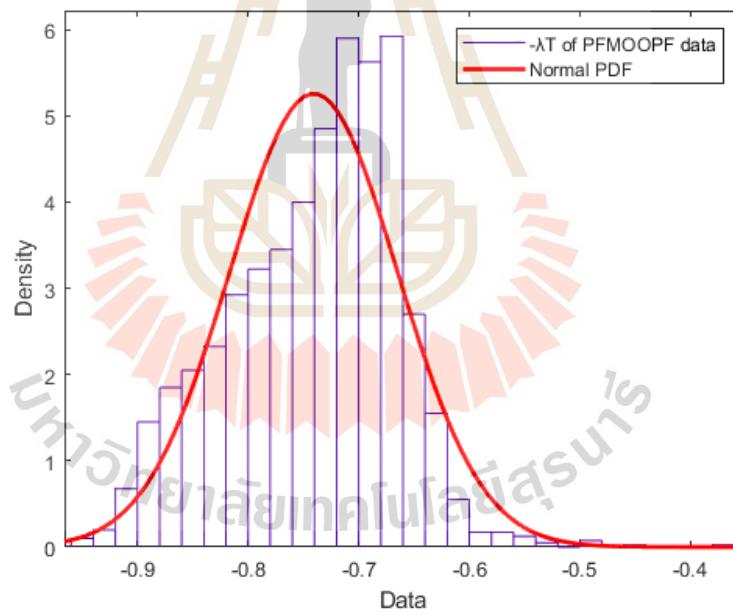
Figure 5.15 The PDF of PFMOOPF for -λ_T
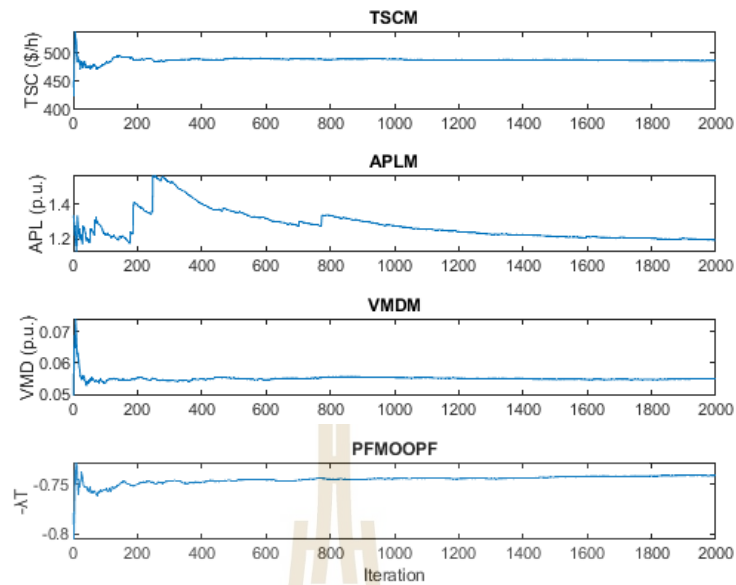
Figure 5.16 The convergence of MCS of PFMOOPF

Figures 5.8 to 5.11 show the PDF of the optimal control variables including the output power of generators, voltage magnitudes of generators, transformer Tap-Changing, and capacitive reactance, respectively. Meanwhile, Figures 5.12 to 5.15 show the PDF results for TSC, APL, VMD, and $-\lambda_T$ of PFMOOPF obtained with 2000 MCS samples.

The results obtained from the proposed method can be compared with the values of the MCS with 2000 runs to indicate the validity and effectiveness of the proposed method, which is shown in Figure 5.16. However, Figure 5.16 shows the convergence of the MCS results of each objective and MO function: TSCM, APLM, VMDM, and PFMOOPF.

CHAPTER 6

CONCLUSION

This thesis proposes the PSO-OPF for optimal operation of the controllable parameters to reduce total system cost. To verify the effectiveness of the proposed PSO-OPF was used with the original IEEE 30-bus test system and the modified IEEE 30-bus test system. Meanwhile, the proposed PSO-OPF considers the optimal active power generation, generator Voltage Magnitude, transformer tap-changing, and SVC reactive value leading to the lowest total system cost. Therefore, the simulation results show that PSO-OPF can reduce the total system cost compared to the reported results.

Moreover, the fuzzy multi-objective optimal power flow (FMOOPF) using the PSO algorithm considers individual objective functions, including total system cost (TSC), active power loss (APL), voltage magnitude deviation (VMD), and multi-objective (MO) that consider all three objective functions simultaneously. To verify the performance of the FMOOPF proposed is used the modified IEEE 30-bus test system, which considers the optimal active power generation, generator Voltage Magnitude, transformer tap-changing, and SVC reactive value. However, the proposed FMOOPF has well performed in obtaining the solution in the middle of conflicting objectives.

Meanwhile, the probabilistic optimal power flow (POPF) is one of the interesting tools for handling uncertainty in power system analysis. Therefore, the proposed PFMOOPF method presents various control variables to determine the uncertainties of PVPP, WPP, and the loads in the system. The proposed method was tested on the modified IEEE 30-bus test system with renewable energy. The uncertainty models can be presented in the PDF. Meanwhile, the objectives considered are individual objectives and multi-objectives such as TSCM, APLM, and VMDM. Therefore, the proposed PFMOOPF using a fuzzy satisfactory function concept with PSO achieves a better multi-objective OPF solution. However, the simulation results indicated that the PFMOOPF can effectively minimize individual-objective and maximize the overall FSF

for multi-objective OPF solutions, incorporating uncertainty of PVPP, WPP, and load in the power system.

REFERENCES

O. Alsac and B. Stott, "Optimal load flow with steady state security", **IEEE trans, Power Apparatus and System**, Vol. PAS93, No. 3, pp.745-751, 1974.

M.A. Abido, "Optimal power flow using particle swarm optimization", **Electrical Power and Energy Systems 24**, pp.563-571, 2002.

A. G. Bakirtzis, Pandel N. Biskas, C. E. Zoumas and V. Petrids, "Optimal Power Flow by Enhanced Genetic Algorithm", **IEEE Transactions on power systems**, Vol.17, No2, pp. 229-236, 2002

A. Bhattacharya, "Solution of Optimal Reactive Power Flow using Biogeography-Based Optimization", **International Journal of Electrical, Computer, Energetic, Electronic and Communication Engineering**, Vol. 4, No. 3 ,2010.

B. Emre and R.Idil, "Optimal Power Flow Solution Using Particle Swarm Optimization Algorithm", **EuroCon 2013**, 2013.

R. Pratap Singh, V. Mukherjee and S.P. Ghoshal, "Optimal power flow by particle swarm optimization with an aging leader and challengers", **International Journal of Engineering, Science and Technology**, Vol. 7, No. 3, 2015, pp. 123-132

H. J. Touma, "Study of The Economic Dispatch Problem on IEEE 30 buses system using Whale Optimization Algorithm", **IJETS**, Vol.5, No.1, 2016.

U. Khaled, A. M. Eltamaly and A. Beroual, "Optimal Power Flow Using Particle Swarm Optimization of Renewable Hybrid Distributed Generation", **Energies**, 2017

D. P. Ladumor, R. H. Bhesdadiya, I. N. Trivedi and P. Jangir, "Optimal Power Flow Problem Solution with SVC using Meta-heuristic Algorithm", 3rd International Conference on Advances in Electrical, **Electronics, Information, Communication and Bio-Informatics (AEEICB17)**, Chennai, India, 2017.

M. Abdo, S. Kamel, M. Ebeed, J. Yu and F. Jurado, "Solving Non-Smooth Optimal Power Flow Problems Using a Developed Grey Wolf Optimizer", **Energies**, 2018.

T. T. Nguyen, "A high performance social spider optimization algorithm for optimal power flow solution with single objective optimization", **Energy 171**, pp. 218-240, 2019.

P. Muangkhiew and K. Chayakulkheeree, "Unified Optimal Power Flow Incorporating Full AC Control Variables", **2021 9th International Electrical Engineering Congress (iEECON)**, 2021.

M. S. Kumari and S. Maheswarapu, "Enhanced Genetic Algorithm based computation technique for multi-objective Optimal Power Flow solution", **Electrical Power and Energy Systems**, Vol. 32, Issue 6, pp. 736-742, 2010.

S. Sivasubramani and K.S. Swarup, "Multi-objective harmony search algorithm for optimal power flow problem", **International Journal of Electrical Power & Energy Systems**, Vol.33, Issue 3, pp.745-752, 2011.

C. Kumar and Dr. Ch. Padmanabha Raju, "Constrained Optimal Power Flow using Particle Swarm Optimization", **International Journal of Emerging Technology and Advanced Engineering**, Vol.2, Issue 2, 2012.

M. Rezaei Adaryani and A. Karami, "Artificial bee colony algorithm for solving multi-objective optimal power flow problem", **International Journal of Electrical Power & Energy Systems**, Vol.53, pp. 219-230, 2013.

H.R.E.H. Bouchekara, "Optimal power flow using black-hole-based optimization approach", **Applied Soft Computing**, Vol.24, pp. 879-888, 2014.

M. Ghasemi, S. Ghavidel, M. Gitizadeh and E. Akbari, "An improved teaching–learning-based optimization algorithm using Lévy mutation strategy for non-smooth optimal power flow", **International Journal of Electrical Power & Energy Systems**, Vol.65, pp. 375-384, 2015.

A. A. El-Fergany and H. M. Hasanien, "Single and Multi-objective Optimal Power Flow Using Grey Wolf Optimizer and Differential Evolution Algorithms", **Electric Power Components and Systems**, Vol. 43, Issue 13, 2015.

X. Yuan, B. Zhang, P. Wang, J. Liang, Y. Yuan, Y. Huang, and X. Lei, "Multi-objective optimal power flow based on improved strength Pareto evolutionary algorithm", **Energy (2017)**, Vol. 122, pp. 70-82, 2017.

M. A. Taher1, S. Kamel, F. Jurado and M. Ebeed, "An improved moth‑flame optimization algorithm for solving optimal power flow problem", **International Transactions on Electrical Energy Systems**, 2018.

Z. Ullah, S. Wang, J. Radosavljevic and J. Lai, "A Solution to the Optimal Power Flow Problem Considering WT and PV Generation", **IEEE. Translations**, Vol.7, 2019.

M. A. Ilyas, G. Abbas, T. Alquthami, M. Awais and M. B. Rasheed, "Multi-Objective Optimal Power Flow with Integration of Renewable Energy Sources Using Fuzzy Membership Function", **IEEE**, Vol.8, 2020.

M. K. Ahmed, M. H. Osman, A. A. Shehata, and N. V. Korovkin, "A Solution of Optimal Power Flow Problem in Power System Based on Multi Objective Particle Swarm Algorithm", **2021 IEEE Conference of Russian Young Researchers in Electrical and Electronic Engineering (ElConRus)**, 2021.

A. K. Khamees , A. Y. Abdelaziz, M. R. Eskaros, H. H. Alhelou, and M. A. Attia, "Stochastic Modeling for Wind Energy and Multi-Objective Optimal Power Flow by Novel Meta-Heuristic Method", **IEEE Access**, Vol. 9, pp. 158353 – 158366, 2021.

E. Naderia, M. Pourakbari-Kasmaeib, F. V. Cernac, M. Lehtonen, "A novel hybrid self-adaptive heuristic algorithm to handle single- and multi-objective optimal power flow problems", **International Journal of Electrical Power & Energy Systems**, Vol. 25, 2021.

S. Li, W. Gong, L. Wang, and Q. Gu, "Multi-objective optimal power flow with stochastic wind and solar power", **Applied Soft Computing**, Vol. 114, 2022.

S. Conti and S. Raiti, "Probabilistic load flow using Monte Carlo techniques for distribution networks with photovoltaic generators", **Solar Energy**, Vol. 81, pp. 1473-1481, 2007.

J. Hetzer, D. C. Yu, and K. Bhattarai, "An Economic Dispatch Model Incorporating Wind Power", **IEEE Transactions on energy conversion**, Vol. 23, No. 2, 2008.

Y. Li, W. Li, W. Yan, J. Yu, and X. Zhao, "Probabilistic Optimal Power Flow Considering Correlations of Wind Speeds Following Different Distributions", **IEEE Transactions on Power Systems**, Vol. 29, No. 4, 2014.

K. Chayakulkheeree, "Probabilistic Optimal Power Flow: An Alternative Solution for Emerging High Uncertain Power Systems", **iEECON**, 2014.

H. Zhang, C. S. Lai, F. Xu and L. L. Lai, "Comparison between Probabilistic Optimal Power Flow and Probabilistic Power Flow with Carbon Emission Consideration", **IEEE International Conference on Systems, Man, and Cybernetics**, 2015.

D. Fang, M. Zou and S. Djokic, "Probabilistic OPF Incorporating Uncertainties in Wind Power Outputs and Line Thermal Ratings", **IEEE**, 2018.

U. Chhor, U. Leeton and K. Chayakulkheeree, "Probabilistic Optimal Power Dispatch Considering Price-Based Real-Time Demand Response", **International Journal of Intelligent Engineering and Systems**, Vol.12, No.1, 2019.

G. Li, W. Lu, J. Bian, F. Qin and J. Wu, "Probabilistic Optimal Power Flow Calculation Method Based on Adaptive Diffusion Kernel Density Estimation", **Energy Res.**, 2019.

K. Rojanaworahiran and K. Chayakulkheeree, "Probabilistic Optimal Power Flow Considering Load and Solar Power Uncertainties Using Particle Swarm Optimization", **GMSARN International Journal**, 2019.

M.U. Keerio, A. Ali, M. Saleem and N. Hussain, "Multi-Objective Optimal Reactive Power Dispatch Considering Probabilistic Load Demand Along with Wind and Solar Power Integration", **International Conference on Smart Power & Internet Energy Systems**, 2020.

A. K. Khamees , A. Y. Abdelaziz, M. R. Eskaros, H. H. Alhelou, and M. A. Attia, "Stochastic Modeling for Wind Energy and Multi-Objective Optimal Power Flow by Novel Meta-Heuristic Method", **IEEE Access**, Vol. 9, pp. 158353 – 158366, 2021.

J. Kennedy and R. Eberhart, "Particle swarm optimization", **International Conference on Neural Networks**, 1995.

H. J. Zimmermann, "Fuzzy Sets. Decision Making, and Expert Systems", **Kluwer Adademic Publishers**, 1987.

M. R. Patal, "Wind and Solar Power Systems Design, Analysis, and Operation", Second Edition,2006.
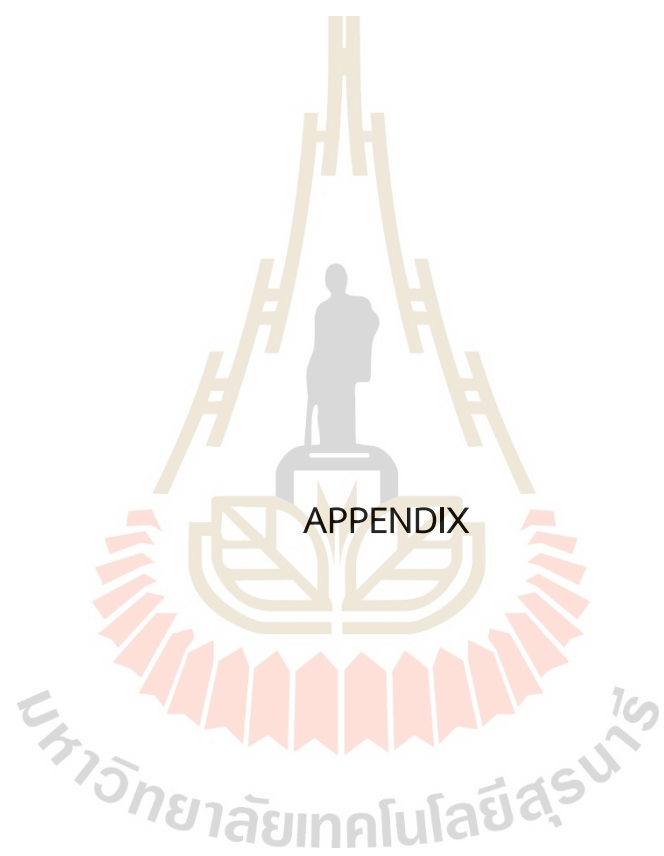
APPENDIX

APPENDIX A

IEEE 30-bus test system data
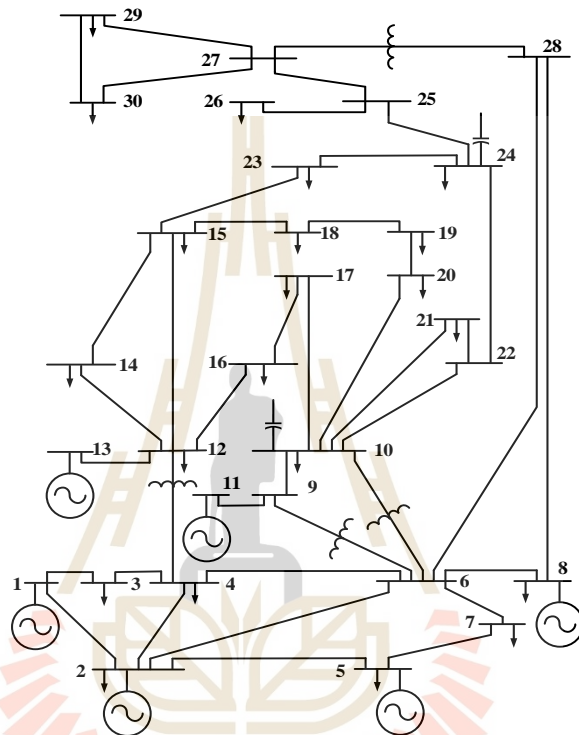
Figure A.1 The IEEE 30-bus test system

Table A.1   Bus load and injection data of IEEE 30-bus test system

Bus	Load (MW)	Bus	Load (MW)
1	0.00	16	3.50
2	21.70	17	9.00
3	2.40	18	3.20
4	67.60	19	9.50
5	34.20	20	2.20
6	0.00	21	17.50
7	22.80	22	0.00
8	30.00	23	3.20
9	0.00	24	8.70
10	5.80	25	0.00
11	0.00	26	3.50
12	11.20	27	0.00
13	0.00	28	0.00
14	6.20	29	2.40
15	8.20	30	10.60

Table A.2   Reactive power limit data of IEEE 30-bus test system

Bus	Qmin (p.u.)	Qmax (p.u.)	Bus	Qmin (p.u.)	Qmax (p.u.)
1	-0.2000	0.0000	16		
2	-0.2000	0.2000	17	-0.0500	0.0500
3			18	0.0000	0.0550
4			19		
5	-0.1500	0.1500	20		
6			21		
7			22		
8	-0.1500	0.1500	23	-0.0500	0.0550
9			24		
10			25		
11	-0.1000	0.1000	26		
12			27	-0.0055	0.0550
13	-0.1500	0.1500	28		
14			29		
15			30		
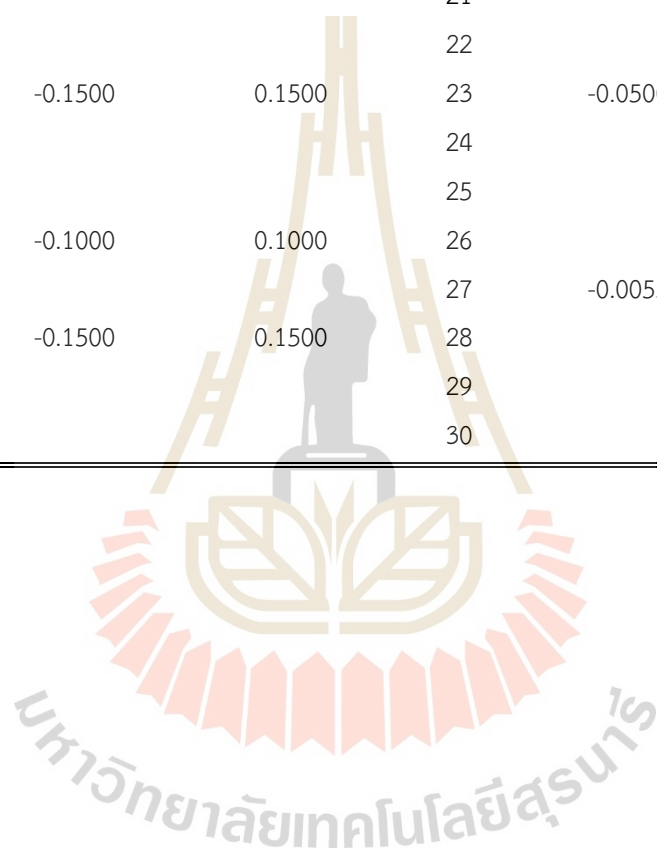
Table A.3   Line parameter of IEEE 30-bus test system

Line	From (Bus)	To (Bus)	R (p.u.)	X (p.u.)	Tap Ratio	Rating (p.u.)
1	1	2	0.0192	0.0575		0.3000
2	1	3	0.0452	0.1852	0.9610	0.3000
3	2	4	0.0570	0.1737	0.9560	0.3000
4	3	4	0.0132	0.0379		0.3000
5	2	5	0.0472	0.1983		0.3000
6	2	6	0.0581	0.1763		0.3000
7	4	6	0.0119	0.0414		0.3000
8	5	7	0.0460	0.1160		0.3000
9	6	7	0.0267	0.0820		0.3000
10	6	8	0.0120	0.0420		0.3000
11	6	9	0.0000	0.2080		0.3000
12	6	10	0.0000	0.5560		0.3000
13	6	11	0.0000	0.2080		0.3000
14	9	10	0.0000	0.1100	0.9700	0.3000
15	4	12	0.0000	0.2560	0.9650	0.6500
16	12	13	0.0000	0.1400	0.9635	0.6500
17	12	14	0.1231	0.2559		0.3200
18	12	15	0.0662	0.1304		0.3200
19	12	16	0.0945	0.1987		0.3200
20	14	15	0.2210	0.1997		0.1600
21	16	17	0.0824	0.1932		0.1600
22	15	18	0.1070	0.2185		0.1600
23	18	19	0.0639	0.1292	0.9590	0.1600
24	19	20	0.0340	0.0680		0.3200
25	10	20	0.0936	0.2090		0.3200
26	10	17	0.0324	0.0845	0.9850	0.3200
27	10	21	0.0348	0.0749		0.3000
28	10	22	0.0727	0.1499		0.3000
29	21	22	0.1160	0.0236		0.3000
30	15	23	0.1000	0.2020		0.1600
31	22	24	0.1150	0.1790		0.3000
32	23	24	0.1320	0.2700	0.9655	0.1600

Table A.3   Line parameter of IEEE 30-bus test system (Continued)

Line	From (Bus)	To (Bus)	R (p.u.)	X (p.u.)	Tap Ratio	Rating (p.u.)
33	24	25	0.1885	0.3292		0.3000
34	25	26	0.2544	0.3800		0.3000
35	25	27	0.1093	0.2087		0.3000
36	28	27	0.0000	0.3960		0.3000
37	27	29	0.2198	0.4153	0.9810	0.3000
38	27	30	0.3202	0.6027		0.3000
39	29	30	0.2399	0.4533		0.3000
40	8	28	0.0636	0.2000	0.9530	0.3000
41	6	28	0.0169	0.0599		0.3000

APPENDIX B

Thailand daily load profile (12:00 p.m. of every day in 2018)

Table B.1   Thailand daily load profile

Day	Load (p.u.)	Day	Load (p.u.)	Day	Load (p.u.)
1	0.4373	28	0.6981	55	0.7893
2	0.4799	29	0.7219	56	0.7613
3	0.6392	30	0.6439	57	0.7279
4	0.7168	31	0.7363	58	0.6243
5	0.7456	32	0.7651	59	0.7191
6	0.7623	33	0.7459	60	0.7282
7	0.7558	34	0.7406	61	0.7453
8	0.7282	35	0.7506	62	0.7667
9	0.6491	36	0.7036	63	0.7928
10	0.7381	37	0.5520	64	0.7722
11	0.7737	38	0.5669	65	0.6714
12	0.7821	39	0.6333	66	0.8288
13	0.7939	40	0.6685	67	0.8466
14	0.7869	41	0.7071	68	0.8448
15	0.7561	42	0.7333	69	0.8483
16	0.6743	43	0.7438	70	0.8583
17	0.7644	44	0.6466	71	0.8085
18	0.8059	45	0.7527	72	0.7085
19	0.7995	46	0.7913	73	0.8594
20	0.7974	47	0.7884	74	0.8607
21	0.8022	48	0.7845	75	0.8689
22	0.7736	49	0.7921	76	0.8649
23	0.6317	50	0.7635	77	0.8577
24	0.6274	51	0.6586	78	0.8229
25	0.6334	52	0.6720	79	0.7003
26	0.6394	53	0.7833	80	0.8623
27	0.6493	54	0.8205	81	0.8729

Table B.1   Thailand daily load profile (Continued)

Day	Load (p.u.)	Day	Load (p.u.)	Day	Load (p.u.)
82	0.8761	115	0.9120	148	0.8250
83	0.8736	116	0.9364	149	0.6925
84	0.8704	117	0.9445	150	0.8323
85	0.7858	118	0.9454	151	0.8396
86	0.6687	119	0.9131	152	0.8299
87	0.8093	120	0.8549	153	0.8415
88	0.8486	121	0.6174	154	0.8428
89	0.8504	122	0.7377	155	0.7802
90	0.8555	123	0.9219	156	0.6983
91	0.8375	124	0.9407	157	0.8437
92	0.8095	125	0.8824	158	0.8601
93	0.7064	126	0.8683	159	0.8314
94	0.8602	127	0.8634	160	0.8477
95	0.8800	128	0.7590	161	0.8552
96	0.8340	129	0.8962	162	0.8199
97	0.9003	130	0.9083	163	0.6861
98	0.8847	131	0.9430	164	0.8484
99	0.8323	132	0.9416	165	0.8599
100	0.7351	133	0.9236	166	0.8554
101	0.8083	134	0.8564	167	0.8277
102	0.7657	135	0.7555	168	0.8103
103	0.5470	136	0.8897	169	0.7646
104	0.5372	137	0.8646	170	0.6827
105	0.5538	138	0.8482	171	0.8454
106	0.6004	139	0.8762	172	0.8060
107	0.6499	140	0.7831	173	0.8157
108	0.8872	141	0.7908	174	0.8297
109	0.9115	142	0.7258	175	0.8179
110	0.9194	143	0.8754	176	0.7829
111	0.9133	144	0.8704	177	0.6731
112	0.9200	145	0.8687	178	0.8137
113	0.8854	146	0.8532	179	0.8132
114	0.7682	147	0.8606	180	0.8155

Table B.1   Thailand daily load profile (Continued)

Day	Load (p.u.)	Day	Load (p.u.)	Day	Load (p.u.)
280	0.8089	309	0.7384	338	0.5943
281	0.7720	310	0.6254	339	0.5319
282	0.6654	311	0.7974	340	0.7418
283	0.8086	312	0.7886	341	0.7398
284	0.8388	313	0.8024	342	0.7330
285	0.8363	314	0.8083	343	0.7298
286	0.8145	315	0.7920	344	0.7009
287	0.8080	316	0.7658	345	0.5881
288	0.7829	317	0.6628	346	0.6973
289	0.6588	318	0.8197	347	0.7603
290	0.7768	319	0.8418	348	0.7665
291	0.8072	320	0.8203	349	0.7689
292	0.8147	321	0.8111	350	0.7331
293	0.8276	322	0.8104	351	0.6646
294	0.8219	323	0.7828	352	0.5737
295	0.7576	324	0.6633	353	0.7123
296	0.6207	325	0.8155	354	0.7304
297	0.6900	326	0.8119	355	0.7450
298	0.8011	327	0.8093	356	0.7482
299	0.7630	328	0.8076	357	0.7511
300	0.8054	329	0.7965	358	0.7286
301	0.7930	330	0.7815	359	0.6111
302	0.7428	331	0.6219	360	0.7437
303	0.6126	332	0.7683	361	0.7132
304	0.7625	333	0.7606	362	0.6288
305	0.7668	334	0.7602	363	0.5557
306	0.7785	335	0.7271	364	0.4786
307	0.7532	336	0.7344	365	0.4233
308	0.7483	337	0.7142		

APPENDIX C

Thailand solar irradiance data (12:00 p.m. of every day in 2021)

Table C.1   Thailand solar irradiance data

Day	Load (p.u.)	Day	Load (p.u.)	Day	Load (p.u.)
1	0.8348	28	0.8205	55	0.9262
2	0.8701	29	0.8415	56	0.8966
3	0.8703	30	0.7885	57	0.9931
4	0.8624	31	0.8883	58	0.9807
5	0.7752	32	0.8907	59	0.9522
6	0.8669	33	0.9190	60	0.9399
7	0.8536	34	0.9077	61	0.8966
8	0.7841	35	0.9127	62	0.6430
9	0.8893	36	0.9089	63	0.8681
10	0.8924	37	0.8684	64	0.9433
11	0.8527	38	0.9116	65	1.0000
12	0.8836	39	0.8259	66	0.9609
13	0.9090	40	0.7219	67	0.8277
14	0.9106	41	0.9169	68	0.7493
15	0.8801	42	0.9850	69	0.8316
16	0.8590	43	0.9707	70	0.8881
17	0.7905	44	0.9433	71	0.8540
18	0.8809	45	0.9200	72	0.8252
19	0.8494	46	0.9420	73	0.7846
20	0.8806	47	0.8755	74	0.8126
21	0.7394	48	0.7562	75	0.7998
22	0.8534	49	0.9229	76	0.7900
23	0.8634	50	0.9582	77	0.7497
24	0.8280	51	0.9703	78	0.8798
25	0.8359	52	0.9330	79	0.8845
26	0.7835	53	0.9593	80	0.8764
27	0.7533	54	0.9347	81	0.4163

Table C.1   Thailand solar irradiance data (Continued)

Day	Load (p.u.)	Day	Load (p.u.)	Day	Load (p.u.)
82	0.9508	115	0.7641	148	0.5257
83	0.9602	116	0.7378	149	0.9330
84	0.8245	117	0.6925	150	0.8938
85	0.8143	118	0.5369	151	0.9614
86	0.9056	119	0.6376	152	0.9762
87	0.9414	120	0.4696	153	0.9420
88	0.9588	121	0.6326	154	0.9640
89	0.7997	122	0.9120	155	0.8913
90	0.9689	123	0.9043	156	0.8567
91	0.8624	124	0.9184	157	0.8874
92	0.9824	125	0.8349	158	0.6306
93	0.7975	126	0.5863	159	0.7524
94	0.0934	127	0.9073	160	0.6647
95	0.1469	128	0.7363	161	0.5987
96	0.1492	129	0.9155	162	0.4355
97	0.6782	130	0.9370	163	0.7417
98	0.8222	131	0.8463	164	0.4980
99	0.8937	132	0.9173	165	0.6161
100	0.8179	133	0.9500	166	0.5160
101	0.7594	134	0.9444	167	0.7443
102	0.7332	135	0.8631	168	0.6886
103	0.8384	136	0.8770	169	0.8477
104	0.6127	137	0.9002	170	0.9786
105	0.9895	138	0.7715	171	0.9362
106	0.8747	139	0.9129	172	0.9577
107	0.8573	140	0.8289	173	0.9479
108	0.8938	141	0.9270	174	0.8833
109	0.8607	142	0.9636	175	0.8708
110	0.8259	143	0.9733	176	0.8453
111	0.8327	144	0.7766	177	0.8870
112	0.8707	145	0.6580	178	0.9712
113	0.8156	146	0.7960	179	0.7833
114	0.8256	147	0.7918	180	0.8554

Table C.1   Thailand solar irradiance data (Continued)

Day	Load (p.u.)	Day	Load (p.u.)	Day	Load (p.u.)
181	0.8693	214	0.7310	247	0.7513
182	0.9250	215	0.6771	248	0.6833
183	0.9599	216	0.8219	249	0.7813
184	0.9850	217	0.8260	250	0.5225
185	0.9731	218	0.8098	251	0.7814
186	0.9535	219	0.7898	252	0.6893
187	0.8506	220	0.9008	253	0.6755
188	0.7531	221	0.9658	254	0.5158
189	0.6611	222	0.9368	255	0.8227
190	0.6722	223	0.7177	256	0.6250
191	0.6669	224	0.7860	257	0.5624
192	0.2722	225	0.8299	258	0.6255
193	0.8863	226	0.5621	259	0.6433
194	0.8813	227	0.4940	260	0.8170
195	0.3892	228	0.7695	261	0.9226
196	0.6202	229	0.9526	262	0.4326
197	0.7420	230	0.9943	263	0.5163
198	0.9117	231	0.9054	264	0.6743
199	0.6956	232	0.8884	265	0.7276
200	0.5688	233	0.4580	266	0.7733
201	0.7985	234	0.7901	267	0.6924
202	0.6367	235	0.9686	268	0.3186
203	0.6246	236	0.9767	269	0.5307
204	0.5466	237	0.9080	270	0.7957
205	0.4769	238	0.5568	271	0.7858
206	0.4265	239	0.5296	272	0.9154
207	0.6194	240	0.4000	273	0.8656
208	0.8202	241	0.7229	274	0.9161
209	0.7287	242	0.8340	275	0.7831
210	0.8407	243	0.7002	276	0.8028
211	0.8326	244	0.8196	277	0.8490
212	0.7167	245	0.8107	278	0.7800
213	0.7248	246	0.5948	279	0.6548

Table C.1   Thailand solar irradiance data (Continued)

Day	Load (p.u.)	Day	Load (p.u.)	Day	Load (p.u.)
280	0.7526	309	0.7741	338	0.8621
281	0.7783	310	0.7353	339	0.7880
282	0.5187	311	0.7569	340	0.8191
283	0.8537	312	0.5366	341	0.8723
284	0.7061	313	0.7193	342	0.8704
285	0.7107	314	0.7225	343	0.7469
286	0.7317	315	0.8600	344	0.8514
287	0.6892	316	0.6838	345	0.8740
288	0.5145	317	0.4193	346	0.8556
289	0.8512	318	0.6055	347	0.8064
290	0.3149	319	0.7326	348	0.8555
291	0.4736	320	0.6194	349	0.8360
292	0.6713	321	0.6912	350	0.8618
293	0.7502	322	0.5998	351	0.7488
294	0.8037	323	0.7797	352	0.8484
295	0.6368	324	0.7400	353	0.6354
296	0.5740	325	0.7343	354	0.8573
297	0.8569	326	0.7811	355	0.8014
298	0.8726	327	0.4762	356	0.8238
299	0.8904	328	0.6825	357	0.8237
300	0.8862	329	0.7863	358	0.7713
301	0.3318	330	0.7588	359	0.7716
302	0.5781	331	0.8379	360	0.7806
303	0.6869	332	0.8889	361	0.8255
304	0.7038	333	0.7660	362	0.8768
305	0.8288	334	0.3426	363	0.7919
306	0.7219	335	0.4832	364	0.7454
307	0.7692	336	0.5269	365	0.7843
308	0.7804	337	0.8412		

APPENDIX D

Thailand wind speed data (12:00 p.m. of every day in 2021)

Table D.1 Thailand wind speed data

Day	Load (p.u.)	Day	Load (p.u.)	Day	Load (p.u.)
1	0.6373	28	0.0140	55	0.3361
2	0.3782	29	0.4776	56	0.1303
3	0.2255	30	0.1513	57	0.0020
4	0.4398	31	0.1401	58	0.0140
5	0.2647	32	0.1176	59	0.4594
6	0.2899	33	0.1891	60	0.3431
7	0.1681	34	0.2941	61	0.2717
8	0.5448	35	0.4860	62	0.5196
9	0.5000	36	0.1933	63	0.1289
10	0.3291	37	0.2157	64	0.0896
11	0.6331	38	0.0020	65	0.0322
12	0.8193	39	0.1345	66	0.2101
13	0.2367	40	0.1849	67	0.0168
14	0.0020	41	0.1891	68	0.0020
15	0.0020	42	0.0020	69	0.0020
16	0.0020	43	0.0020	70	0.0020
17	0.3193	44	0.0020	71	0.0020
18	0.6499	45	0.0350	72	0.0924
19	0.1275	46	0.3375	73	0.0798
20	0.0020	47	0.3039	74	0.2773
21	0.0020	48	0.2507	75	0.3599
22	0.0020	49	0.5826	76	0.3277
23	0.0020	50	0.6176	77	0.0238
24	0.0490	51	0.2157	78	0.2465
25	0.0020	52	0.0020	79	0.3754
26	0.0020	53	0.0020	80	0.1359
27	0.0938	54	0.0252	81	0.6008

Table D.1   Thailand wind speed data (Continued)

Day	Load (p.u.)	Day	Load (p.u.)	Day	Load (p.u.)
82	0.2605	115	0.3992	148	0.2703
83	0.0020	116	0.0020	149	0.4132
84	0.2549	117	0.0020	150	0.4104
85	0.1261	118	0.1751	151	0.3263
86	0.3081	119	0.0020	152	0.3445
87	0.3431	120	0.0020	153	0.0784
88	0.2815	121	0.0020	154	0.0252
89	0.2003	122	0.0020	155	0.0504
90	0.3221	123	0.0020	156	0.2717
91	0.1975	124	0.0020	157	0.4678
92	0.2689	125	0.0020	158	0.6289
93	0.1569	126	0.0020	159	0.6106
94	0.4076	127	0.2003	160	0.5266
95	0.0070	128	0.0020	161	0.4020
96	0.0020	129	0.0020	162	0.6513
97	0.0020	130	0.0020	163	0.4062
98	0.0020	131	0.1303	164	0.6429
99	0.0020	132	0.0476	165	0.6947
100	0.0742	133	0.1429	166	0.5042
101	0.0020	134	0.0994	167	0.5140
102	0.0020	135	0.1597	168	0.2381
103	0.0020	136	0.3824	169	0.1134
104	0.0644	137	0.0266	170	0.0154
105	0.0020	138	0.1737	171	0.3613
106	0.0020	139	0.0020	172	0.3697
107	0.0020	140	0.0020	173	0.2675
108	0.0020	141	0.0020	174	0.3978
109	0.0020	142	0.3725	175	0.4958
110	0.0020	143	0.4244	176	0.2479
111	0.0020	144	0.2101	177	0.3179
112	0.0020	145	0.1008	178	0.4398
113	0.0560	146	0.1022	179	0.3221
114	0.0020	147	0.1905	180	0.1485

Table D.1   Thailand wind speed data (Continued)

Day	Load (p.u.)	Day	Load (p.u.)	Day	Load (p.u.)
181	0.2535	214	0.5980	247	0.4090
182	0.2367	215	0.5504	248	0.5700
183	0.0224	216	0.6289	249	0.1695
184	0.2409	217	0.5882	250	0.7255
185	0.0700	218	0.5084	251	0.2885
186	0.0020	219	0.4524	252	0.1485
187	0.1723	220	0.2241	253	0.3768
188	0.1064	221	0.1863	254	0.3557
189	0.2157	222	0.1947	255	0.5378
190	0.1583	223	0.4594	256	0.7045
191	0.0056	224	0.5056	257	0.4062
192	0.6569	225	0.4384	258	0.0020
193	0.2185	226	0.4412	259	0.4076
194	0.0020	227	0.7451	260	0.1331
195	0.0020	228	0.1261	261	0.0020
196	0.0020	229	0.0020	262	0.0020
197	0.2591	230	0.0020	263	0.0420
198	0.4258	231	0.0020	264	0.3908
199	0.6499	232	0.0020	265	0.2703
200	1.0000	233	0.2563	266	0.0020
201	0.7409	234	0.1555	267	0.2199
202	0.8347	235	0.2479	268	0.1737
203	0.5504	236	0.2507	269	0.2171
204	0.4650	237	0.2437	270	0.0020
205	0.7927	238	0.1303	271	0.0020
206	0.7479	239	0.3053	272	0.0020
207	0.6779	240	0.4468	273	0.0020
208	0.5798	241	0.0336	274	0.1611
209	0.5336	242	0.0504	275	0.0560
210	0.5098	243	0.0020	276	0.0840
211	0.4048	244	0.0020	277	0.0020
212	0.6303	245	0.0020	278	0.2101
213	0.6162	246	0.6555	279	0.0980

Table D.1   Thailand wind speed data (Continued)

Day	Load (p.u.)	Day	Load (p.u.)	Day	Load (p.u.)
280	0.0020	309	0.0020	338	0.4566
281	0.1695	310	0.0168	339	0.4622
282	0.3950	311	0.0020	340	0.4384
283	0.4076	312	0.7325	341	0.2619
284	0.3796	313	0.5056	342	0.2577
285	0.1989	314	0.2185	343	0.4454
286	0.2871	315	0.2479	344	0.4230
287	0.2857	316	0.3305	345	0.2297
288	0.7143	317	0.6261	346	0.4174
289	0.1919	318	0.5350	347	0.7199
290	0.6162	319	0.3739	348	0.1499
291	0.0364	320	0.3768	349	0.1401
292	0.0020	321	0.2997	350	0.0364
293	0.0020	322	0.6008	351	0.4090
294	0.0020	323	0.1134	352	0.6499
295	0.0020	324	0.0020	353	0.5266
296	0.2437	325	0.0924	354	0.1555
297	0.3417	326	0.3319	355	0.0070
298	0.4090	327	0.5154	356	0.0020
299	0.1709	328	0.4818	357	0.0020
300	0.3557	329	0.4482	358	0.0020
301	0.1737	330	0.3137	359	0.1933
302	0.1148	331	0.4230	360	0.2815
303	0.1485	332	0.4566	361	0.5056
304	0.0020	333	0.6331	362	0.4636
305	0.0518	334	0.8810	363	0.5490
306	0.0020	335	0.7241	364	0.6723
307	0.0686	336	0.5798	365	0.5140
308	0.0020	337	0.5028		

APPENDIX E

Line flow results data

Table E.1 Line flow results data of the IEEE 30-bus test system for TSCM (Table 3.2)

From Bus	To Bus	Forward Power Flow		Power Loss		MVA Flow	MVA Limit
		MW	MVAR	MW	MVAR	MVA	MVA
1	2	118.5000	-15.6100	2.2500	0.4300	119.5200	130.0000
1	3	58.9900	-2.5600	1.3000	0.4800	59.0500	130.0000
2	1	-116.2400	16.0400	2.2500	0.4300	117.3500	130.0000
2	4	33.9200	-4.6000	0.5600	-2.6100	34.2300	65.0000
2	5	63.7500	0.1000	1.6200	1.9900	63.7500	130.0000
2	6	45.5400	-1.5200	1.0200	-1.2400	45.5700	65.0000
3	1	-57.6900	3.0400	1.3000	0.4800	57.7700	130.0000
3	4	55.2900	-4.2400	0.3500	0.0200	55.4600	130.0000
4	2	-33.3600	2.0000	0.5600	-2.6100	33.4200	65.0000
4	3	-54.9500	4.2600	0.3500	0.0200	55.1100	130.0000
4	6	51.8900	12.1000	0.2900	-0.0100	53.2800	90.0000
4	12	28.8200	-19.9500	0.0000	3.2900	35.0500	130.0000
5	2	-62.1200	1.8900	1.6200	1.9900	62.1500	130.0000
5	7	-10.7800	8.1800	0.0800	-2.0800	13.5300	70.0000
6	2	-44.5200	0.2800	1.0200	-1.2400	44.5200	65.0000
6	4	-51.5900	-12.1100	0.2900	-0.0100	52.9900	90.0000
6	7	33.9300	-0.4400	0.2700	-1.0800	33.9400	130.0000
6	8	11.2400	-14.0900	0.0300	-0.9100	18.0300	32.0000
6	9	22.2900	33.8300	0.0000	2.6200	40.5100	130.0000
6	10	13.4500	-5.3800	0.0000	1.1400	14.4900	65.0000
6	28	15.2000	-2.0900	0.0300	-1.3500	15.3400	32.0000
7	5	10.8600	-10.2600	0.0800	-2.0800	14.9400	70.0000
7	6	-33.6600	-0.6400	0.2700	-1.0800	33.6700	130.0000
8	6	-11.2100	13.1800	0.0300	-0.9100	17.3100	32.0000
8	28	2.2600	-0.1000	0.0100	-4.8500	2.2600	32.0000

Table E.1 Line flow results data of the IEEE 30-bus test system for TSCM
(Table 3.2) (Continued)

From Bus	To Bus	Forward Power Flow		Power Loss		MVA Flow	MVA Limit
		MW	MVAR	MW	MVAR	MVA	MVA
9	6	-22.2800	-31.2000	0.0000	2.6200	38.3400	130.0000
9	10	34.1200	36.2300	0.0000	2.3400	49.7700	65.0000
9	11	-11.8400	-5.0300	0.0000	0.3000	12.8600	65.0000
10	6	-13.4500	6.5200	0.0000	1.1400	14.9500	65.0000
10	9	-34.1200	-33.8900	0.0000	2.3400	48.0900	65.0000
10	17	6.8900	8.9900	0.0400	0.1000	11.3300	32.0000
10	20	10.1300	5.9300	0.1200	0.2600	11.7400	32.0000
10	21	16.6000	8.9800	0.1100	0.2500	18.8800	32.0000
10	22	8.1500	3.9200	0.0500	0.1100	9.0400	32.0000
11	9	11.8400	5.3200	0.0000	0.3000	12.9800	65.0000
12	4	-28.8200	23.2400	0.0000	3.2900	37.0300	130.0000
12	13	-12.0000	-32.8000	0.0000	1.6000	34.9300	65.0000

Table E.2   Line flow results of the modified IEEE 30-bus test system for TSCM
(Table 4.1)

From	To	Forward Power Flow		Power Loss		MVA Flow	MVA Limit
Bus	Bus	MW	MVAR	MW	MVAR	MVA	MVA
1	2	118.0100	-16.3100	2.2400	0.3800	119.1300	130.0000
1	3	59.0400	-2.0400	1.3000	0.4900	59.0800	130.0000
2	1	-115.7700	16.6900	2.2400	0.3800	116.9700	130.0000
2	4	34.2400	-3.7500	0.5700	-2.5800	34.4400	65.0000
2	5	63.3300	0.1600	1.6000	1.9000	63.3300	130.0000
2	6	45.2000	-5.0800	1.0100	-1.3100	45.4800	65.0000
3	1	-57.7400	2.5300	1.3000	0.4900	57.7900	130.0000
3	4	55.3400	-3.7300	0.3500	0.0300	55.4600	130.0000
4	2	-33.6700	1.1700	0.5700	-2.5800	33.6900	65.0000
4	3	-54.9900	3.7600	0.3500	0.0300	55.1200	130.0000
4	6	48.7500	-6.5900	0.2500	-0.1700	49.2000	90.0000
4	12	32.3100	0.0600	0.0000	2.4500	32.3100	130.0000
5	2	-61.7200	1.7400	1.6000	1.9000	61.7500	130.0000
5	7	-11.1700	5.0300	0.0700	-2.1300	12.2500	70.0000
6	2	-44.1900	3.7800	1.0100	-1.3100	44.3500	65.0000
6	4	-48.5100	6.4200	0.2500	-0.1700	48.9300	90.0000
6	7	34.3100	2.6600	0.2800	-1.0800	34.4200	130.0000
6	8	11.1800	1.6200	0.0100	-0.9800	11.3000	32.0000
6	9	18.4900	-12.7200	0.0000	1.0500	22.4400	130.0000
6	10	13.0700	-1.4600	0.0000	0.9200	13.1500	65.0000
6	28	15.6500	-0.3000	0.0400	-1.3600	15.6500	32.0000
7	5	11.2400	-7.1600	0.0700	-2.1300	13.3200	70.0000
7	6	-34.0400	-3.7400	0.2800	-1.0800	34.2400	130.0000
8	6	-11.1600	-2.6100	0.0100	-0.9800	11.4600	32.0000
8	28	2.3000	-2.8500	0.0000	-4.8800	3.6600	32.0000
9	6	-18.4900	13.7800	0.0000	1.0500	23.0500	130.0000
9	10	30.4400	-3.4400	0.0000	0.9800	30.6400	65.0000
9	11	-11.9500	-10.3400	0.0000	0.4900	15.8000	65.0000
10	6	-13.0700	2.3800	0.0000	0.9200	13.2800	65.0000
10	9	-30.4400	4.4200	0.0000	0.9800	30.7600	65.0000

Table E.2   Line flow results of the modified IEEE 30-bus test system for TSCM
                 (Table 4.1) (Continued)

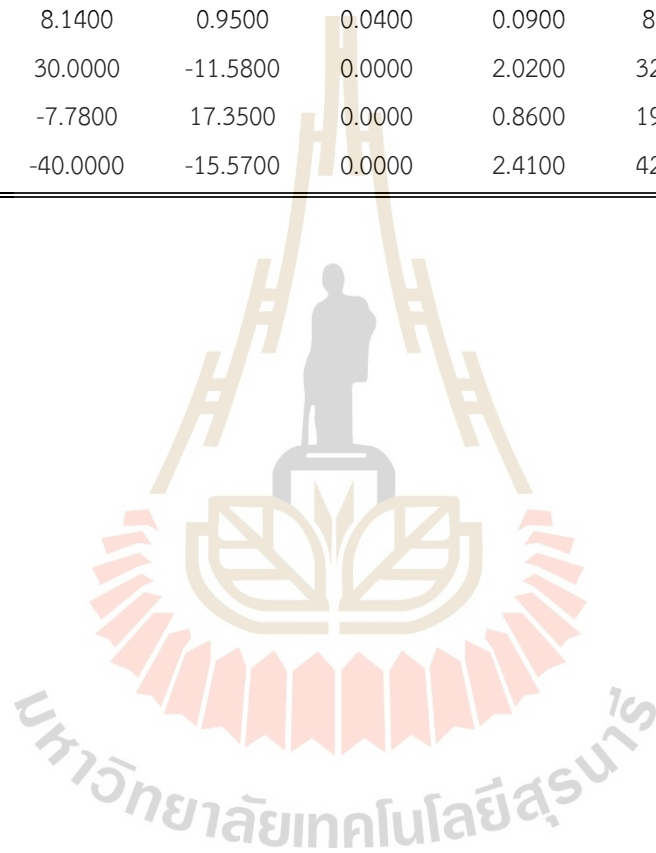| From Bus	To Bus	Forward Power Flow		Power Loss		MVA Flow	MVA Limit
		MW	MVAR	MW	MVAR	MVA	MVA
10	17	5.3600	-2.1100	0.0100	0.0300	5.7600	32.0000
10	20	9.0100	0.6300	0.0700	0.1600	9.0400	32.0000
10	21	15.8000	-0.1300	0.0800	0.1800	15.8000	32.0000
10	22	7.5500	-0.1900	0.0400	0.0800	7.5500	32.0000
11	9	11.9500	10.8300	0.0000	0.4900	16.1300	65.0000
12	4	-32.3100	2.3900	0.0000	2.4500	32.4000	130.0000
12	13	-12.0000	28.4500	0.0000	1.2200	30.8700	65.0000

Table E.3   Line flow results of the modified IEEE 30-bus test system for APLM
(Table 4.1)

From Bus	To Bus	Forward Power Flow		Power Loss		MVA Flow	MVA Limit
		MW	MVAR	MW	MVAR	MVA	MVA
1	2	27.5600	-7.5700	0.1200	-6.0000	28.5800	130.0000
1	3	23.9100	-4.0300	0.2100	-4.0300	24.2500	130.0000
2	1	-27.4300	1.5700	0.1200	-6.0000	27.4800	130.0000
2	4	20.2100	-4.5400	0.2000	-3.8100	20.7200	65.0000
2	5	39.5500	-0.8700	0.6100	-2.3800	39.5500	130.0000
2	6	25.9700	-1.2700	0.3300	-3.4600	26.0100	65.0000
3	1	-23.7000	0.0000	0.2100	-4.0300	23.7000	130.0000
3	4	21.3000	-1.2000	0.0500	-0.8600	21.3300	130.0000
4	2	-20.0200	0.7300	0.2000	-3.8100	20.0300	65.0000
4	3	-21.2500	0.3400	0.0500	-0.8600	21.2500	130.0000
4	6	25.8900	13.8100	0.0900	-0.7600	29.3400	90.0000
4	12	7.7800	-16.4900	0.0000	0.8600	18.2300	130.0000
5	2	-38.9300	-1.5100	0.6100	-2.3800	38.9600	130.0000
5	7	-5.2700	5.9300	0.0300	-2.2900	7.9300	70.0000
6	2	-25.6500	-2.1900	0.3300	-3.4600	25.7400	65.0000
6	4	-25.8000	-14.5700	0.0900	-0.7600	29.6300	90.0000
6	7	28.2800	1.2700	0.1800	-1.4200	28.3100	130.0000
6	8	-1.2700	-9.6600	0.0100	-1.0300	9.7500	32.0000
6	9	4.6600	29.0600	0.0000	1.4600	29.4300	130.0000
6	10	8.3000	-1.6700	0.0000	0.3700	8.4600	65.0000
6	28	11.4800	-2.2300	0.0200	-1.4600	11.7000	32.0000
7	5	5.3000	-8.2200	0.0300	-2.2900	9.7800	70.0000
7	6	-28.1000	-2.6800	0.1800	-1.4200	28.2300	130.0000
8	6	1.2800	8.6300	0.0100	-1.0300	8.7300	32.0000
8	28	3.7200	-1.1800	0.0100	-5.0100	3.9000	32.0000
9	6	-4.6600	-27.6000	0.0000	1.4600	27.9900	130.0000
9	10	34.6600	14.0000	0.0000	1.3700	37.3800	65.0000
9	11	-30.0000	13.6000	0.0000	2.0200	32.9400	65.0000
10	6	-8.3000	2.0500	0.0000	0.3700	8.5500	65.0000
10	9	-34.6600	-12.6300	0.0000	1.3700	36.8900	65.0000

Table E.3   Line flow results of the modified IEEE 30-bus test system for APLM
(Table 4.1) (Continued)

From	To	Forward Power Flow		Power Loss		MVA Flow	MVA Limit
Bus	Bus	MW	MVAR	MW	MVAR	MVA	MVA
10	17	3.8200	4.2400	0.0100	0.0300	5.7000	32.0000
10	20	8.5000	4.1500	0.0800	0.1700	9.4600	32.0000
10	21	16.6900	1.6700	0.0900	0.1900	16.7800	32.0000
10	22	8.1400	0.9500	0.0400	0.0900	8.2000	32.0000
11	9	30.0000	-11.5800	0.0000	2.0200	32.1600	65.0000
12	4	-7.7800	17.3500	0.0000	0.8600	19.0100	130.0000
12	13	-40.0000	-15.5700	0.0000	2.4100	42.9200	65.0000

Table E.4 Line flow results of the modified IEEE 30-bus test system for VMDM (Table 4.1) (Continued)

From Bus	To Bus	Forward Power Flow		Power Loss		MVA Flow	MVA Limit
		MW	MVAR	MW	MVAR	MVA	MVA
10	17	1.2100	-0.7500	0.0000	0.0000	1.4200	32.0000
10	20	6.8700	2.3900	0.0500	0.1200	7.2800	32.0000
10	21	15.1900	-3.6700	0.0900	0.1900	15.6300	32.0000
10	22	7.1200	-2.3100	0.0400	0.0900	7.4900	32.0000
11	9	17.2900	0.0900	0.0000	0.6900	17.2900	65.0000
12	4	-14.0800	-24.4400	0.0000	2.1100	28.2100	130.0000
12	13	-39.3500	24.3100	0.0000	3.1000	46.2500	65.0000

Table E.5 Line flow results of the modified IEEE 30-bus test system for MO
(Table 4.1)

From Bus	To Bus	Forward Power Flow		Power Loss		MVA Flow	MVA Limit
		MW	MVAR	MW	MVAR	MVA	MVA
1	2	72.8100	-10.0200	0.9800	-2.5200	73.5000	130.0000
1	3	38.4200	-3.7800	0.6400	-1.5900	38.6000	130.0000
2	1	-71.8300	7.5000	0.9800	-2.5200	72.2200	130.0000
2	4	23.2100	-5.3500	0.3100	-2.8200	23.8200	65.0000
2	5	50.4500	-0.3100	1.1700	0.7200	50.4500	130.0000
2	6	31.0500	-1.2100	0.5500	-2.1200	31.0700	65.0000
3	1	-37.7800	2.1900	0.6400	-1.5900	37.8400	130.0000
3	4	35.3800	-3.3900	0.1600	-0.3900	35.5400	130.0000
4	2	-22.9000	2.5200	0.3100	-2.8200	23.0400	65.0000
4	3	-35.2200	3.0000	0.1600	-0.3900	35.3400	130.0000
4	6	35.1600	17.1800	0.1800	-0.2700	39.1300	90.0000
4	12	15.3600	-24.3100	0.0000	2.3900	28.7500	130.0000
5	2	-49.2700	1.0300	1.1700	0.7200	49.2900	130.0000
5	7	-10.8000	7.8700	0.0900	-1.7600	13.3700	70.0000
6	2	-30.5000	-0.9100	0.5500	-2.1200	30.5200	65.0000
6	4	-34.9800	-17.4500	0.1800	-0.2700	39.0900	90.0000
6	7	34.0100	0.5600	0.3100	-0.7100	34.0100	130.0000
6	8	-1.0000	-10.9300	0.0100	-0.8500	10.9800	32.0000
6	9	9.7800	31.9700	0.0000	1.9000	33.4300	130.0000
6	10	10.2600	-2.3000	0.0000	0.6000	10.5100	65.0000
6	28	12.4400	-0.9300	0.0300	-1.1900	12.4700	32.0000
7	5	10.9000	-9.6300	0.0900	-1.7600	14.5400	70.0000
7	6	-33.7000	-1.2700	0.3100	-0.7100	33.7200	130.0000
8	6	1.0100	10.0800	0.0100	-0.8500	10.1300	32.0000
8	28	3.9800	-0.1700	0.0100	-4.2100	3.9800	32.0000
9	6	-9.7800	-30.0700	0.0000	1.9000	31.6200	130.0000
9	10	36.3600	18.1400	0.0000	1.6600	40.6300	65.0000
9	11	-26.5800	11.9300	0.0000	1.6100	29.1300	65.0000
10	6	-10.2600	2.9000	0.0000	0.6000	10.6600	65.0000
10	9	-36.3600	-16.4800	0.0000	1.6600	39.9200	65.0000

Table E.5   Line flow results of the modified IEEE 30-bus test system for MO
(Table 4.1) (Continued)

From Bus	To Bus	Forward Power Flow		Power Loss		MVA Flow	MVA Limit
		MW	MVAR	MW	MVAR	MVA	MVA
10	17	5.9200	6.9300	0.0300	0.0700	9.1100	32.0000
10	20	9.7200	5.0300	0.1100	0.2400	10.9500	32.0000
10	21	16.9000	2.2000	0.1000	0.2100	17.0400	32.0000
10	22	8.2800	1.4700	0.0500	0.1000	8.4000	32.0000
11	9	26.5800	-10.3200	0.0000	1.6100	28.5100	65.0000
12	4	-15.3600	26.7000	0.0000	2.3900	30.8000	130.0000
12	13	-27.5600	-24.0600	0.0000	1.8500	36.5900	65.0000

APPENDIX F

LIST OF PUBLICATION

P. Muangkhiew and K. Chayakulkheeree (2021), Unified Optimal Power Flow Incorporating Full AC Control Variables, 2021 International Electrical Engineering Congress (iEECON2021), Pattaya, Thailand.

P. Muangkhiew and K. Chayakulkheeree (2022), Multi-objective Optimal Power Flow Using Fuzzy Satisfactory Stochastic Optimization, International Energy Journal (IEJ).

P. Muangkhiew and K. Chayakulkheeree (2022), Probabilistic Fuzzy Multi-Objective Optimal Power Flow, GMSARN International Journal.

Unified Optimal Power Flow Incorporating Full AC Control Variables

Prakaipetch Muangkhiew   Keerati Chayakulkheeree

School of Electrical Engineering
Institute of Engineering, Suranaree University of Technology
Nakhonratchasima, Thailand
E-mail: prakaipetch.m@gmail.com, keerati.ch@sut.ac.th

Abstract—This paper introduces a particle swarm optimization based unified optimal power flow (PSO-UOPF). The main objective of the proposed method is to minimize the total system generation cost considering full AC control variables. In the proposed PSO-UOPF, the IEEE 30 buses system is used for base case and extended SVCs case. The results showed that the proposed PSO-UOPF method can efficiently and effectively provide the minimum total system generation cost comparing to the existing methods.

Keywords— optimal power flow, particle swarm optimization, total system generation cost minimization, power system control variables.

Nomenclature

c_1, c_2 : the acceleration constants
f_i : the MVA flow of line l (MVA)
f_l^{max} : the maximum limit of line l (MVA)
$F(P_{Gi})$: the cost function of the generator at bus i ($/h.)
$gbest_i^t$: the best group position of particle i at iteration t
NB : the number of buses
NC : the number of shunt compensators
NG : the number of generators
NP : the number of particles
NT : the number of transformers
p_i : the position of particle i
$pbest_i^t$: the best particle position of particle i at iteration t
PNF : the penalty function for constraints violation ($/h.)
P_{Di} : the real power demand at bus i (MW, p.u.)
P_{Gi} : the real power of generator at bus i (MW, p.u.)
P_{Gi}^{min} : the minimum real power of generator at bus i (MW, p.u.)
P_{Gi}^{max} : the maximum generation limit at bus i (MW, p.u.)
Q_{Di} : the reactive power demand at bus i (MVAR, p.u.)
Q_{Gi} : the reactive power of generator at bus i (MVAR, p.u.)
Q_{Gi}^{min} : the minimum reactive power of generator at bus i (MVAR, p.u.)
Q_{Gi}^{max} : the maximum reactive power of generator at bus i (MVAR, p.u.)
r_1, r_2 : the random values within the range of [0,1]
t : the total number of iterations
TC : the total system generation cost ($/h.)
T_{i-j} : the tap change of transformer between buses i and j
v_i^t : the particle i 's velocity at iteration t
$|V_i|$: the magnitude of generator voltage at bus i (p.u.)
$|V_i|^{min}$: the minimum magnitude of generator voltage at bus i (p.u.)
$|V_i|^{max}$: maximum the voltage magnitude of generator at bus i (p.u.)
w : the inertia weight factor
X_{Ci} : the reactance values of SVCs (ohm)
$|y_{ij}|$: the magnitude of the y_{ij} element of Y_{bus} (mho)
ρ : the set of PSO population
θ_{ij} : the angle of the y_{ij} element of Y_{bus} (radian)
δ_{ij} : the voltage angle difference between bus i and j (radian)

I. INTRODUCTION

In the hour-to-hour operation of power system, the generators share the power generation based on the individual generation cost, respected to physical constraints [1]. The important analysis tool for power system operation and control is known as optimal power flow (OPF) has received extensive attention in today's power system operation and control, especially for economic operation. The OPF problem aims to determine optimal power system operation and planning, including electricity prices [1]. However, due to several controls and unknown variables in power system analysis, OPF problem requires intensive computation resources procedure.

In the past decades, a large variability of optimization techniques has been applied to solve the OPF problem for determining the optimal operating conditions for electric power generations and control variables in power system, with the main objective of total system operation cost minimization. Formerly, traditional (deterministic) methods like nonlinear programming [2] and [3] Newton-based method, Gradient method, Quadratic Programming method, the simplex method [4] have been used to determine OPF problem solution. However, the OPF problem is a highly non-linear optimization problem that intensively difficult to obtain global optimal solution with deterministic methods. Therefore, the recent computational intelligence tools with stochastic optimization technique had been used to handle the OPF problem. For instance, genetic algorithm (GA) was earlier used to solve OPF in [5]. Meanwhile, the more recent stochastic search methods such as black-hole-based optimization (BHBO) in [6], grey wolf optimization (GWO) in [7], harmony search (HS) in [8], and particle swarm optimization (PSO) in [9-11], had been proposed. Nonetheless, due to the high complexity of OPF problem, some research proposed the approximation models for simplicity but leading to a non-global optimal solution [12]. Accordingly,

118

2021 International Electrical Engineering Congress (iEECON2021)
March 10-12, 2021, Pattaya, THAILAND

the global optimal solution in OPF problem is still challenging with different problem formulations and searching techniques.

The major contribution of this paper is to apply the PSO for determining OPF solution in unified form with several full AC load flow control variables. The proposed PSO based unified OPF (PSO-UOPF) problem is formulated with the objective of total system generation cost minimization. The optimal real power generations, the optimal generator voltage magnitudes, the optimal transformer tap changing, and the optimal static VAR compensators (SVCs) are obtained simultaneously, as the outputs of the proposed method. The simulations result with IEEE 30 buses system showed that the proposed method can potentially minimize the total system generation cost, satisfying generation, and network constraints. The comparison results with IEEE 30 buses system of the proposed method and other existing methods are illustrated and discussed.

This article is arranged as follows. Section II addressed the OPF problem formulation. Then, section III introduces the PSO method for solving the OPF in unified form. The results of the proposed PSO-UOPF with IEEE 30 buses system are addressed and discussed in Section IV. Finally, conclusion is provided in Section V.

II. UOPF PROBLEM FORMULATION

In this paper, the UOPF model represents the problem of determining the optimal control variables for minimizing total system operation cost, subjected to several equality and inequality limit constraints. The proposed UOPF problem formulations are as follows:

A. The objective functions

The objective function is total operating cost minimization considering penalty function for constraints violation as,

$$TC = \sum_{i=1}^{NG} F(P_{Gi}) + PNF .$$ (1)

B. The contraints

• The equality constraints

These equality constraints are the power balances equation as below;

$$P_{Gi} - P_{Di} = \sum_{j=1}^{NB} |V_i| |V_j| |y_{ij}| \cos(\theta_{ij} - \delta_{ij}), i = 1,...,NB ,$$ (2)

and,

$$Q_{Gi} - Q_{Di} = \sum_{j=1}^{NB} |V_i| |V_j| |y_{ij}| \sin(\theta_{ij} - \delta_{ij}), i = 1,...,NB .$$ (3)

• The inequality constraints

The inequality limit constraints are as follows:

- generator voltage magnitude limit constraints,

$$|V_i|^{\min} \leq |V_i| \leq |V_i|^{\max}, i = 1,...,NG ,$$ (4)

- generator real power output limit constraints,

$$P_{Gi}^{\min} \leq P_{Gi} \leq P_{Gi}^{\max}, i = 1,...,NG ,$$ (5)

- generator reactive power output limit constraints,

$$Q_{Gi}^{\min} \leq Q_{Gi} \leq Q_{Gi}^{\max}, i = 1,...,NG ,$$ (6)

- transformer tap changing limit constraints,

$$T_i^{\min} \leq T_i \leq T_i^{\max}, i = 1,...,NT ,$$ (7)

- shunt capacitor limit constraints,

$$Q_{ci}^{\min} \leq Q_{ci} \leq Q_{ci}^{\max}, i = 1,...,NC ,$$ (8)

- line flow limit constraints,

$$f_l \leq f_i^{\max} .$$ (9)

III. PSO BASED OPF

The PSO system proposed by [13], is the stochastic search optimization method inspired by bird flocking and the emergent behavior, which search for a population of each particle to obtain the best solution. With this concept, the population is defined as *swarm* and the potential solutions are then *particles*. The system is initialized by random positions of population in a searching space. Then the particles are updated in the next generations (iterations). The particles are updated by the adaptive velocities and record the best position it has ever been.
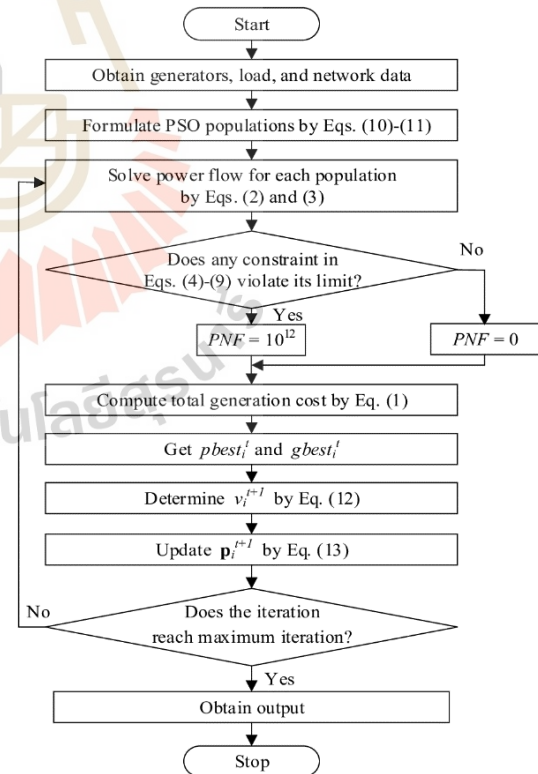

Fig.1 Flow chart of the PSO-UOPF

All other particles are ideally communicated by each particle for updating their velocity. The best value in each iteration called *pbest*[t]. If the value is better than *pbest* of the current iteration, the *pbest* value is then replaced. The best value among all

populations is a global best value (*gbest*). In this paper, the set of populations is formulated as,

$$\mathbf{\rho} = [\mathbf{p}_1, \ \mathbf{p}_2, \ ..., \ \mathbf{p}_{NP}]^T \ , \qquad (10)$$

$$\mathbf{p}_i = [\mathbf{P}_{Gi}, \ |\mathbf{V}_i|, \ \mathbf{T}_{i-j}, \ \mathbf{X}_{Ci}]^T \ . \qquad (11)$$

Where $\mathbf{P}_{Gi}$, $|\mathbf{V}_i|$, $\mathbf{T}_{i-j}$, and $\mathbf{X}_{Ci}$ are the column matrices consisted of P_{Gi}, $|V_i|$, T_{i-j}, and X_{Ci}, respectively.

The control variables in Eq. (11) are solved by Eqs. (1)-(9), simultaneously. Then, the particles velocities and updating equation can be expressed as,

$$v_i^{t+1} = wv_i^t + c_1 r_1 (pbest_i^t - \mathbf{p}_i^t) + c_2 r_2 (gbest_i^t - \mathbf{p}_i^t) \ , \quad (12)$$

$$\mathbf{p}_i^{t+1} = \mathbf{p}_i^t + v_i^{t+1} \ . \qquad (13)$$

Where superscript *t* and *t+1* denote the iteration number of the variables. Therefore, $pbest_i^t$ is the particle that gives the minimum *TC* of particle *i* at iteration *t* and $gbest_i^t$ is the particle that gives the global minimum *TC* among all particle. In this paper, *w* is decreased from 0.9 to 0.4 at the maximum iteration. c_1 and c_2 are 2.00. The PSO computational can be illustrated in Fig.1.

IV. Test Results

The proposed PSO-UOPF has been investigated by the IEEE 30 buses system and the modified IEEE 30 buses system, as shown in Fig.2. The IEEE 30 buses system information including network data, generation and load data, and control variables including their limits, are given in [3] and [5].
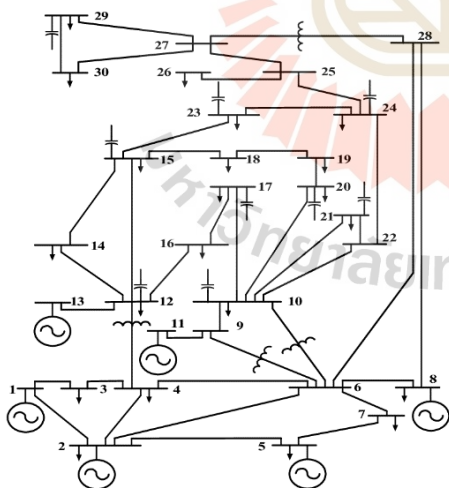

Fig.2 The modified IEEE 30 buses system

In this paper, two case studies were carried out, which are;

Case I: Base case with IEEE 30 buses system, for comparison to [3] and

Case II: Further SVCs connected to bus numbers 12, 15, 17, 20, 21, 23, and 29, to compare with [6] and [8].

The comparison results with IEEE 30 buses system of [3], [6], [8], and the proposed method are given in Table I. In Table I, the control variables

including generators' real power generations (P_{G2} - P_{G6}), generators' voltage magnitudes (V_1 -V_6), transformers' tap changings (T_{6-9} -T_{28-27}), and the reactance values of SVCs (X_{C10} - X_{C29}) are represented in the left column.

In Case I, the SVCs are connected to only buses 10 and 24. The results showed that the total system generation cost proposed PSO-UOPF is 799.43 $/h., lower than those of [3].

In Case II, the total system generation cost is supposed to be lower than Case I, due to more control variables of SVCs. Similarly, the proposed PSO-UOPF of Case II resulted in the lowest total system generation cost of 798.582 $/h., comparing to those of BHBO method in [6] and HS method in [8]. Meanwhile, the convergence plot of the proposed UOPF for Case II is shown in Fig.3.

As a result, it is seen that the proposed PSO-UOPF method can successfully minimize the total system generation cost considering full AC load flow variables in power system, in unified form.

TABLE I. COMPARISON RESULTS OF THE IEEE 30 BUSES SYSTEM

Variables	Case I		Case II		
	Deter-ministic [3]	The proposed PSO-UOPF	BHBO [6]	HS [8]	The proposed PSO-UOPF
P_{G2}	48.8400	48.629	48.3518	48.2275	48.696
P_{G5}	21.5100	21.302	21.5323	21.2792	21.264
P_{G8}	22.1500	21.182	20.0198	21.2049	21.010
P_{G11}	12.1400	11.939	13.4241	11.6715	11.907
P_{G13}	12.0000	12.000	13.4081	12.3595	12.000
$|V_1|$	1.0500	1.100	1.0965	1.0997	1.100
$|V_2|$	1.0382	1.087	1.0790	1.0829	1.087
$|V_5|$	1.0114	1.061	1.0506	1.0505	1.061
$|V_8|$	1.0194	1.068	1.0604	1.0558	1.068
$|V_{11}|$	1.0912	1.100	1.0831	1.0972	1.097
$|V_{13}|$	1.0913	1.100	1.0650	1.0978	1.100
T_{6-9}	1.0028	1.036	1.0164	1.0194	0.970
T_{6-10}	0.9602	0.937	1.0033	0.9015	0.900
T_{4-12}	1.0047	0.985	1.0265	0.9857	0.900
T_{28-27}	0.9416	0.959	1.0033	0.9558	0.900
X_{C10}	-5.260	-5.000	-33.231	-47.393	-3.164
X_{C12}	-	-	-33.690	-20.120	-2.000
X_{C15}	-	-	-28.935	-20.920	-23.613
X_{C17}	-	-	-28.160	-21.459	-18.649
X_{C20}	-	-	-40.839	-21.789	-32.238
X_{C21}	-	-	-36.033	-20.000	-12.302
X_{C23}	-	-	-35.737	-23.640	-44.999
X_{C24}	-25.000	-20.000	-29.522	-20.120	-18.937
X_{C29}	-	-	-37.213	-42.016	-44.802
Total system generation cost ($/h)	802.400	799.430	799.921	798.800	798.582

Table II illustrates the results from 30 trials of the proposed method. The minimum and maximum total system generation costs obtained by PSO-UOPF are 798.582 $/h. and 800.730 $/h. respectively. The average of total system generation cost from 30 trials is 798.871 $/h. The plot of 30 trial solutions is also shown in Fig.4. Therefore, it is obviously shown that,

the proposed method is reliable and robust in solving OPF with various numbers of control variables.

TABLE II.   THE MINIMUM, AVERAGE, AND MAXIMUM TOTAL SYSTEM GENERATION COST FROM 30 TRIAL SOLUTIONS OF CAES II

	PSO-UOPF		
	Min.	Avg.	Max.
Total system generation cost ($/h)	798.582	798.871	800.730
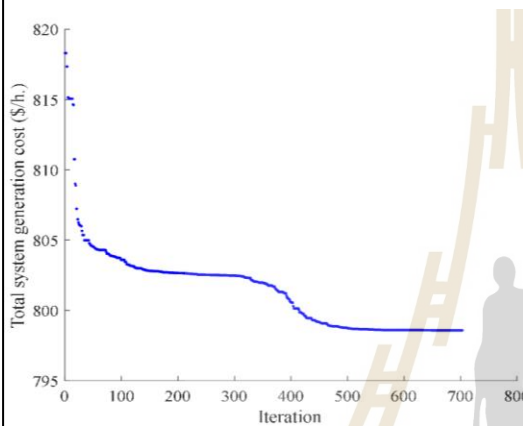
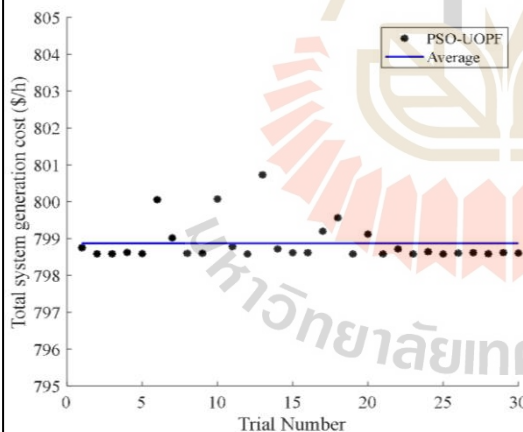Fig.3   The convergence plot of the proposed UOPF for Case II.

Fig.4   The solution with 30 trials of UOPF run for Case II.

V. CONCLUSION

In this article, the PSO-UOPF is proposed for optimal operation of the controllable parameters to minimize the total system generation cost. The results showed that the PSO-UOPF can potentially provide the total system generation cost minimization considering all control variables in power system operation. In the proposed PSO-UOPF, the optimal real power generations, the magnitudes of generators' voltages, the tap changings of transformers, and the reactance values of SVCs are obtained concurrently in a unified form, leading to the lowest total system generation cost.

REFERENCES

[1] T. Niknam, M.R. Narimani, M. Jabbari, A.R. Malekpour, "A modified shuffle frog leaping algorithm for multi-objective optimal power flow", Energy ,vol.36, no.11, pp. 6420–6432, 2011.

[2] Dommel H, Tinny W, "Optimal power flow solution", IEEE Trans Pwr Appar Syst 1968;PAS-87(10):1899-76.

[3] O. Alsac and B. Stott, "Optimal load flow with steady state security", IEEE trans, Power Apparatus and System,. vol.PAS93, no. 3, pp.745-751, May 1974.

[4] Allen J. Wood, Bruce F. Wollenrg and Gerald B. Sheble., "Power Generation, Operation and Control", Third Edition, John Wiley&Sons, INC., Hoboken, New Jersey, 2014.

[5] Anastasios G. Bakirtzis, Pandel N. Biskas, Christoforos E. Zoumas and Vasilios Petrids, "Optimal Power Flow by Enhanced Genetic Algorithm", IEEE Transactions on power systems, vol.17, no2, pp. 229-236, May 2002

[6] H.R.E.H. Bouchekara, "Optimal power flow using black-hole-based optimization approach", Applied Soft Computing , vol.24, pp.879-888, 2014.

[7] Dilip P Ladumor, R.H.Bhesdadiya, Indrajit N. Trivedi and Pradeep Jangir, "Optimal Power Flow Problem Solution with SVC using Meta-heuristic Algorithm", 3rd International Conference on Advances in Electrical, Electronics, Information, Communication and Bio-Informatics (AEEICB17), Chennai, India, 2017.

[8] S. Sivasubramani and K.S. Swarup, "Multi-objective harmony search algorithm for optimal power flow problem", Electrical Power and Energy Systems 33, pp.745-752, 2011.

[9] M.A. Abido, "Optimal power flow using particle swarm optimization", Electrical Power and Energy Systems 24, pp.563-571, 2002.

[10] C.Kumar1 and Dr. Ch. Padmanabha Raju, "Constrained Optimal Power Flow using Particle Swarm Optimization", ISSN 2250-2459, volume 2, Issue 2, February 2012.

[11] Belgin Emre TURKAY and Rengin Idil CABADAG, "Optimal Power Flow Solution Using Particle Swarm Optimization Algorithm", EuroCon 2013, Zagreb, Crotia, 2013.

[12] Haider J.Touma, "Study of The Economic Dispatch Problem on IEEE 30 buses system using Whale Optimization Algorithm", IJETS, vol.5, no.1, 2016.

[13] Kennedy J. and Eberhart R., "Particle swarm optimization", IEEE International Conference on Neural Networks, vol.4, pp.1942-1948, 1995.

Biography

Ms. Prakaipetch Muangkhiew received her B.Eng in EE (First Class Honors) from Suranaree University of Technology, Thailand, in 2020. She is currently pursuing M.Eng in EE at School of Electrical Engineering, Institute of Engineering, Suranaree University of Technology. Her research interests currently focuses on power system analysis, power systems optimization, AI application in power system, and related fields.

Associate Professor Dr. Keerati Chayakulkheeree received his B.Eng in EE from King Mongkut Institute of Technology Ladkrabang, Thailand, in 1995, M.Eng. and D.Eng. degrees in EPSM from Asian Institute of Technology, in 1999 and 2004, respectively. He is presently an Associate Professor at School of Electrical Engineering, Institute of Engineering, Suranaree University of Technology. His research interests lie primarily in the fields of power systems optimization, power system protection, smart grid and related fields.

Multi-objective Optimal Power Flow Using Fuzzy Satisfactory Stochastic Optimization

Prakaipetch Muangkhiew[1] and Keerati Chayakulkheeree[2,*]

Abstract – The optimal power flow (OPF) has been widely used in power system operation and planning of power systems. Recently, many advanced optimization methods have been used to solve the OPF problem with different objectives. However, traditional OPF cannot effectively handle multiple objectives, at the same time. Therefore, the main contribution of this is to propose the fuzzy multi-objective optimal power flow (FMOPF) using the stochastic search optimization technique. In the proposed method, particle swarm optimization (PSO) is used to solve the FMOPF by incorporating to minimizing the objective function's fuzzy satisfaction function, including the total system cost, active power loss, and voltage magnitude deviation. The proposed FMOPF is applied to solve the optimal condition for the IEEE 30-bus test system for verification. The simulation results showed that the proposed FMOPF using the PSO method could potentially and effectively determine the best solution for single-objective OPF compared to existing methods. From the results, the proposed method gave the compromise solution among different objectives in the proposed FMOPF in a fuzzy manner by comparing the results obtained with the existing method under the same system data, and control variables.

Keywords – **active power loss, fuzzy satisfactory function, optimal power flow, total system cost, voltage magnitude deviation.**

1. INTRODUCTION

In power system operation, the optimal operation of system equipment for economic, security, quality of supply, and environmental concern is the most required. The vital tool for power system day-to-day operation and planning is optimal power flow (OPF). The OPF was first introduced by Carpentier [1], to operate cost minimization. Nowadays, the OPF has been constantly developed with several objectives and security constraints including solving methods. The OPF is a complex non-convex optimization problem [2] and [3], for determining the optimal solution of a power system considering security constraints. In the OPF formulation, the best operating condition of the power system is determined depending on the desired objectives, for example, total system cost minimization (TSCM), active power loss minimization (APLM), and voltage magnitude deviation minimization (VMDM). Therefore, the best suitable values of control variables are the outputs of OPF. Meanwhile, the power balance and system operating constraints are needed to be met in the OPF problem [4]. The dependent variable obtained and handled by OPF is the generators' reactive power, voltage magnitudes at load buses, and the MVA flow at each branch [5].

In the past decades, non-deterministic search optimization techniques have been continuously developed to solve complex OPF problems, for example, genetic algorithm (GA) in [6] and tabu search (TS) in [7]. Meanwhile, the recent stochastic optimization methods have also been continuously proposed. The black-hole-based optimization (BHBO) was proposed to solve the

OPF problem in [8]. Meanwhile, the authors in [9] used the meta-heuristic algorithm to solve the OPF with SVCs consideration. An enhanced adaptive differential evolution (JADE) with a self-adaptive penalty constraint handling technique (EJADE-SP) is proposed to obtain the OPF problem in [10]. Among the modern stochastic optimization techniques, particle swarm optimization (PSO) is one of the most widely-used methods, [11] to [13]. Meanwhile, the improved PSO algorithm, stochastic weight trade-off PSO (SWT-PSO), is applied to solve the OPF problem in [14]. However, due to the complex behavior that difficult to find global solutions for OPF, further development to get a better solution is still beneficial.

Moreover, the practical operation of a power system is commonly included in multiple objectives. The best solution for some objectives may lead to a bad solution for some other objectives. Therefore, the multi-objective OPF has been proposed in several kinds of research [15] to [18]. When the optimization problem has two or more objective functions, the problems are called multi-objective optimization problems (MOOP) [16]. Generally, MOOP has to be optimized for more than one objective function at the same time. There are many methods proposed for solving MOOP. The classical approach for solving such problems focuses on aligning multi-objective to a single-objective. The MOOP can be defined as conflicting objectives by the Pareto optimal method or a fuzzy method [17] to [20] for extracting the best compromise solution obtained from the Pareto front or fuzzy trade-off. Furthermore, various methods can solve the MOOP. For example, the authors in [21] used Mayfly and Aquila (MA) Optimizer algorithms to solve MOOP considering Pareto front solutions. Also, the multi-objective differential evolution (MDE) solution aims to focus only on the required parts of the Pareto set was proposed in [22] In addition, self-adaptive particle swarm

[1,2]School of Electrical Engineering, Institute of Engineering, Suranaree University of Technology, Nakhon Ratchasima, Thailand.

*Corresponding author;
E-mail: [1]prakaipetch.m@gmail.com , [2]keerati.ch@sut.ac.th*.

optimization (SPSO)-differential evolution (DE) algorithms [23] and manta ray foraging optimization (MRFO) [24] can solve the problem of MOOP as well. Nevertheless, compromised trade-off among multiple objectives may be preferred by the system operator.

Therefore, this paper proposes the fuzzy multi-objective OPF (FMOPF) that is solved by PSO. In the proposed method, the OPF problem is formulated to MOOP. The objective functions include the TSCM, APLM, and VMDM. Several case studies were conducted with different combinations of the three objectives mentioned above. The standard and modified IEEE 30-bus test systems were used to test the proposed OPF problem formulation using PSO for individual single-objective TSCM, APLM, and VMDM. In addition, the FMOPF for trade-off among TSCM, APLM, and VMDM has also been investigated.

In this paper, the problem formulation is discussed in Section 2. Next, the strategy for objective functions fuzzification is offered in Section 3. Furthermore, the simulation result and discussion are given in Section 4. The conclusion is addressed in Section 5. Finally, the nomenclature is given at the end part.

2. PROBLEM FORMULATION

Mathematically, the OPF problem can be represented as follow:

$$\text{Minimize} \quad f(\mathbf{P_G}, |\mathbf{V_G}|, \mathbf{T}, \mathbf{X_C}) , \tag{1}$$

$$\text{Subject to:} \quad g(\mathbf{P_G}, |\mathbf{V_G}|, \mathbf{T}, \mathbf{X_C}) = 0 , \tag{2}$$

$$h(\mathbf{P_G}, |\mathbf{V_G}|, \mathbf{T}, \mathbf{X_C}) \leq 0 . \tag{3}$$

In Equation 1, matrix f represents the set of objective functions that are to be minimized. Meanwhile, matrices g and h, in Equations 2 and 3, are the sets of equality and inequality constraints required. Where $\mathbf{P_G}$ is the matrix of active power generation excluding slack bus generation as,

$$\mathbf{P_G} = [P_{G2}, P_{G3}, ..., P_{GNG}]_{1\times(NG-1)} . \tag{4}$$

$|\mathbf{V_G}|$ is the matrix of voltage magnitude of generator bus,

$$|\mathbf{V_G}| = [|V_{G1}|, |V_{G2}|..., |V_{GNG}|]_{1\times NG} . \tag{5}$$

$\mathbf{T}$ is the matrix of transformer tap-changing,

$$\mathbf{T} = [T_1, ..., T_{NT}]_{1\times NT} . \tag{6}$$

$\mathbf{X_C}$ is the matrix of SVCs reactance values,

$$\mathbf{X_C} = [X_{C1}, ..., X_{CNC}]_{1\times NC} . \tag{7}$$

2.1 Objective function

In this article, TSCM, APLM, and VMDM objective functions are considered.

2.1.1 Total system cost minimization (TSCM)

The TSCM problem can be represented as below:

$$\min TSC(\mathbf{P_G}, |\mathbf{V_G}|, \mathbf{T}, \mathbf{X_C}) , \tag{8}$$

where,

$$TSC(\mathbf{P_G}, |\mathbf{V_G}|, \mathbf{T}, \mathbf{X_C}) = \sum_{i=1}^{NG} (a_i + b_i P_{Gi} + c_i P_{Gi}^2) . \tag{9}$$

2.1.2 Active power loss minimization (APLM)

The APLM is to reduce the transmission losses as:

$$\min APL(\mathbf{P_G}, |\mathbf{V_G}|, \mathbf{T}, \mathbf{X_C}) , \tag{10}$$

where,

$$APL(\mathbf{P_G}, |\mathbf{V_G}|, \mathbf{T}, \mathbf{X_C}) = \sum_{L=1}^{NTL} g_{L,ij} \left[V_i^2 + V_j^2 - 2 V_i V_j \cos\theta_{ij} \right] \tag{11}$$

2.1.3 Voltage magnitude deviation minimization (VMDM)

The VMDM is to keep the voltage quality of a power system, can be formulated as:

$$\min VMD(\mathbf{P_G}, |\mathbf{V_G}|, \mathbf{T}, \mathbf{X_C}) , \tag{12}$$

where,

$$VMD(\mathbf{P_G}, |\mathbf{V_G}|, \mathbf{T}, \mathbf{X_C}) = \sum_{i=1}^{NL} |V_i - V_i^{ref}| . \tag{13}$$

V_i^{ref} is generally considered as 1 p.u.

2.1.4 FMOPF

The FMOPF problem is simultaneously solved for the optimal solution of TSCM, APLM, and VMDM, based on a fuzzy trade-off concept.

2.2 System constraints

The common OPF constraints including power balance and operation are taken into consideration in the proposed method.

2.2.1 Power balance constraints

The power balance constraint can be represented by the Newton-Raphson power flow equations. These constraints are handled by solving the power flow solution. Therefore, a feasible solution can be ensured. In addition, the other dependent variables are obtained from this process. The power balance constraints can be described as:

$$P_{Gi} - P_{Di} = \sum_{j=1}^{NB} \left[G_{ij} |V_i||V_j| \cos(\theta_{ij}) + B_{ij} |V_i||V_j| \sin(\theta_{ij}) \right] , \tag{14}$$

$$Q_{Gi} - Q_{Di} = \sum_{j=1}^{NB} \left[G_{ij} |V_i||V_j| \sin(\theta_{ij}) - B_{ij} |V_i||V_j| \cos(\theta_{ij}) \right] , \tag{15}$$

where, $i=1,...,NB$.

2.2.2 System operating limit constraints

The system operating constraints are as follows.
(1) Generator constraints are,
 - The limit on generators' voltage magnitude,

$$|V_{Gi}|^L \leq |V_{Gi}| \leq |V_{Gi}|^U , \tag{16}$$

- The generators' real and reactive power operating limit,

$$P_{Gi}^L \leq P_{Gi} \leq P_{Gi}^U \quad , \tag{17}$$

$$Q_{Gi}^L \leq Q_{Gi} \leq Q_{Gi}^U \quad , \text{ and} \tag{18}$$

$$i = 1,...,NG.$$

(2) Transformer tap-changing limit,

$$T_i^L \leq T_i \leq T_i^U \quad , i = 1,...,NT \quad . \tag{19}$$

(3) The SVCs setting limits,

$$Q_{ci}^L \leq Q_{ci} \leq Q_{ci}^U \quad , i = 1,...,NC \quad . \tag{20}$$

(4) Network operating limit constraints include,
- The limit on bus voltage magnitude,

$$|V_{Li}|^L \leq |V_{Li}| \leq |V_{Li}|^U \quad , i = 1,...,NPQ \quad , \tag{21}$$

- The transmission lines and transformers loading limit,

$$|S_{Li}| \leq S_{Li}^U \quad , i = 1,...,NL \quad . \tag{22}$$

3. STRATEGY FOR OBJECTIVE FUNCTIONS FUZZIFICATION

This section illustrates a multi-objective optimization technique using a fuzzy satisfactory approach which is proposed by Zimmermann [25]. With this approach, the optimization of MOOP can be solved by compromising trade-offs among all objectives. The MOOP is compared to a single-objective optimization problem by considering the solution at the edge of the fuzzy satisfactory functions, in this paper. The proposed FMOPF using PSO is categorized into:

1. TSCM in Equation 9,
2. APLM in Equation 11, and
3. VMDM in Equation 13.

The objective functions in Equations 9 to 13 are used to formulate the fuzzy satisfactory functions (FSF) as shown in Figures 1 to 3.

In the fuzzification process, the MOOP is converted into FSF, μ_{TSC}, μ_{APL}, and μ_{VMD}, as shown in Figures 1 to 3, respectively. This process defines a FSFs associated with each objective because high value of each objective is given by a low FSF value. In the same manner, the best value for each objective is obtained by optimizing a single-objective. Meanwhile, the maximum objective value is determined by minimizing other objective functions.
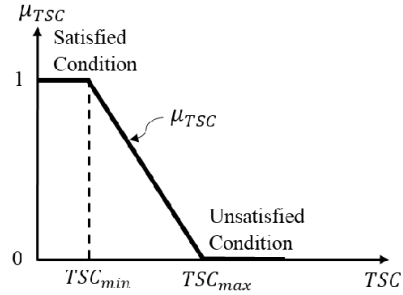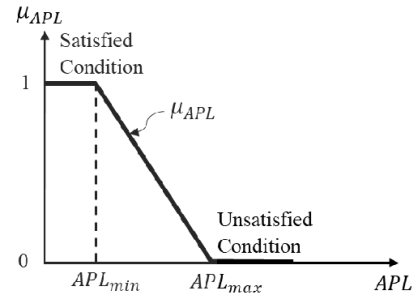

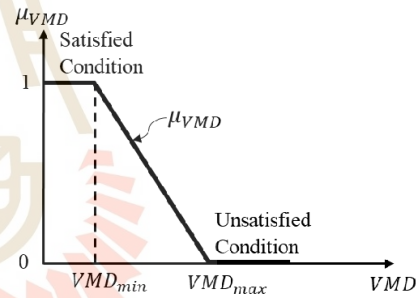**Fig. 1. FSF of TSC.**

Fig. 2. FSF of APL.

Fig. 3. FSF of VMD.

The FSF of the individual objective functions can be represented by Equations 23 to 25, for TSCM, APLM, and VMDM, respectively. A FSF can take any value in [0,1]. The FSF value of 1 is assigned to the minimum value for each objective. When the other objective provides that objective value is greater than the minimum value, the FSF is decreased to zero. Lastly, the multi-objective problem can be formulated as fuzzy maximization problem as Equation 26.

$$\mu_{TSC} = \begin{cases} 1 & , \text{for } TSC \leq TSC_{\min} \\ \dfrac{-1}{TSC_{\max} - TSC_{\min}} \cdot TSC \\ + \dfrac{TSC_{\max}}{TSC_{\max} - TSC_{\min}} & , \text{for } TSC_{\min} \leq TSC < TSC_{\max} \\ 0 & , \text{for } TSC \geq TSC_{\max} \end{cases} \tag{23}$$

$$\mu_{APL} = \begin{cases} 1 & , \text{for } RPL \le RPL_{\min} \\ \dfrac{-1}{APL_{\max} - APL_{\min}} \cdot APL \\ + \dfrac{APL_{\max}}{APL_{\max} - APL_{\min}} & , \text{for } APL_{\min} \le APL < APL_{\max} \\ 0 & , \text{for } APL \ge APL_{\max} \end{cases}$$

(24)

$$\mu_{VMD} = \begin{cases} 1 & , \text{for } VMD \le VMD_{\min} \\ \dfrac{-1}{VMD_{\max} - VMD_{\min}} \cdot VMD \\ + \dfrac{VMD_{\max}}{VMD_{\max} - VMD_{\min}} & , \text{for } VMD_{\min} \le VMD < VMD_{\max} \\ 0 & , \text{for } VMD \ge VMD_{\max} \end{cases}$$

(25)

Maximize $\mu_T = \min\{\mu_{TSC}, \mu_{APL}, \mu_{VMD}\}$ (26)

3.1 PSO based FMOPF

The PSO was proposed in 1995 [26], as one of the bio-inspired algorithms and it is a simple one to search for an optimal search in the solution space, like the motion of bird flocks. In the proposed PSO based FMOPF, the individual single-object for TSCM, APLM, and VMDM are solved, in order to obtain the FSF of TSCM, APLM, and VMDM.
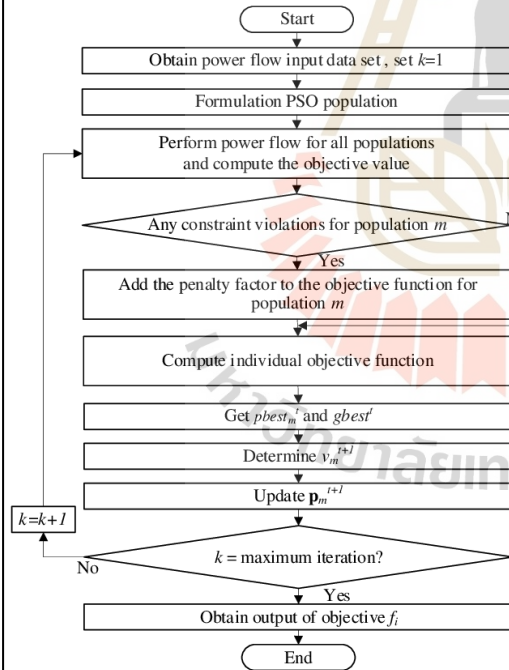

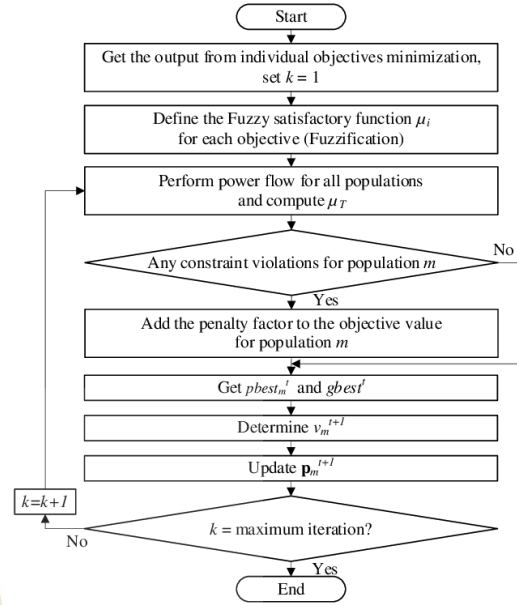Fig. 4. Flow chart of the individual objective.

Fig. 5. Flow chart of the FMOPF using PSO.

The PSO population i for single-objective is

$$\mathbf{p_i} = [\mathbf{P_{Gi}}, |\mathbf{V_{Gi}}|, \mathbf{T_i}, \mathbf{X_{Ci}}].$$ (27)

Then, velocity of particle m can be computed by,

$$v_m^{t+1} = wv_m^t + c_1 r_1(pbest_m^t - \mathbf{p}_i^t) + c_2 r_2(gbest^t - \mathbf{p}_m^t).$$ (28)

The particle's position is, then, updated as,

$$\mathbf{p}_m^{t+1} = \mathbf{p}_m^t + v_m^{t+1}.$$ (29)

The standard parameters of PSO are used for investigation of this work. Therefore, w is reduced from 0.9 at the first iteration to 0.4 at the maximum iteration, and c_1 and c_2 are 2.00. The proposed, the individual objective, computational procedure is shown in Figure 4. For FMOPF, the FSF is used to obtain μ_T. The computational can be illustrated as Figure 5.

4. SIMULATION RESULT AND DISCUSSION

In this section, the TSCM, APLM, VMDM are studied, which were tested on the standard and the modified IEEE 30-bus test systems, as shown in Figures 6 and 7, respectively. The system data is taken from [27] and [28]. The proposed FMOPF has been investigated in three cases study as follows.
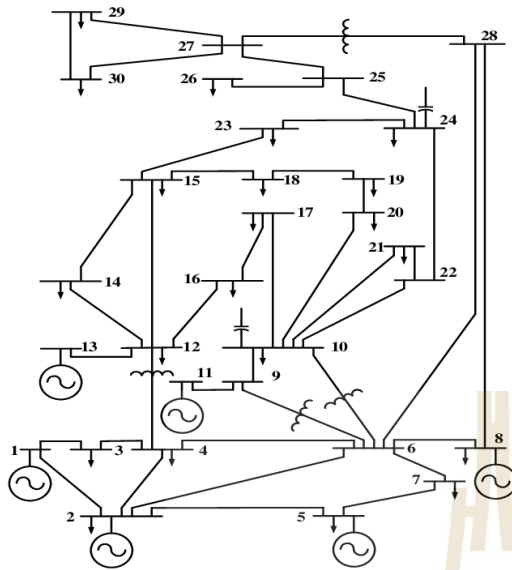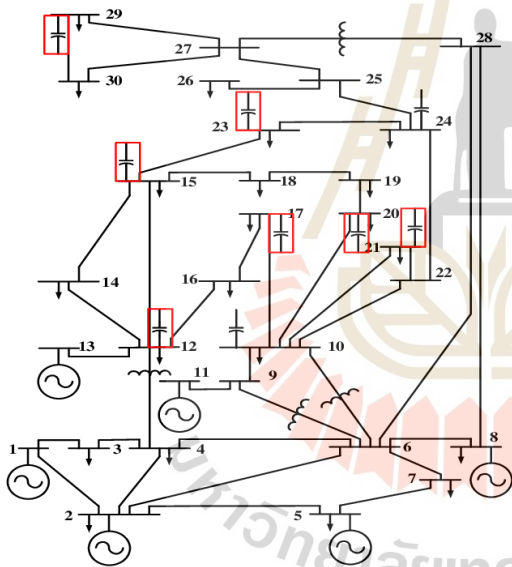
Fig. 6. The IEEE 30 buses system [27].

Fig. 7. The modified IEEE 30-bus test system [28].

Table 2. Comparison results of the IEEE 30-bus test system for TSCM.

Control Variables	Deterministic method	Proposed method
Power Generation (P_{Gi}) at Bus (MW)		
2	48.84	48.63
5	21.51	21.30
8	22.15	21.18
11	12.14	11.94
13	12.00	12.00
Generator Voltage ($|V_i|$) Magnitude at Bus (p.u.)		
1	1.05	1.10
2	1.04	1.09
5	1.01	1.06
8	1.02	1.07
11	1.09	1.10
13	1.09	1.10
Transformer Tap-Changing (T_{i-j}) between Buses		
6-9	1.00	1.04
6-10	0.96	0.94
4-12	1.00	0.99
28-27	0.94	0.96
SVC Reactance Values (X_{Ci}) at Bus (p.u.)		
10	-5.26	-5.00
24	-25.00	-20.00
TSC ($/h.)	**802.400**	**799.430**

Table 2 shows the results obtained from the convention deterministic method and the proposed method. The results showed that the proposed method can determine a lower TSC than the conventional deterministic method. Therefore, the proposed PSO-based OPF problem formulation can successfully minimize the TSC of the power system to satisfy system operating constraints. Further comparison result with the modified IEEE 30-bus test system is illustrated compared to more recent stochastic methods in Section 4.2.

4.2 The single-objective with modified IEEE 30-bus test system

The control variables of the modified IEEE 30-bus test system are shown in Table 3. The TSCM sing objective solution has been carried out and investigated compared to the enhanced genetic algorithm (EGA) method [29], BHBO method [30], and enhanced genetic algorithm-decoupled quadratic load flow (EGA-DQLF) method [31], as shown in Table 4.

Table 3. The control variables of standard case.

Control Variables	Number	At bus number
Real power generations	5	2, 5, 8, 11, 13
Generators' voltage magnitudes	6	1 (slack), 2, 5, 8, 11, 13
Transformer tap-changes	4	6-9, 6-10, 4-12, 27-28
SVCs' setting values	9	10, 12, 15, 17, 20, 21, 22, 23, 24

From Table 4, the EGA method resulted in the highest TSC of 802.06 $/h. Meanwhile, the BHBO and EGA-DQLF methods can provide the lower TSC at 799.922 and 799.56 $/h, respectively. However, the TSC

4.1 Base case for TSCM with standard IEEE 30-bus test system

For the base case, the control variables are as shown in Table 1. This case study investigates the performance of the proposed PSO-based OPF by comparing it to the widely-used standard case in [27].

Table 1. The control variables of standard case.

Control Variables	Number	At bus number
Real power generations	5	2, 5, 8, 11, 13
Generators' voltage magnitudes	6	1 (slack), 2, 5, 8, 11, 13
Transformer tap-changes	4	6-9, 6-10, 4-12, 27-28
SVCs' setting values	2	10, 24

obtained by the proposed problem formulation is the lowest among all other methods. Therefore, the proposed method is potentially competitive with other existing stochastic methods for TSC minimization.

**Table 4. Comparison results of the modified IEEE 30-bus test system for TSCM.**

Control Variables	EGA [29]	BHBO [30]	EGA-DQLF [31]	Proposed method
Power Generation (P_{Gi}) at Bus (MW)				
2	48.75	48.35	48.11	48.84
5	21.44	21.53	21.28	21.36
8	21.95	20.02	20.93	20.93
11	12.42	13.42	12.50	11.91
13	12.02	13.41	12.00	12.00
Generator Voltage ($|V_i|$) Magnitude at Bus (p.u.)				
1	1.05	1.10	1.10	1.10
2	1.04	1.08	1.08	1.09
5	1.01	1.05	1.05	1.06
8	1.01	1.06	1.06	1.07
11	1.08	1.08	1.10	1.04
13	1.07	1.07	1.09	1.07
Transformer Tap-Changing (T_{i-j}) between Buses				
6-9	1.01	1.02	0.95	1.08
6-10	0.95	1.00	1.04	0.99
4-12	1.00	1.03	1.00	1.05
28-27	0.96	1.00	0.98	1.04
SVC Reactance Values (X_{Ci}) at Bus (p.u.)				
10	-20.00	-33.23	-25.00	-18.02
12	-20.00	-33.69	-50.00	-29.56
15	-33.33	-28.94	-20.00	-34.91
17	-20.00	-28.16	-20.00	-15.66
20	-20.00	-40.84	-50.00	-45.00
21	-20.00	-36.03	-25.00	-9.42
23	-25.00	-35.74	-25.00	-44.99
24	-20.00	-29.52	-33.33	-15.65
29	-33.33	-37.21	-100.00	-44.99
TSC($/h.$)	**802.060**	**799.922**	**799.560**	**799.3862**

### 4.3 The FMOPF with modified IEEE 30-bus test system

The proposed FMOPF for trading-off among TSCM, APLM, and VMDM had been investigated in this case study. This case study was done by the input data as in Table 3. To further verify the reliability of the proposed method, 20 trials for TSCM, APLM, VMDM, and μ_T of FMOPF have been performed, as shown in Table 5. It is seen that the results from several trials guarantee the reliability to get the feasible solution of the proposed method. Figures 8 to 11 showed the convergence behavior of the TSCM, APLM, VMDM, and μ_T of FMOPF, respectively. μ_T is the maximum FSF value among the minimum values of μ_{TSC}, μ_{APL}, and μ_{VMD}. Note that the minimization of $-\mu_T$ is solved for μ_T maximization.
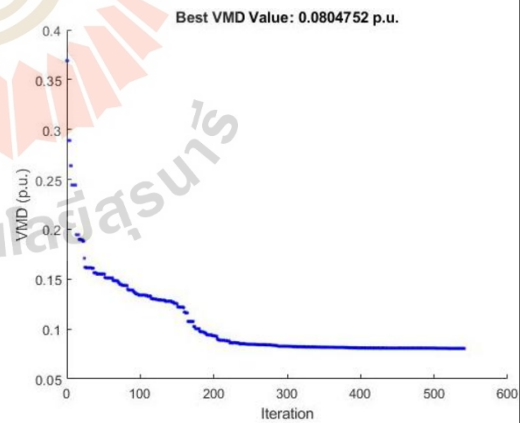
Table 5. The results from 20 trials.

	Best	Avg.	Worst
TSCM ($/h.$)	799.386	799.512	800.539
APLM (p.u.)	2.966	2.984	3.076
VMDM (p.u.)	0.081	0.089	0.141
μ_T of FMOPF	0.834	0.685	0.563
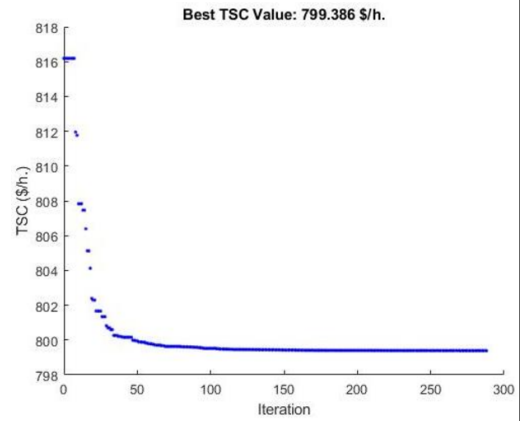
Fig. 8. The convergence behavior of TSCM.
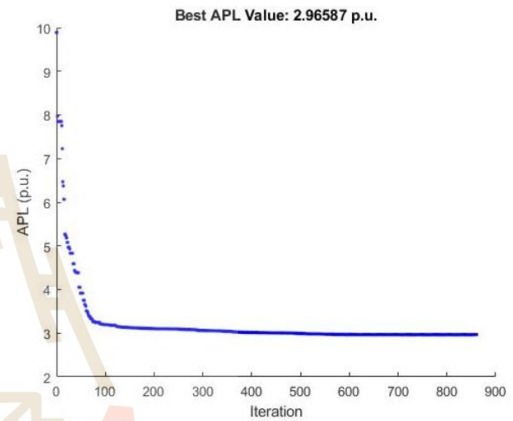
Fig. 9. The convergence behavior of APLM.

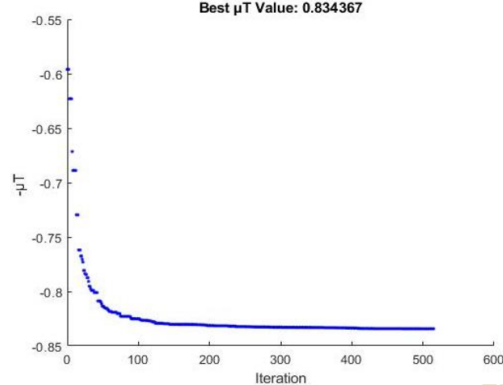Fig. 10. The convergence behavior of VMDM.

Fig. 11. The convergence behavior of μ_T of FMOPF.

The results of individual objectives and FMOPF are shown in Table 6. In FMOPF overview, it is obvious that when minimizing an individual single-objective can result in a higher solution for other objectives. The minimum TSC obtained from the proposed method is 799.386 $/h. Under this condition, the APL and VMD are 8.718 p.u. and 0.807 p.u., respectively. Meanwhile, when minimizing APL by APLM, the lowest value of APL is 2.966 p.u. However, the minimum APL condition is lead

to the highest solution of TSC of 967.342 $/h. Similarly, the lowest VDM condition is lead to the higher value of TSC and APL at 929.577 $/h and 8.751 p.u.

To obtain a fair comparison with the PPSOGSA method [32], the simulations were tested under the same system data and control variables. A comparison of the proposed FMOPF and PPSOGSA method showed that the FMOPF yielded the results for the individual objective, including TSCM, ALPM, and VMDM, better than the results of the PPSOGSA method, as shown in Table 6. However, the performance of the system is significantly improved by simultaneous minimization of TSC, APL, and VMD. Therefore, the cooperative solution among individual objectives may gain benefit to the system depending on the operator's requirement. When solving the MOOP using the proposed FMOPF for this case, the soft computational bargain between the contradiction objectives can be obtained. It is shown that a slightly increasing in TSC can decrease the VMD from 0.807 to 0.221 p.u. Simultaneously, the APL is reduced from 8.718 to 6.802 p.u. As a result, the proposed FMOPF can compromise among TSCM, APLM, and VMDM, under the fuzzy trade-off concept. Meanwhile, the PPSOGSA method uses the weighted sum method to solve the MOOP.

Table 6. Comparison results of the modified IEEE 30-bus test system for MOOP.

Control Variables	TSCM		APLM		VMDM		MOOP	
	PPSOGSA [32]	FMOPF	PPSOGSA [32]	FMOPF	PPSOGSA [32]	FMOPF	PPSOGSA [32]	FMOPF
Power Generation (P_{Gi}) at Bus (MW)								
2	48.58	48.84	80.00	80.00	49.04	80.00	52.66	46.40
5	21.37	21.36	50.00	50.00	44.74	49.97	31.73	36.64
8	21.44	20.93	35.00	35.00	18.41	35.00	34.94	34.94
11	11.94	11.91	30.00	30.00	24.13	10.11	25.28	17.20
13	12.00	12.00	40.00	40.00	14.50	29.80	20.38	16.17
Generator Voltage ($|V_i|$) Magnitude at Bus (p.u.)								
1	1.08	1.10	1.06	1.10	1.01	0.99	1.03	1.03
2	1.07	1.09	1.06	1.10	1.00	1.05	1.02	1.02
5	1.03	1.06	1.04	1.08	1.02	1.02	1.00	0.99
8	1.04	1.07	1.04	1.09	1.01	0.99	1.01	1.00
11	1.09	1.04	1.06	1.03	1.00	1.04	1.01	1.10
13	1.04	1.07	1.05	1.06	1.02	0.96	1.01	1.02
Transformer Tap-Changing ($T_{i\text{-}j}$) between Buses								
6-9	1.02	1.08	1.02	1.10	1.02	1.05	1.03	1.02
6-10	0.95	0.99	0.94	0.97	0.90	1.08	0.91	1.04
4-12	0.96	1.05	0.99	1.05	1.01	0.94	0.98	0.98
28-27	0.98	1.04	0.98	1.05	0.96	0.99	0.97	0.98
SVC Reactance Values (X_{Ci}) at Bus (p.u.)								
10	-1.39	-18.02	-0.26	-45.00	-0.22	-20.03	-0.20	-43.29
12	-0.72	-29.56	-0.47	-29.31	-0.28	-23.77	-0.95	-24.25
15	-0.22	-34.91	-0.21	-28.98	-0.20	-45.00	-0.21	-44.67
17	-0.20	-15.66	-0.20	-15.77	-3.08	-13.63	-1.40	-42.37
20	-0.25	-45.00	-0.22	-45.00	-0.20	-44.20	-0.20	-45.00
21	-0.20	-9.42	-0.20	-9.59	-0.20	-7.41	-0.20	-22.24
23	-0.26	-44.99	-0.29	-45.00	-0.20	-26.95	-0.20	-43.25
24	-0.20	-15.65	-0.20	-14.14	-0.20	-8.72	-0.20	-44.39
29	-0.30	-44.99	-0.37	-45.00	-0.77	-43.30	-0.34	-45.00
TSC ($/h.)	800.528	**799.386**	967.669	967.342	849.613	929.577	829.598	**827.206**
APL (p.u.)	9.027	8.718	3.103	**2.966**	7.420	8.751	6.110	**6.802**
VMD (p.u.)	0.911	0.807	0.891	0.888	0.090	**0.081**	0.110	**0.221**

5. CONCLUSION

This paper proposed the FMOPF formulation with various control variables using PSO. The proposed method can successfully provide the optimal operating condition of the active power generation, the generator voltage magnitudes, the transformers tap changings, and the SVCs setting values. The considered objectives are TSCM, APLM, and VMDM. The fuzzy concept is applied to solve the MOOP, tested on the original and the modified IEEE 30-bus test system. The proposed FMOPF has the ability and good performance to obtain the compromised solution among conflictual objectives.

NOMENCLATURE

$|S_{Li}|$ = the MVA flow of line i (MVA).
$|V_{Gi}|$ = the voltage magnitude of generator at bus i (p.u.).
$|V_i|$ = the voltage magnitudes at bus i (p.u.).
$|V_i^{ref}|$ = the reference value of the voltage magnitude at bus i.
$|V_j|$ = the voltage magnitudes at bus j (p.u.).
$|V_{Li}|$ = the voltage magnitude at load bus i (p.u.).
μ_{APL} = the fuzzy satisfaction function of active power loss.
μ_T = the fuzzy satisfaction function.
μ_{TSC} = the fuzzy satisfaction function of total system cost.
μ_{VMD} = the fuzzy satisfaction function of voltage magnitude deviation.
a_i, b_i, c_i = the cost coefficients parameters of generator i.
APL = the active power loss (p.u.).
APL_{max} = the maximum acceptable active power loss obtained by TSCM and VDM.
APL_{min} = the minimum active power loss obtained by RPLM.
B_{ij} = the imaginary of admittance between buses i and j.
f_i = the objective function to be optimize.
g = the equality constraints representing nonlinear power flow equations.
G_{ij} = the real parts of admittance between buses i and j.
$g_{L,ij}$ = the conductance of line L between buses i and j.
h = the system operating constraints.
NB = the buses total number.
NC = the shunt compensators total number.
NG = the generators total number.
NL = the branches total number.
N_{obj} = the objectives total number.
NPQ = the PQ buses total number.
NT = the transformers total number.
NTL = the transmission line total number.
P_{Di} = the real power load demand at bus i (MW, p.u.).
P_{Gi} = the real power generation at bus i (MW, p.u.).
Q_{Ci} = the shunt VAR compensator (p.u.).
T_i = the transformer tap changing (p.u.).
TSC = the total system cost ($/h.).
TSC_{max} = the maximum acceptable total system cost obtained by RPLM and VDM.
TSC_{min} = the minimum total system cost obtained by TSCM.
u = the column vector of independent control variables.

VD = the voltage deviation (p.u.).
VD_{max} = the maximum acceptable voltage deviation obtained by TSCM and RPLM.
VD_{min} = the minimum voltage deviation obtained by VDM.
x = the vector of dependent variables.
θ_{ij} = the voltage angles between buses i and j (radian).

Superscript
L = lower limit.
U = upper limit.

REFERENCES

[1] J. Carpentier, "Contribution á l'étude du dispatching économique," Bulletin de la Société Française des Électriciens, 1962.

[2] Bernard C. Lesieutre. "Convexity of the Set of Feasible Injections and Revenue Adequacy in FTR Markets", IEEE Transactions on Power Systems, 2005.

[3] Daniel K. Molzahn, "Identifying and Characterizing Non-Convexities in Feasible Spaces of Optimal Power Flow Problems", IEEE Transactions on circuits and systems, 2018.

[4] Dan Wu and Bernard C. Lesieutre, "A Deterministic Method to Identify Multiple Local Extrema for the AC Optimal Power Flow Problem", IEEE Transactions on Power Systems, 2018.

[5] Thang Trung Nguyen, "A high performance social spider optimization algorithm for optimal power flow solution with single objective optimization", Energy, 2019.

[6] Anastasios G. Bakirtzis, Pandel N. Biskas, Christoforos E. Zoumas and Vasilios Petrids, "Optimal Power Flow by Enhanced Genetic Algorithm", IEEE Transactions on power systems, 2002.

[7] M.A. Abido, "Optimal Power Flow Using Tabu Search Algorithm", Electric Powe r Components and Systems, 2002.

[8] H.R.E.H. Bouchekara, "Optimal power flow using black-hole-based optimization approach", Applied Soft Computing, 2014.

[9] Dilip P Ladumor, R.H.Bhesdadiya, Indrajit N. Trivedi and Pradeep Jangir, "Optimal Power Flow Problem Solution with SVC using Meta-heuristic Algorithm", 3rd International Conference on Advances in Electrical, Electronics, Information, Communication and Bio-Informatics (AEEICB17) , 2017.

[10] S. Li, W. Gong, L. Wang, X. Yah, and C. Hu, "Optimal power flow by means of improved adaptive differential evolution", Energy 198, Vol. 198, 2020.

[11] M.A. Abido, "Optimal power flow using particle swarm optimization", Electrical Power and Energy Systems 24, 2002.

[12] C. Kumar1 and Dr. Ch. Padmanabha Raju, "Constrained Optimal Power Flow using Particle Swarm Optimization", ISSN 2250-2459, 2012.

[13] Belgin Emre TURKAY and Rengin Idil CABADAG, "Optimal Power Flow Solution

Using Particle Swarm Optimization Algorithm", EuroCon 2013, 2013.

[14] L.D. Le, L.D. Ho, J. Polprasert, W. Ongsakul, D.N. Vo, and D.A. Le, "Stochastic Weight Trade-Off Particle Swarm Optimization for Optimal Power Flow", Journal of Automation and Control Engineering, Vol. 2, No. 1, 2014.

[15] S. Sivasubramani and K.S. Swarup, "Multi-objective harmony search algorithm for optimal power flow problem", Electrical Power and Energy Systems 33, 2011.

[16] Bakirtzis Anastasios G, Biskas Pandel N, Zoumas Christoforos E., "Multi-objective optimization using evolutionary algorithms", Kalyanmoy Deb: John Wiley & Sons, Ltd., 2001.

[17] V.C. Ramesh and Member Xuan Li, "A Fuzzy Multiobjective Approach to Contingency Constrained OPF", IEEE Transactions on Power Systems, 1997.

[18] A. Khorsandi, S.H. Hosseiniana and A. Ghazanfari, "Modified artificial bee colony algorithm based on fuzzy multi-objective technique for optimal power flow problem", Electric Power Systems Research 95, 2013.

[19] R.H. Liang and Y.Y. Hsu, "Fuzzy linear programming: an application to hydroelectric generation scheduling", *IEE*, 1994.

[20] Keerati Chayakulkheeree, "Unified Multi-Objective Optimal Power Flow Considering Emissions with Fuzzy Network and Generators Ramp-Rate Constraints", *ECTI-CON* 2011, 2011.

[21] A.K.Khamees , A.Y. Abdelaziz, M.R. Eskaros, H.H. Alhelou, and M.A. Attia, "Stochastic Modeling for Wind Energy and Multi-Objective Optimal Power Flow by Novel Meta-Heuristic Method", IEEE Access, Vol. 9, pp. 158353-158366, 2021.

[22] A.M. Shaheen, S.M. Farrag, ans R.A. El-Sehiemy, "MOPF solution methodology", IET Gener. Transm. Distrib, Vol. 11, Iss. 2, pp. 570–581, 2017.

[23] E. Naderia, M. Pourakbari-Kasmaeib, F.V. Cernac, and M. Lehtonen, "A novel hybrid self-adaptive heuristic algorithm to handle single- and multi-objective optimal power flow problems", International Journal of Electrical Power & Energy Systems, Vol. 125, 2021.

[24] H.T. Kahraman, M. Akbel, and S. Duman, "Optimization of Optimal Power Flow Problem Using Multi-Objective Manta Ray Foraging Optimizer" Applied Soft Computing, Vol. 116, 2022.32

[25] H. J. Zimmermann, *Fuzzy Sets. Decision Making, and Expert Systems*: Kluwer Adademic Publishers, 1987.

[26] James Kennedy and Russell Eberhart, "Particle Swarm Optimization", IEEE, 1995.

[27] O. Alsac and B. Stott, "Optimal load flow with steady state security", IEEE trans, Power Apparatus and System, 1974.

[28] S. Sivasubramani and K.S. Swarup, "Multi-objective harmony search algorithm for optimal power flow problem", International Journal of Electrical Power & Energy Systems, 2011.

[29] Anastasios G. Bakirtzis, Pandel N. Biskas, Christoforos E. Zoumas and Vasilios Petrids, "Optimal Power Flow by Enhanced Genetic Algorithm", IEEE Transactions on power systems, 2002.

[30] H.R.E.H. Bouchekara, "Optimal power flow using black-hole-based optimization approach", 2014.

[31] M. Sailaja Kumari and Sydulu Maheswarapu, "Enhanced Genetic Algorithm based computation technique for multi-objective Optimal Power Flow solution", Electrical Power and Energy Systems, 2010.

[32] Z. Ullah,S. Wang, J. Radosavlievic, and J. Lai, "A solution to the optimal power flow problem considering WT and PV generation" *IEEE Access*, Vol. 7, pp. 46763-46772.

Probabilistic Fuzzy Multi-Objective Optimal Power Flow

Prakaipetch Muangkhiew[1]   Keerati Chayakulkheeree[1*]

ABSTRACT

This paper presents the probabilistic fuzzy multi-objective optimal power flow (PFMOPF) considering photovoltaic power plant (PVPP) generation, wind power plant (WPP) generation, and load uncertainty. In the proposed method, the output power of PVPP and WPP generation is based on probabilistic models of wind speed and solar irradiance. Furthermore, the active power of PVPP and WPP are dependent variables, while the magnitude of the voltage at PVPP and WPP buses are control variables in the OPF formulation. The objective functions used in this paper are the total system cost minimization (TSCM), active power loss minimization (APLM), voltage magnitude deviation minimization (VMDM), and multi-objective minimization. A fuzzy satisfaction function of the objective is used to solve the best solution of multi-objective coordination with particle swarm optimization (PSO). The PFMOPF is verified on the IEEE 30-bus test system with modifications to include PVPP and WPP using probabilistic density function (PDF) and Monte-Carlo simulation (MCS). The proposed method can maximize the satisfaction function of the multi-objective optimal power flow considering the PVPP, WPP, and load uncertainty into the system.

NOMENCLATURES

σ	= the standard deviation of load demand.
$\lvert S_{Li} \rvert$	= the MVA flow of line i.
$\lvert \tilde{V}_{Gi} \rvert$	= the PDF of voltage magnitude of generator at bus i.
$\lvert \tilde{V}_i \rvert$	= the PDF of voltage magnitudes at bus i.
$\lvert \tilde{V}_i^{ref} \rvert$	= the PDF of reference value of the voltage magnitude at bus i.
$\lvert \tilde{V}_j \rvert$	= the PDF of voltage magnitudes at bus j.
$\lvert \tilde{V}_{Li} \rvert$	= the PDF of voltage magnitude at load bus i.
μ	= the mean value of load demand.
a_i, b_i, c_i	= the cost coefficients parameters of generator i.
APL	= the active power loss.
APL_{max}	= the maximum acceptable active power loss obtained by TSCM and VMDM.
APL_{min}	= the minimum active power loss obtained by APLM.
B_{ij}	= the imaginary of admittance between buses i and j.
c	= the scale parameter of the Weibull distribution.
$f_G(G)$	= the PDF of solar irradiance.
F_i	= the objective function to be optimized.
$f_{Pd}(P_d)$	= the PDF of load demand.
$f_v(v)$	= the Weibull PDF of wind speed.
g	= the equality constraints representing nonlinear power flow equations.

G_{ij}	= the active parts of admittance between buses i and j.
$g_{L,ij}$	= the conductance of line L between buses i and j.
h	= the system operating constraints.
k	= the shape parameter of the Weibull distribution.
$M\tilde{V}A_{Li}$	= the PDF of MVA flow of line i.
NB	= the buses total number.
NC	= the shunt compensators total number.
NG	= the generators total number.
NL	= the branches total number.
N_{obj}	= the objectives total number.
NPQ	= the PQ buses total number.
NT	= the transformers total number.
NTL	= the transmission line total number.
P_d	= the load demand.
$\tilde{P}_{Di}$	= the active power load demand at bus i.
$\tilde{P}_{Gi}$	= the PDF of active power generation at bus i.
$\tilde{P}_{pvn}$	= the nominal output power of the PV unit.
$\tilde{P}_{PVPi}$	= the PDF of active power PVPP generation at bus i.
$\tilde{P}_{WPPi}$	= the PDF of active power WPP generation at bus i.
$\tilde{Q}_{ci}$	= the PDF of shunt VAR compensator.
$\tilde{Q}_{Di}$	= the PDF of reactive power load demand at bus i.
$\tilde{Q}_{Gi}$	= the PDF of reactive power generation at bus i.

[1]School of Electrical Engineering, Institute of Engineering, Suranaree University of Technology, Nakhon Ratchasima, Thailand.
Corresponding author; Email: prakaipetch.m@gmail.com, keerati.ch@sut.ac.th

R_c	=	the certain irradiance point.
S	=	the solar irradiance on the PV module surface.
S_{stc}	=	the solar irradiance at standard test conditions.
$\tilde{T}_i$	=	the PDF of transformer tap changing.
TSC	=	the total system cost.
TSC_{max}	=	the maximum acceptable total system cost obtained by APLM and VMDM.
TSC_{min}	=	the minimum total system cost obtained by TSCM.
$\tilde{u}$	=	the column vector of PDF of control variables.
v	=	the wind speed.
v_{ci}	=	the cut-in wind speed.
v_{co}	=	the cut-out wind speed.
VMD	=	the voltage magnitude deviation.
VMD_{max}	=	the maximum acceptable voltage magnitude deviation obtained by TSCM and APLM.
VMD_{min}	=	the minimum voltage magnitude deviation obtained by VMDM.
v_n	=	the nominal wind speed.

$\tilde{x}$	=	the vector of PDF of dependent variables.
$\tilde{\theta}_{ij}$	=	the PDF of voltage angles between buses i and j.
λ_{APL}	=	the fuzzy satisfaction function of active power loss.
λ_{OB}	=	the fuzzy satisfaction function of individual objective.
λ_T	=	the overall fuzzy satisfaction function.
λ_{TSC}	=	the fuzzy satisfaction function of total system cost.
λ_{VMD}	=	the fuzzy satisfaction function of voltage magnitude deviation.

Superscript

~	=	probabilistic variable.
L	=	lower limit.
U	=	upper limit.

1. INTRODUCTION

The optimal power flow (OPF) has remained a subject of widespread interest in power system research since its inception about half a century ago, by Carpentier [1]. The OPF model is a complex non-convex optimization by [2-3] for determining the best solution for a power system based on safety constraints. In the OPF formulation, the best operating condition of the power system are determined depending on the intended objective. Therefore, the optimal value of the control variable is the result of the OPF. Meanwhile, the balance of power and functional constraints of the system are also needed to be addressed in the OPF problem [4]. The OPF solution adjusts the electrical system's network settings to function for its purpose and meet the requirements of equipment operating constraints, power flow equation, and electrical system safety [5].

In the last decades, renewable energy has been heavily pursued and largely infiltrated the power system. Of course, this type of power is a good alternative to conventional thermal units [6]. Additionally, the problem with photovoltaic power plant (PVPP) and wind power plant (WPP) generation in power systems is the uncertainty of solar irradiance and wind speed in each region, respectively. It also considers the load uncertainty in the system. Thus, correctly assessing the PVPP and WPP generators in power systems requires the use of probabilistic load flow [7]. Probabilistic load flow (PLF) was first proposed to address load uncertainty by B. Borkowska [8]. Contains inputs, such as load uncertainty, wind speed, and solar irradiance, with the appropriate properties, such as PDF, are required for calculating the state variables of a system with uncertainty properties.

Under the emerging high penetration of distributed energy resources condition, probabilistic optimal power flow (POPF) is a handy tool to analyze uncertainty in power systems and hence has gained a lot of attention over the year.

The POPF treats each uncertain variable in the power system as a random variable in some probability distribution model and aims to obtain the optimal solution statistical interval. Meanwhile, several methods for the probabilistic optimal power flow (POPF) were also proposed in many articles. For example, analytical POPF methods [9], Point estimation method [10], and Monte-Carlo simulation. The most common way of numbers is the Monte-Carlo simulation (MCS). The MCS is widely used to present the true characteristics of power systems, it is simple in operation and has high accuracy [11-21]. Several approaches have been proposed in the relevant papers focusing on PLF, including PVPP and WPP generators [14-17]. The main approaches such as non-linear MCS, linear MCS, convolution-based approach [18], Markov-based approach [19], special distribution-based approach, Bayesian-based approach, and hybrid approaches, are described in [20].

Recently, stochastic models that accurately describe the behavior of power generation and load demand are critical for planning and operations of the power system. Meanwhile, these models need further improvements to accurately capture the behavior of solar irradiance and wind speed. In this paper, the practical load profiles of the power system are considered to estimate load PDF. The load uncertainty is expressed by Normal PDF in the proposed method, and the uncertainty of solar irradiance is expressed by Normal PDF as well as the load uncertainty [22]. Weibull PDF is widely used to model wind speed [23], however, a discrete PDF will be used to model the output power due to the wind energy conversion system (WECS) [6].

In this article, the OPF consists of three objective functions including the total system cost minimization (TSCM), active power loss minimization (APLM), and voltage magnitude deviation minimization (VMDM). The main contribution of this paper is the use of the fuzzy satisfactory functions (FSF) for determining the probabilistic multi-objective optimal power flow by particle

swarm optimization (PSO). The simulations result with the modified IEEE 30-bus test system including PVPP and WPP have been used as a case study.

The organization of this paper is as follow. Section 2 represents problem formulation, and PFOPF formulation is addressed in Section 3. Furthermore, the simulation results and discussion are illustrated in Section 4. Finally, conclusion is addressed in Section 5.

2. PROBLEM FORMULATION

2.1. Problem

In this paper, the probabilistic fuzzy multi-objective OPF (PFMOPF) problem can be represented as follows:

$$\text{Minimize} \quad F_i(\tilde{\mathbf{x}}, \tilde{\mathbf{u}}), \ i = 1, 2, ..., N_{obj} \quad (1)$$

$$\text{Subject to:} \quad g(\tilde{\mathbf{x}}, \tilde{\mathbf{u}}) = 0, \quad (2)$$

$$h(\tilde{\mathbf{x}}, \tilde{\mathbf{u}}) \le 0. \quad (3)$$

In Equation 1, matrix F_i represents the set of objective functions that are to be minimized consisting of total system cost (TSC), active power loss (APL), and voltage magnitude deviation (VMD). Meanwhile, the vector of dependent variables is denoted by $\tilde{\mathbf{x}}$, consisting of,
1. Slack bus generated active power ($\tilde{P}_{Gl}$),
2. Voltage magnitudes at load bus ($\tilde{V}_{Ll}$),
3. Generators' reactive power output ($\tilde{Q}_{Gi}$), and
4. Transmission lines and transformers loading (branches flow) ($\tilde{S}_l$).

Hence, $\tilde{\mathbf{x}}$ can be expressed as:

$$\tilde{\mathbf{x}} = [\tilde{P}_{G1}, \tilde{V}_{L1}...\tilde{V}_{LNL}, \tilde{Q}_{G1}...\tilde{Q}_{GNG}, \tilde{Q}_{WPP}, \tilde{Q}_{PVPP}, \tilde{S}_{l1}...\tilde{S}_{lNTL}]^T \quad (4)$$

Whereas, $\tilde{\mathbf{u}}$ is the vector of probabilistic control variables as follows:

$$\tilde{\mathbf{u}} = [\tilde{\mathbf{P}}_{\mathbf{G}}, |\tilde{\mathbf{V}}_{\mathbf{G}}|, \tilde{\mathbf{T}}, \tilde{\mathbf{X}}_{\mathbf{C}}]^T \quad (5)$$

Where $\tilde{\mathbf{P}}_{\mathbf{G}}$ is the matrix of active power generation excluding slack bus generation. $|\tilde{\mathbf{V}}_{\mathbf{G}}|$ is the matrix of voltage magnitude of generator bus, including WT and PV. $\tilde{\mathbf{T}}$ is the matrix of transformer tap-changing. And $\tilde{\mathbf{X}}_{\mathbf{C}}$ is the matrix of SVCs reactance values.

$$\tilde{\mathbf{P}}_{\mathbf{G}} = [\tilde{P}_{G2}, \tilde{P}_{G3}, ..., \tilde{P}_{GNG}]_{1\times(NG-1)} \quad , \quad (6)$$

$$|\tilde{\mathbf{V}}_{\mathbf{G}}| = [|\tilde{V}_{G1}|, |\tilde{V}_{G2}|, ..., |\tilde{V}_{GNG}|, |\tilde{V}_{WPP}|, |\tilde{V}_{PVPP}|]_{1\times NG} \quad , \quad (7)$$

$$\tilde{\mathbf{T}} = [\tilde{T}_1, ..., \tilde{T}_{NT}]_{1\times NT} \quad , \quad (8)$$

$$\tilde{\mathbf{X}}_{\mathbf{C}} = [\tilde{X}_{C1}, ..., \tilde{X}_{CNC}]_{1\times NC} \quad . \quad (9)$$

2.2. Objective Function

In this article, TSCM, APLM, VMDM, and multi-objective functions are considered, subject to the power flow equations and the system constraints as follows.

2.2.1. Total System Cost Minimization (TSCM)

The TSCM problem aims to save the generation cost of the power system. The objective function can be expressed as below:

$$\min_u F_1(\tilde{\mathbf{x}}, \tilde{\mathbf{u}}) = \min_u TSC(\tilde{\mathbf{x}}, \tilde{\mathbf{u}}) \quad (10)$$

where,

$$TSC(\tilde{\mathbf{x}}, \tilde{\mathbf{u}}) = \sum_{i=1}^{NG} (a_i + b_i \tilde{P}_{Gi} + c_i \tilde{P}_{Gi}^2) \quad (11)$$

2.2.2. Active Power Loss Minimization (APLM)

The APLM is to reduce the transmission loss as:

$$\min_u F_2(\tilde{\mathbf{x}}, \tilde{\mathbf{u}}) = \min_u APL(\tilde{\mathbf{x}}, \tilde{\mathbf{u}}) \quad (12)$$

where,

$$APL(\tilde{\mathbf{x}}, \tilde{\mathbf{u}}) = \sum_{L=1}^{NTL} g_{L,ij} \left[\tilde{V}_i^2 + \tilde{V}_j^2 - 2\tilde{V}_i \tilde{V}_j \cos \tilde{\theta}_{ij} \right] \quad (13)$$

2.2.3. Voltage Magnitude Deviation Minimization (VMDM)

The VMDM is to keep the voltage quality of a power system. To make the system stable and more secure by maintaining the voltage within tight control. In the order to avoid this situation, $\tilde{V}_i^{ref}$ is generally considered as 1 p.u. The objective function can be formulated as:

$$\min_u F_3(\tilde{\mathbf{x}}, \tilde{\mathbf{u}}) = \min_u VMD(\tilde{\mathbf{x}}, \tilde{\mathbf{u}}) \quad (14)$$

where,

$$VMD(\tilde{\mathbf{x}}, \tilde{\mathbf{u}}) = \sum_{i=1}^{NL} |\tilde{V}_i - \tilde{V}_i^{ref}| \quad (15)$$

2.2.4. Fuzzy Multi-Objective OPF Formulation (FMOPF)

The PFMOPF problem is simultaneously solved for the optimal solution of TSCM, APLM, and VMDM, based on a fuzzy trade-off concept.
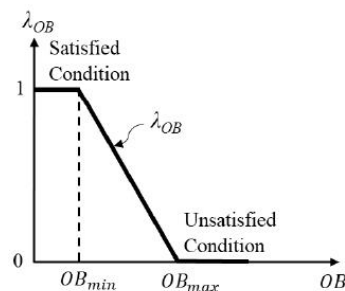

Fig. 1. FSF of TSC.

The fuzzy multi-objective optimization technique formulates the fuzzy satisfaction for individual objectives [24]. In this way, the multi-objective optimization problem can be solved by compromising all objectives.

$$
\lambda_{OB} = \begin{cases} 1 & ,\text{for } OB \le OB_{\min} \\ \dfrac{-1}{OB_{\max} - OB_{\min}} \cdot OB \\ + \dfrac{OB_{\max}}{OB_{\max} - OB_{\min}} & ,\text{for } OB_{\min} \le OB < OB_{\max} \\ 0 & ,\text{for } OB \ge OB_{\max} \end{cases} \tag{16}
$$

$$
\text{Maximize } \lambda_T = \min\{\lambda_{TSC}, \lambda_{APL}, \lambda_{VMD}\} \tag{17}
$$

The objective function in Equation 16 is used to formulate the fuzzy satisfactory functions (FSF) as shown in Figure 1 and Equation 16, where *OB* represents the individual objective (TSCM, APLM, and VMDM).

This process defines FSFs associated with each objective because the high value of each objective is obtained from the low FSF value. In some way, the best value for each objective is obtained from individual objective optimization. The FSF of the individual objective functions can be represented by Equation 16, for TSCM, APLM, and VMDM. FSF can take any value in [0,1]. The FSF value of one is assigned to the minimum value for each objective. When the other objective provides that the objective value is greater than the minimum value, the FSF is decreased to zero. Lastly, the multi-objective problem can be formulated as a fuzzy maximization problem as Equation 17.

2.3. System constraints

The OPF constraints including power balance and operation are taken into consideration in the proposed method.

2.3.1. Power balance constraints

The power balance constraint can be represented by the Newton-Raphson power flow equations. These constraints are handled by solving the power flow solution. In addition, the other dependent variables are obtained from this process. The objective functions discussed above should be simultaneously optimized considering the following constraints.

$$
\tilde{P}_{Gi} + \tilde{P}_{PVi} + \tilde{P}_{WTi} - \tilde{P}_{Di} = \sum_{j=1}^{NB}\left[G_{ij}|\tilde{V}_i||\tilde{V}_j|\cos(\tilde{\theta}_{ij}) + B_{ij}|\tilde{V}_i||\tilde{V}_j|\sin(\tilde{\theta}_{ij})\right], \tag{18}
$$

$$
\tilde{Q}_{Gi} - \tilde{Q}_{Di} = \sum_{j=1}^{NB}\left[G_{ij}|\tilde{V}_i||\tilde{V}_j|\sin(\tilde{\theta}_{ij}) - B_{ij}|\tilde{V}_i||\tilde{V}_j|\cos(\tilde{\theta}_{ij})\right], \tag{19}
$$

where, $i=1,\dots,NB$.

2.3.2. System operating limit constraints

The generator constraints are the limit on generators' voltage magnitude and the generators' active and reactive power operating limit at the *i*th bus, respectively. Equations 23 to 24 are transformer tap-changing limits and the SVCs setting limits, respectively. Whereas, network operating limit constraints include the limit on bus voltage magnitude and the transmission lines and transformers loading limit, respectively.

$$
|V_{Gi}|^L \le |\tilde{V}_{Gi}| \le |V_{Gi}|^U \qquad, i = 1, 2, \dots, NG, \tag{20}
$$

$$
P_{Gi}^L \le \tilde{P}_{Gi} \le P_{Gi}^U \qquad, i = 1, 2, \dots, NG, \tag{21}
$$

$$
Q_{Gi}^L \le \tilde{Q}_{Gi} \le Q_{Gi}^U \qquad, i = 1, 2, \dots, NG, \tag{22}
$$

$$
T_i^L \le \tilde{T}_i \le T_i^U \qquad, i = 1, 2, \dots, NT, \tag{23}
$$

$$
Q_{ci}^L \le \tilde{Q}_{ci} \le Q_{ci}^U \qquad, i = 1, 2, \dots, NC, \tag{24}
$$

$$
|V_{Li}|^L \le |\tilde{V}_{Li}| \le |V_{Li}|^U \qquad, i = 1, 2, \dots, NPQ, \tag{25}
$$

$$
|MVA_{Li}| \le M\tilde{V}A_{Li}^U \qquad, i = 1, 2, \dots, NL. \tag{26}
$$

3. PFOPF FORMULATION

Monte-Carlo simulation (MCS) is a traditional numerical method for dealing with probability problems. The MCS can generate random numbers and random sampling with the cumulative density function, and repeat the power flow one by one. In the proposed, the procedure for calculating the MCS concept can be defined as follows [21]:

Step 1: Obtain power flow input data set.
Step 2: Specify the control variables, dependent variables, and security limits.
Step 3: Set the average total power generation at $k = 0$ to zeros ($PGT_{AV}^0 = 0$). Set iteration $k = 1$.
Step 4: Obtain system load, PVPP power generation, and WPP power generation, form PDFs.
Step 5: Solve OPF for individual objective function (TSC, APL, and VMD in Equation 10, 12, and 14, respectively) using PSO.
Step 6: Define a satisfying Fuzzy function for individual objections.
Step 7: Compute a satisfying Fuzzy function for multi-objective.
Step 8: Solve FMOPF for λ_T maximization in Equation 17, using PSO.
Step 9: Calculate the average total power generation (PGT_{AV}^k) obtained from iterations k
Step 10: If $|PGT_{AV}^k - PGT_{AV}^{k-1}| > \varepsilon$, $k = k+1$ and go to Step 4,
If $|PGT_{AV}^k - PGT_{AV}^{k-1}| \le \varepsilon$,, go to Step 11.
Step 11: Calculate the PDF of control and output variables.
Step 12: Stop.

Meanwhile, PVPP generation, WPP generation, and load are modeled as uncertain variables as follows.

3.1. PVPP Model

The solar radiation follows a normal distribution probability theory. A normal distribution is a continuous probability distribution of a continuous random variable in which a normal logarithm distribution is given. In the proposed, the PVPP is intermittent and uncertain output, and it is modeled as a continuous random variable of Thailand. Therefore, the output power generated by the PVPP unit is dependent on solar irradiance [25], as follows.

$$\tilde{P}_{PVPPi}(S) = \begin{cases} \tilde{P}_{pvn} \dfrac{S^2}{S_{stc}R_c} & \text{for } S < R_c \quad \text{,for bus } i \\ \tilde{P}_{pvn} \dfrac{S}{S_{stc}} & \text{for } S \geq R_c \quad \text{,for bus } i \end{cases} \tag{27}$$

The probability of solar irradiance *(G)* following normal PDF with mean 'μ', variance 'σ', and mean of a normal distribution are defined in Equations 30 and 31, respectively.

$$f_G(G) = \frac{1}{G\sigma\sqrt{2\pi}} \exp\left\{ \frac{-(\ln x - \mu)^2}{2\sigma^2} \right\} \quad \text{for } G > 0 \tag{28}$$

$$M_{lgn} = \exp(\mu + \frac{\sigma^2}{2}) \tag{29}$$

3.2. WPP model

Power generated from a wind power plant (WPP) depends on the fluctuation of wind speed over time. Because the geographic location of wind resources is highly variable. Wind speed distributions are often characterized by a Weibull distribution [26]. The output power of WPP can be analyzed as follows:

$$\tilde{P}_{WPP}(v) = \begin{cases} 0 & v \leq v_{ci} \\ \dfrac{v - v_{ci}}{v_n - v_{ci}} & v_{ci} < v \leq v_n \\ P_{wtn} & v_n < v \leq v_{co} \\ 0 & v \geq v_{co} \end{cases} \tag{30}$$

Weibull distribution can be formulated as follows:

$$f_v(v) = \frac{k}{c} \cdot \left(\frac{v}{c} \right)^{k-1} \cdot e^{-\left(\frac{v}{c} \right)^k} \tag{31}$$

3.3. Load Model

Probabilistic load modeling (PLM) can be found in several probabilistic load flows. Like PVPP and WPP, the load is modeled as a continuous random variable of energy consumption in Thailand. The total load connected to the bus can be probabilistically described by a normal distribution. The relevant PDF is as follows:

$$f_{P_d}(P_d) = \frac{1}{\sqrt{(2\pi)}\sigma} \exp\left(-\frac{(P_d - \mu)^2}{2\sigma^2} \right) \tag{32}$$

4. SIMULATION RESULT AND DISCUSSION

The PFMOPF simulation is performed on the modified IEEE 30-bus test system consisting of PVPP, WPP, and load, which were studied TSCM, APLM, VMDM, and multi-objective, as shown in Figure 2. The system data is taken from [27].
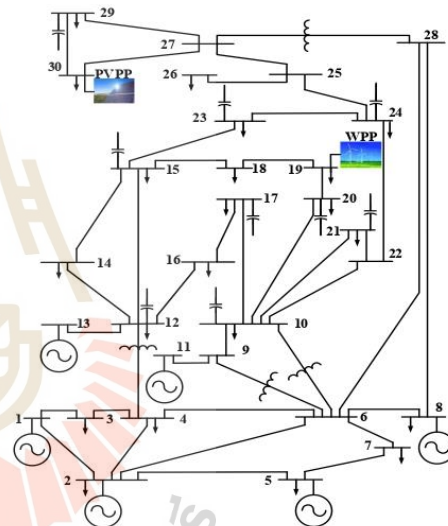

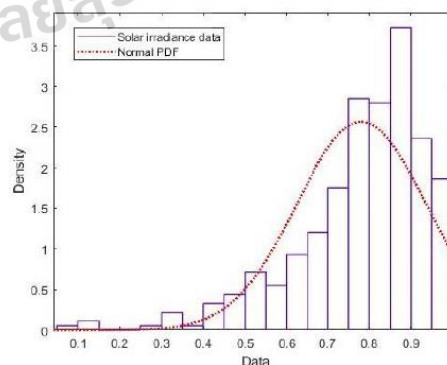**Fig. 2. The modified IEEE 30 buses system by renewable energy.**

Fig. 3. The PDF of solar irradiance data.

The IEEE 30-bus test system was modified by adding two

renewable energy sources: WPP and PVPP generator, considering load uncertainty, obtained from the PDF models. The MCS is performed until the average total power generation is close to the previous iteration. In the proposed, Figure 3 shows the normal fitting of normalized solar irradiance after running an MCS. In the proposed, the mean value 'μ' is taken as 0.7805 and the variance 'σ' is taken as 0.0242. The rated power of PVPP connected at bus 30 is 25 MW [27].
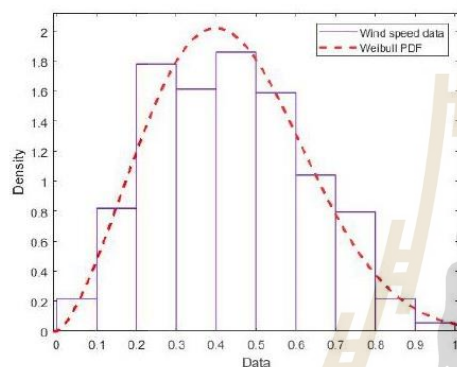

Fig. 4. The PDF of wind speed data of Thailand.
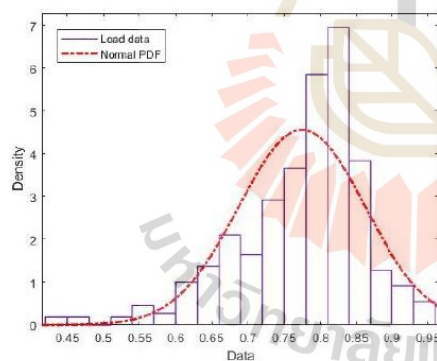
Fig. 5. The PDF of active power load.

The probability distribution of wind speed is usually represented by the Weibull distribution. A general Weibull distribution can take various shapes depending on the parameters. In this paper, the wind speed is modeled using a Weibull distribution [26]. The WPP connected at bus 19 with a normal wind speed of 10 m/s, cut-in wind speed of 2.7 m/s, and cut-out wind speed of 25 m/s [27]. The normalized wind speed is approximated with a two-parameter Weibull distribution, the scale factor 'c' is taken as 0.493 and the shape factor 'k' is taken as 2.459, as in Figure 4.

The normalized loading characteristic showed in Figure 5. The load probability density function (PDF) is usually

represented by a normal PDF, where the PLM can be rendered more realistically by daily hourly loading. In Figure 5, the active power is assumed to have normal density distribution. The μ is taken as 0.7748 and the σ is taken as 0.0077.

Table 1. The results obtained by proposed PFMOPF

Control Variables	Mean	variance
Power Generation (P_{Gi}) at Bus (MW)		
2	38.868	7.449
5	31.338	5.238
8	23.779	7.414
11	19.010	5.348
13	17.874	5.190
Generator Voltage ($|V_i|$) Magnitude at Bus (p.u.)		
1	1.036	0.032
2	1.029	0.032
5	1.013	0.031
8	1.022	0.031
11	1.011	0.036
13	1.011	0.026
19(WPP)	1.014	0.019
30(PVPP)	1.040	0.020
Transformer Tap-Changing (T_{i-j}) between Buses		
6-9	1.014	0.055
6-10	1.006	0.067
4-12	1.004	0.042
28-27	1.003	0.038
SVC Reactance Values (X_{Ci}) at Bus (p.u.)		
10	-27.570	14.487
12	-24.442	15.428
15	-36.064	9.614
17	-28.078	10.760
20	-37.298	9.629
21	-21.742	12.649
23	-37.993	8.437
24	-25.489	10.274
29	-40.195	7.344
TSC ($/h.)	**535.123**	**9612.92**
APL (p.u.)	**2.523**	**3.594**
VMD (p.u.)	**0.429**	**0.022**
-μT of PFMOPF	**-0.741**	**0.006**

Table 1 shows control variables of the proposed PFMOPF. The PDF in terms of μ and σ for PFMOPF are shown in Table 1.

The PVPP power generation characteristic is obtained from the solar irradiance data of Thailand. The selected dispatch hour is noon of every day because it is the time with the highest solar irradiation. The PVPP is connected to bus 30. The wind speed data is obtained from NASA's online database for Bangkok, Thailand at noon, similar to solar irradiance data. The WPP is connected to bus 19. Similar to solar irradiance and wind speed, the load characteristic is derived from the load demand of Thailand, which is distributed proportionally throughout the IEEE 30-bus test system.

Figures 6 to 9 shows the PDF of the optimal control variables, and Figures 10 to 13 presents the PDF for TSC,

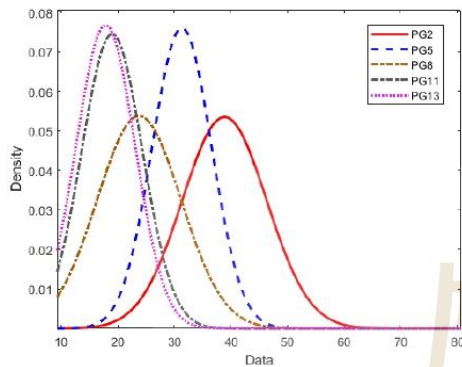APL, VMD, and -λ_T of PFMOPF, obtained with 2000 sample MCS.

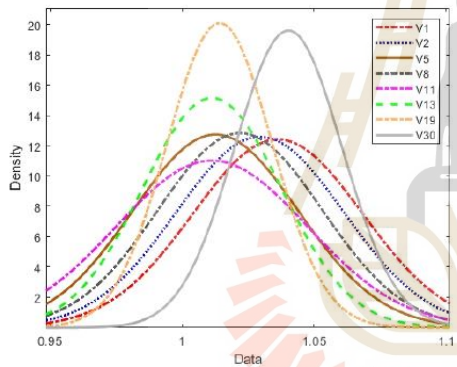Fig. 6. The PDF of PFMOPF for output power of generators.

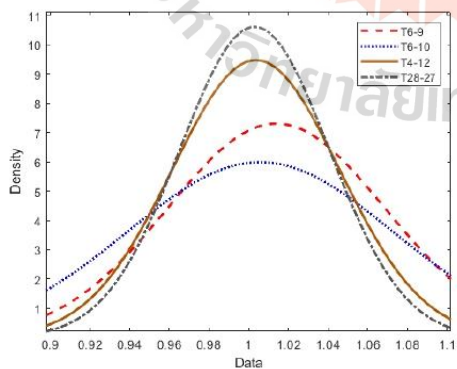Fig. 7. The PDF of PFMOPF for voltage magnitudes of generators.

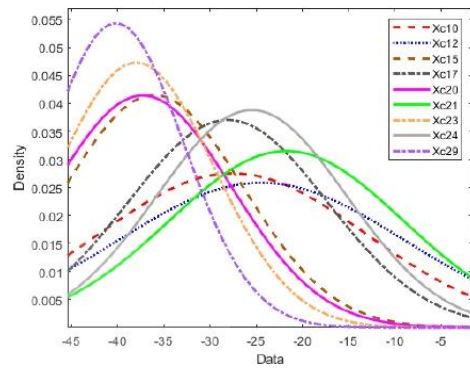Fig. 8. The PDF of PFMOPF for transformer Tap-Changing.

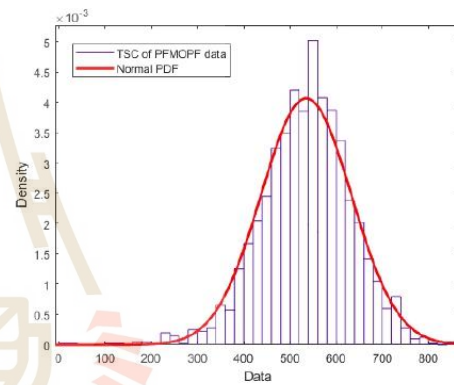Fig. 9. The PDF of PFMOPF for SVC Reactance Values.
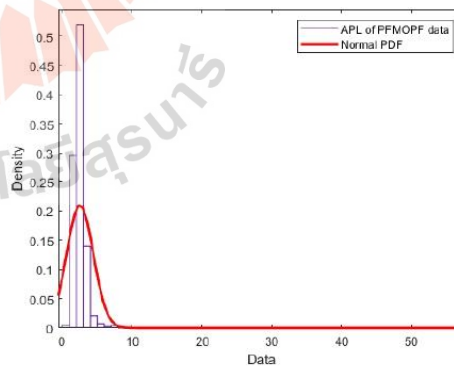

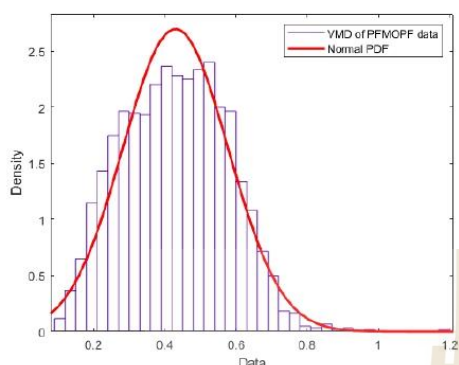Fig. 10. The PDF of PFMOPF for TSC.

Fig. 11. The PDF of PFMOPF for APL.
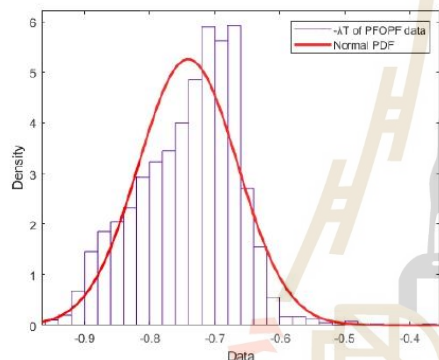
Fig. 12. The PDF of PFMOPF for VMD.

Fig. 13. The PDF of PFMOPF for -λ_T.

To indicate the accuracy and effectiveness of the proposed method. The results are compared with the MCS, which are considered reference methods. The results obtained from the proposed method can be compared with the values of the MCS with 2000 runs. Figure 14 illustrates the convergence of the MCSs results of four objective functions: TSCM, APLM, VMDM, and PFMOPF.
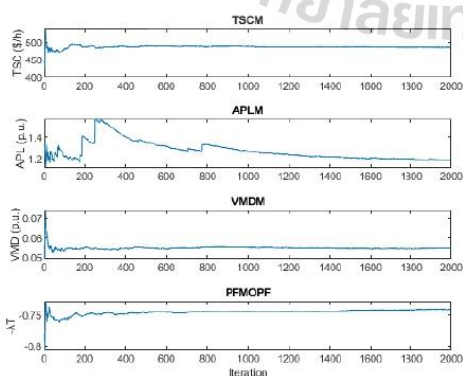

Fig. 14. The convergence of MCS of PFMOPF.

5. CONCLUSIONS

This article proposes the PFMOPF method with various control variables using PSO integrated PVPP, WPP, and load uncertainty. The proposed method was tested under the modified IEEE 30-bus test system. The proposed problem formulation provides the optimal operating conditions for active power generation, generator voltage magnitude, transformer tap change, and SVCs setting values in probabilistic term. The objectives considered are TSCM, APLM, and VMDM, and traded of by using the fuzzy concept. The simulation results indicated that the PFMOPF can effectively minimize individual-objective and maximize the overall FSF for multi-objective OPF solutions, incorporating uncertainty of PVPP, WPP, and load in power system.

REFERENCES

[1] J. Carpentier, "Contribution á l'étude du dispatching économique," *Bulletin de la Société Française des Électriciens,* Vol. 3, pp. 431-447, 1962.

[2] Bernard C. Lesieutre. "Convexity of the Set of Feasible Injections and Revenue Adequacy in FTR Markets", *IEEE Transactions on Power Systems*, Vol. 20, No. 4, 2005.

[3] Daniel K. Molzahn, "Identifying and Characterizing Non-Convexities in Feasible Spaces of Optimal Power Flow Problems", *IEEE Transactions on circuits and systems*, Vol. 65, pp.672-676, 2018.

[4] Dan Wu and Bernard C. Lesieutre, "A Deterministic Method to Identify Multiple Local Extrema for the AC Optimal Power Flow Problem", *IEEE Transactions on Power Systems*, Vol. 33, pp. 654-668, 2018.

[5] Yu-Cheng Chang, Tsung-Ying Lee, Chun-Lung Chen, Rong-Mow Jan, "Optimal power flow of a wind-thermal generation system", *Electrical Power and Energy Systems*, Vol. 55, pp. 312-320, 2014.

[6] John Hetzer, David C. Yu, "An Economic Dispatch Model Incorporating Wind Power", *IEEE transactions on energy conversion*, Vol. 23, No. 2, 2008.

[7] S. Conti and S. Raiti, "Probabilistic load flow using Monte Carlo techniques for distribution networks with photovoltaic generators", *Solar Energy 81*, pp. 1473-1481, 2007.

[8] B. Borkowska, "Probabilistic load flow", *IEEE Trans. Power Apparatus and Systems*, Vol. PAS-93, No. 3, pp. 752-755, 1974.

[9] A. Schellenberg; W. Rosehart; and J. Aguado, "Introduction to cumulant-based probabilistic optimal power flow (P-OPF)", *IEEE Transactions on Power Systems*, Vol. 20, 2005.

[10] Y. Li; W. Li; W. Yan; J. Yu; and X. Zhao, "Probabilistic Optimal Power Flow Considering Correlations of Wind

Speeds Following Different Distributions", *IEEE Transactions on Power Systems*, Vol. 29, 2014.

[11] Ripley, *Stochastic Simulation*, 1st ed. Wiley, 2006.

[12] G. Carpinelli, P. Caramia, P. Varilone, "Multi-linear monte carlo simulation method for probabilistic load flow of distribution systems with wind and photovoltaic generation systems", *Renewable Energy 76*, pp.283-295, 2015.

[13] Anselmo B. Rodrigues and Maria G. Da Silva, "Probabilistic Assessment of Available Transfer Capability Based on Monte Carlo Method With Sequential Simulation", *IEEE transactions on power systems*, Vol. 22, No. 1, 2007.

[14] K.C. Divya, P.S. Nagendra Rao, "Models for wind turbine generating systems and their application in load flow studies", *Electric Power Systems Research 76*, pp. 844-856, 2006.

[15] Yan Chen, Jinyu Wen, and Shijie Cheng, "Probabilistic Load Flow Method Based on Nataf Transformation and Latin Hypercube Sampling", *IEEE transactions on sustainable energy*, Vol. 4, No. 2, 2013.

[16] F.J. Ruiz-Rodriguez, J.C. Herna´ndez, F. Jurado, "Probabilistic load flow for radial distribution networks with photovoltaic generators", *IET Renewable Power Generation*, Vol. 6, Iss. 2, pp. 110 –121, 2012.

[17] Miao Fan, Vijay Vittal, Gerald T. Heydt, and Raja Ayyanar, "Probabilistic Power Flow Analysis with Generation Dispatch Including Photovoltaic Resources", *IEEE Transactions on power systems*, Vol. 28, No. 2, 2013.

[18] N.D. Hatziargyriou, T.S. Karakatsanis, M. Papadopoulos, "Probabilistic load flow in distribution systems containing dispersed wind power generation", *IEEE Transactions on Power Systems*, Vol. 8, No. 1, 1993.

[19] W. Sun, M. Zamani, H.T. Zhang, and Y. Li, "Probabilistic Optimal Power Flow with Correlated Wind Power Uncertainty via Markov Chain Quasi-Monte Carlo Sampling", IEEE Transactions on Industrial Informatics, Vol. 15, pp. 6058-6069, 2019.

[20] Guido Carpinelli, Pierluigi Caramia, Pietro Varilone, "Multi-linear Monte Carlo simulation method for probabilistic load flow of distribution systems with wind and photovoltaic generation systems", *Renewable Energy 76*, PP. 283-295, 2015.

[21] K. Chayakulkheeree, "Probabilistic Optimal Power Flow with Weibull Probability Distribution Function of System Loading Using Percentiles Estimation", *Electric Power Components and Systems*, pp. 252-270, 2013.

[22] J. Reinders, N.G. Paterakis, J. Morren, and J.G. Slootweg, "A Linearized Probabilistic Load Flow Method to deal with Uncertainties in Transmission Networks", *IEEE International Conference on Probabilistic Methods Applied to Power Systems (PMAPS)*, 2018.

[23] Mukund R. Patal, "Wind and Solar Power Systems Design, Analysis, and Operation", Second Edition,2006.

[24] H. J. Zimmermann, Fuzzy Sets. Decision Making, and Expert Systems: *Kluwer Adademic Publishers*, 1987.

[25] Partha P. Biswas, P.N. Suganthan, Gehan A.J. Amaratunga, "Optimal power flow solutions incorporating stochastic wind and solar power", *Energy Conversion and Management 148*, pp. 1194-1207, 2017.

[26] Imad Abouzahr, R. Ramkumar, "An approach to assess the performance of utility-interactive wind electric conversion systems", *IEEE Transactions on Energy Conversion*, Vol. 6, No.4, 1991.

[27] Zia Ullah, Shaorong Wang, and Jinmu Lai, "A Solution to the Optimal Power Flow Problem Considering WT and PV Generation", *IEEE Access*, Vol. 7, pp. 46763-46772, 2019.

CURRICULUM VITAE

My name is Prakaipetch Muangkhiew. I received my Bachelor of Engineering in Electrical Engineering (First Class Honors) from Suranaree University of Technology, Thailand, in 2020. I am currently a graduate student in a Master of Engineering in Electrical Engineering at Suranaree University of Technology. I am also working as a teaching assistant and research assistant at the School of Electrical Engineering, Institute of Engineering, Suranaree University of Technology. My research interests currently focus on power system analysis, power systems optimization, Artificial intelligence (AI) application in power systems, the probabilistic method in power system analysis, renewable energy, and related fields.

When I was studying for my bachelor's degree at Suranaree University of Technology, I interned at Bosch Automotive (Thailand) Co., Ltd. I have experience in the manufacturing process of electrical equipment.

After I graduated with a bachelor's degree, I immediately studied for a master's degree at Suranaree University of Technology. I am so proud of my teaching assistant position duty to teach laboratories for electrical engineering students. I received the best paper award in power systems at the 2021 International Electrical Engineering Congress (iEECON2021). Moreover, I also published a research article about multi-objective optimal power flow in the International Energy Journal (IEJ) and probabilistic optimal power flow in the GMSARN International Journal.

Moreover, I have experience in consulting assistance of PV power plants, my duty is analyzing and energy management systems for the installation of PV power plants in power systems.

Finally, I have experience as a project engineer for the project-related induction motor efficiency estimation at Suranaree University of Technology. This work also helps me develop my electrical engineering skills.